Absorption into Stirred Emulsions

Von der Fakultät für Lebenswissenschaften

der Technischen Universität Carolo-Wilhelmina zu Braunschweig

zur Erlangung des Grades

einer Doktorin der Naturwissenschaften

(Dr. rer. nat.)

genehmigte

D i s s e r t a t i o n

von Elmira Mohsenzadeh
aus Arak / Iran

1. Referentin oder Referent: Professor Dr. Adrian Schumpe
2. Referentin oder Referent: Privatdozent Dr. Ulf Christian Prüße
eingereicht am: 14.02.2018
mündliche Prüfung (Disputation) am: 27.04.2018

Druckjahr 2018

Vorveröffentlichungen der Dissertation

Teilergebnisse aus dieser Arbeit wurden mit Genehmigung der Fakultät für Lebenswissenschaften, vertreten durch den Mentor der Arbeit,
in folgenden Beiträgen vorab veröffentlicht:

Tagungsbeiträge

Elmira Mohsenzadeh and Adrian Schumpe (2016). "Absorption of Carbon Dioxide into Stirred Emulsions." *Jahrestreffen Reaktionstechnik*, 2-4 May, Würzburg, Germany.

Elmira Mohsenzadeh and Adrian Schumpe (2017). "Absorption of Carbon Dioxide into Stirred Emulsions." *3rd International Symposium on Multiscale Multiphase Process Engineering* (MMPE), 8-11 May, Toyama, Japan.

Acknowledgements

I would like to take this opportunity to express my deepest gratitude to all those who assisted and supported me in creating my dissertation.

First, I am sincerely thankful and greatly indebted to Prof. Dr. Adrian Schumpe for his tremendous support, expert guidance and remarkable patience through all these years. He is not only a perfectly knowledgeable supervisor for me, but also an excellent teacher and wise mentor. He genuinely checks in to make sure that things are going well not only for my dissertation, but also my everyday wellbeing. I am honored and grateful to be a part of his research group.

Many thanks go to all my committee members, PD Dr. Ulf Prüße and Prof. Dr. Uwe Schröder for their dedicated time and helpful feedback. I would also like to thank Prof. Dr. Hans-Joachim Jördening for accepting to be my second supervisor.

I would like to extend my thanks to all the supporting staff at the Technical Chemistry Institute, especially Gabriele Schirmer, Birgit Niehoegen and Dr. Dirk-Christian Eiting. I am indebted to them for their help.

I am also thankful to Dr. Willy Tchowa Medjiade. He gave me a lot of valuable advice during my hard time and helped me in every possible way. I deeply appreciate Boris Beese for his great collaboration.

Finally, I want to thank my loving family and friends, who have helped me along my journey. I am extremely thankful to my little sister Samira Mohsenzadeh for her love and continuous support. In particular, my parents who always encourage me to pursue my goals and help me overcome difficulties. Dear Mom and Dad, I could not be where I am today without your unselfish and unconditional love and support. I will never be able to express how blessed and grateful I am for everything you have done for me. Thank you so much for always being there for me.

Table of Contents

List of Figures

List of Tables

List of symbols

$\boldsymbol{A}$	Transfer surface area	m^2
$\boldsymbol{a}$	Specific interfacial area	m^{-1}
$\boldsymbol{a_{chem}}$	Chemical effective specific interfacial area	m^{-1}
$\boldsymbol{a_{geo}}$	Geometrical specific interfacial area	m^{-1}
$\boldsymbol{C}$	Constant in Eq. (43)	-
$\boldsymbol{c^*}$	Gas solubility	mol m^{-3}
$\boldsymbol{c_{A,i}}$	Liquid phase concentration of dissolved gas at the gas-liquid interface	mol m^{-3}
$\boldsymbol{c_{A,L}}$	Concentration of dissolved gas in the liquid bulk	mol m^{-3}
$\boldsymbol{c_{B,0}}$	Bulk concentration of *B*	mol m^{-3}
$\boldsymbol{c_i}$	Concentration of ion	mol m^{-3}
$\boldsymbol{c_L^*}$	Equilibrium concentration of dissolved gas in the liquid phase	mol m^{-3}
$\boldsymbol{D}$	Gas diffusion coefficient	m^2 s^{-1}
$\boldsymbol{E}$	Enhancement factor	-
$\boldsymbol{H}$	Henry's constant	Pa m^3 mol^{-1}
$\boldsymbol{Ha}$	Hatta number	-
$\boldsymbol{h_G}$	Gas-specific parameter	m^3 mol^{-1}
$\boldsymbol{h_i}$	Ion-specific parameter	m^3 mol^{-1}
$\boldsymbol{k_G}$	Gas-side mass transfer coefficient	m s^{-1}
$\boldsymbol{k_L}$	Liquid-side mass transfer coefficient	m s^{-1}
$\boldsymbol{k_La}$	Volumetric mass transfer coefficient	s^{-1}
$\boldsymbol{K_m}$	Overall absorption coefficient for pseudo-*m*th order reaction	mol m^{-2} s^{-1} $Pa^{-(m+1)/2}$
$\boldsymbol{k_{m,n}}$	*m*,*n*th order reaction rate constant	$(mol\ m^{-3})^{1-(m+n)}$ s^{-1}
$\boldsymbol{m}$	Reaction order of *A*	-
$\boldsymbol{m_R}$	Gas solubility ratio oil / water	-
$\boldsymbol{M_s}$	Molecular weight of solvent	kg mol^{-1}
$\boldsymbol{N}$	Mass transfer flux at a gas-liquid interphase	mol m^{-2} s^{-1}
$\boldsymbol{N}$	Stirrer speed in Eq. (43)	s^{-1}

n	Reaction order of *B*	-
P	Total pressure	Pa
$p_{A,G}$	Partial pressure of gas A in the gas bulk	Pa
$p_{A,i}$	Partial pressure of dissolved gas A at the gas-liquid interface	Pa
P_f	Final total pressure	Pa
p_G^*	Equilibrium partial pressure of the dissolved gas	Pa
P_i	Initial total pressure	Pa
p_O	Oil partial pressure	Pa
p_W	Water partial pressure	Pa
R	Gas constant	Pa m^3 mol^{-1} K^{-1}
R_A	Absorption rate per unit volume	mol m^{-3} s^{-1}
r_A	Reaction rate	mol m^{-3} s^{-1}
s	Surface renewal frequency	s^{-1}
$S_{O/W}$	Oil-water spreading coefficient	N m^{-1}
T	Temperature	K
t	Temperature in Eq. (40)	˚C
V_L	Volume of liquid	m^3
V_{O_2}	Molar volume of oxygen at normal boiling point	m^3 mol^{-1}
V_s	Superficial gas velocity in Eq. (43)	m s^{-1}
X	association parameter	-
x	mole fraction	-
z	Stoichiometric coefficient	-

Greek symbols

γ	Interfacial tension	N m^{-1}
δ	Film thickness	m
θ	Contact time	s
μ	Dynamic viscosity	Pa s
ϕ	Volume fraction	-

List of abbreviations

A	Gas phase reactant
B	Liquid phase reactant
cont.	Continuous
disp.	dispersed
DPBI	Down-pumping pitched blade impeller
exp	Experimental
G	Gas
GIR	Gas induced reactor
GSR	Gas sparged reactor
L	Liquid
O,o	Oil
PBI	Pitched blade impeller
S	Stirring vessel with flat surface
SAR	Surface aerated reactor
UPBI	Up-pumping pitched blade impeller
W,w	Water

Chapter 1

Introduction

There are different types of gas-liquid contactors, *e.g.*, bubble columns, airlift reactors, hollow fiber membrane and agitated vessels. Mechanically agitated reactors are the standard and most used reactors in the chemical and biochemical industry for physical/chemical absorption, gas-liquid and gas-liquid-solid processes. They are applied for fermentation, chlorination, oxidation, hydrogenation, polymerization, chemical synthesis and wastewater treatment.

Stirred tank reactors are preferred over bubble columns as they show better performance and provide higher gas-liquid mass transfer coefficients, better circulation and control flexibility. One of the most important research subjects in stirred tanks is gas dispersion which has a strong influence on gas-liquid mass transfer. In order to recycle gas from the head space to the liquid phase without the need of a sparger, surface aerators and self-induced gas-liquid reactors are used. The benefit of using this rector is where the gas is available at a relatively low pressure.

Gas-liquid-liquid systems are encountered in several important fields of biochemical processes, wastewater treatment and chemical applications. It is known that the volumetric mass transfer coefficient k_La is one of the key parameters determining the performance of these systems in multiphase reactors. k_La depends on several factors such as tank geometry, impeller type, physical properties of the liquids and its rheology and the presence of surface active agents. It has been frequently reported that the addition of an immiscible organic liquid to a gas-liquid system may significantly enhance the mass transfer rate through shuttle or bubble covering mechanism. Some limited work has also been undertaken to observe the effect of the presence of a second liquid phase on carbon dioxide transfer such as n-hexadecane (Ngo and Schumpe, 2012a), n-dodecane (Cents *et al.*, 2001; Ngo and Schumpe 2012a) and n-heptane (Cents *et al*., 2001; Zhang *et al*., 2010; Ngo and Schumpe, 2012a). However, no general trend can be derived from the reported results. Additional research in this area is desired. Despite the vast amount of publications on oil-in-water emulsions, studies on water-in-oil emulsions formed at high oil volume fractions are rare (Linek and Beneš, 1976; Ngo and Schumpe, 2012a,b).

Systems with contaminants are important in bioreactors with emulsion stabilizer and in biological treatment of wastewaters of the petroleum industries (Asgharpour *et al*., 2010). The presence of surfactants at the gas liquid interface may increase the gas absorption rate by reducing the coalescence rate of bubbles. It is possible that a reduction of k_L may be counteracted by increased interfacial area and therefore the values of k_La may increase. Very limited investigations related to the influence of surfactants on mass transfer have been carried out.

The main purpose of this study is to investigate and determine the volumetric mass transfer coefficient (k_La) of carbon dioxide in oil-in-water and water-in-oil emulsions by pressure technique in a surface-aerated stirred vessel under isothermal (25˚C) condition. The effect of an anionic surfactant on k_La is also investigated. Some preliminary experiments were performed to determine the specific interfacial area in O/W emulsions of n-hexadecane by cobalt-catalyzed sulfite oxidation.

Chapter 2

Theory and Literature Review

2.1 Physical Absorption

Mass transfer in multiphase systems occurs whenever two phases of different activity are brought into contact. For instance, if a liquid solution is brought into contact with carbon dioxide, the gas will be dissolved in the liquid until a state of equilibrium composition is reached. Without chemical reactions, physical solubility plays the essential role in the absorption rate:

$$N_{CO_2} = k_{\mathrm{L}}\left(c_{CO_2,i} - c_{CO_2,L}\right) = k_{\mathrm{L}}\left(\frac{p_{CO_2,i}}{H_{CO_2}} - c_{CO_2,L}\right) \quad (1)$$

where

N_{CO_2}= mass transfer flux at a gas-liquid interphase, mol m^{-2} s^{-1}

k_{L}= liquid-side mass transfer coefficient, m s^{-1}

$c_{CO_2,i}$ = CO_2 concentration at the gas-liquid interface, mol m^{-3}

$c_{CO_2,L}$ = bulk concentration of CO_2, mol m^{-3}

H_{CO_2}= Henry's constant of carbon dioxide, Pa m^3 mol^{-1}.

When a substance is transferred from a phase of high activity to one of low activity across a separating interface, the resistance in each phase can be divided to the diffusional resistance in the film and resistance in the bulk (Treybal, 1981). It is commonly assumed that the major resistance to mass transfer occurs in a thin film on both sides of the interface and the bulk resistance is negligible. Three important mass transfer models (surface renewal, and penetration theory) will be briefly reviewed in the sequel in this section.

2.1.1 Two-film theory

The film theory is the oldest mass transfer model and was developed by Lewis and Whitman in 1924. They assumed that stationary films of low thickness exist on either side of the gas-liquid interface. The linear concentration gradient represents the driving force that is causing molecular diffusion to take place in the films while there is no concentration gradient in the gas- and liquid-bulk (Fig. 1).

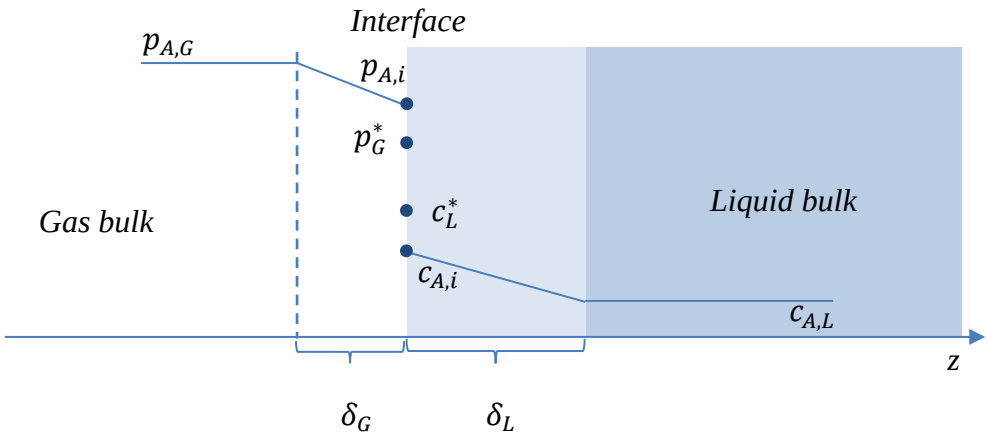

Fig. 1 Schematic of two film theory.

Fick's law can be applied to calculate the mass flux of the gas (A) in the liquid-side film:

$$N_A = -D_{AB}\frac{dc_A}{dz} = -\frac{D_{AB}}{\delta_L}\left(c_{A,i} - c_{A,L}\right) \tag{2}$$

where

D_{AB} = diffusion coefficient, $m^2\ s^{-1}$

δ_L = liquid film thickness, m.

The liquid-side mass transfer coefficient for the stationary film theory k_L, is expressed by

$$k_L = \frac{D_{AB}}{\delta_L} \tag{3}$$

2.1.2 Penetration theory

The penetration theory proposed by Higbie (1935) improved the two-film theory since the most industrial processes are time-dependent. The basic presumptions of the theory are: (1) The contact time between gas and each liquid element is short so that the mass exchange takes place by unsteady-state diffusion. (2) The exposure time is the same for all fluid elements. (3) After contact, the liquid elements return back to the bulk and are replaced by the fresh ones. An illustration of this model is given in Figure 2.

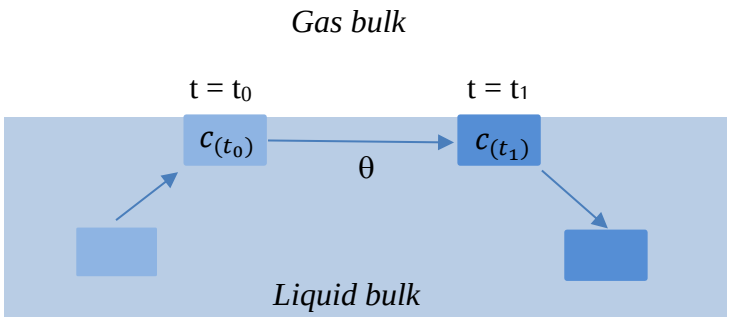

Fig. 2 Schematic of Higbie's theory.

For this instationary process, k_L turns into

$$k_L = 2\sqrt{D_{AB}/\pi\theta} \tag{4}$$

where

θ = Contact time, s.

2.1.3 Surface renewal theory

Danckwerts (1955) modified the penetration theory by assuming that the exposure times of fluid elements at the interface are non-uniform, specifically, he assumed an exponential age-distribution.

The liquid-side mass transfer coefficient depends on the surface renewal frequency *s* and the molecular diffusion coefficient D_{AB}:

$$k_{\mathrm{L}} = \sqrt{D_{AB} s} \tag{5}$$

2.1.4 Mass transfer between two phases

The molar flux in a two-phase system not at physical equilibrium describes the number of moles that pass a certain area in a certain time (Bird *et al*., 2002):

Molar flux = mass transfer coefficient × driving force

The flux of constituent *A*, in terms of the mass transfer coefficients for each phase, can be written as:

$$N_A = k_{\mathrm{G}}\left(p_{A,G} - p_{A,i}\right) = k_{\mathrm{L}}\left(c_{A,i} - c_{A,L}\right) \tag{6}$$

where

N_A = molar flux of component *A*, mol m^{-2} s^{-1}

k_{G} = gas-side mass transfer coefficient, mol m^{-2} s^{-1} Pa^{-1}

$\left(p_{A,G} - p_{A,i}\right)$ = driving force in the gas film, Pa

k_{L} = liquid-side mass transfer coefficient, m s^{-1}

$\left(c_{A,i} - c_{A,L}\right)$ = concentration driving force in liquid film, mol m^{-3}.

The volumetric mass transfer rate can be developed by multiplying equation (6) by the specific interfacial area *a*:

$$R_A = N_A \cdot a = k_L \cdot a \cdot (c_{A,i} - c_{A,L}) \quad (7)$$

where

$$a = \frac{A}{V_L} = \frac{transfer\ surface\ area}{volume\ of\ liquid}, \text{ m}^{-1}.$$

It can usually be assumed that the principal resistance to mass transfer lies in the liquid phase and the interfacial concentration $c_{A,i}$ is in equilibrium to $p_{A,i}$, *i.e.*, $c_{A,i} = p_{A,i}/H \approx p_{A,G}/H = c_L^*$ where H is Henry's constant (Fig. 1).

For the design and scale-up of multiphase bioreactors, evaluation of the overall volumetric mass transfer coefficient $k_L a$ is essential. In order to overcome the difficulties of measuring the specific interfacial area and the liquid side mass transfer coefficient, separately, the determination of $k_L a$ as one parameter is preferred.

2.1.5 Overall volumetric mass transfer coefficient

The gas absorption rate is usually characterized by the overall volumetric mass transfer coefficient which can be measured by both physical and chemical methods.

Table 1 summarizes some investigations dealing with measured $k_L a$ for gas-liquid-liquid systems in the three different type of stirred tanks: gas sparged reactors (GSR), surface-aerated reactors (SAR) and gas induced reactors (GIR).

Table 1

Literature studies on $k_L a$ in stirred tanks with emulsions.

Reference	***Gas***	***Liquid-Liquid-system***	***Reactor***	***Operating condition***
Yoshida *et al*. (1970)	O_2	Water+kerosene, paraffin/toluene/oleic acid	GSR	303 K, 200-650 rpm
Hassan and Robinson (1977)	O_2	Na_2SO_4+n-dodecane/n-hexadecane	GSR	303 K, 800-1800 rpm
Ledakowicz *et al*. (1984)	H_2, CO, N_2, CO_2	Vestowax SH105	SAR	453-553 K, 1-60 bar
Karandikar *et al*. (1987)	H_2, CO, CH_4, CO_2	Heavy fraction of Fischer-Tropsch liquid	GIR	423-498 K, 10-40 bar, 700-1200 rpm
Albal *et al*. (1988)	He, O_2	Glycerin/water+glass beads/oil shale particles/CMC	SAR	295 K, 13.8-96.5 bar, 400-1000 rpm
Miller *et al*. (1990)	H_2, CO	n-Octacosane	SAR	528 K, 10-30 bar, 250-1750 rpm
Rols and Goma (1991)	O_2	Soybean oil	GSR	308 K, 7-35 bar, 500 rpm
Hichri *et al*. (1992)	H_2	2-propanol/o-cresol/mixture ($^1/_3$ o-cresol + $^2/_3$ 2-propanol)/pyrex beads	GIR	303-393 K, 0-30 bar, 800-1500 rpm

Nocentini *et al*. (1992)	Air	Water+glycerol	GSR	Ambient condition, 500 rpm
Hsu *et al*. (1997)	O_3	Water	GIR	298 K, 500-1600 rpm
Inga and Morsi (1997)	H_2, CO, N_2, CH_4, C_2H_4	Hexane mixture/iron oxide catalyst	SAR	298-373 K, 2-25 bar, 400-1200 rpm
Lekhal *et al*. (1997)	H_2, CO	1-octane/ethanol/water	GIR	323 K, 10-150 bar, 1100-2500 rpm
Tekie *et al.* (1997)	N_2, O_2	Cyclohexane	GIR SAR	330-430K, 7-35 bar, 400-1200 rpm
Kierzkowska-Pawlak and Zarzycki (2000)	CO_2	Water + toluene	SAR	293 K, 400-600 rpm
Maalej *et al*. (2001)	N_2	Water	GSR	328-428 K, 1-50 bar, 800-1200 rpm
Hsu *et al*. (2002)	O_3	Water	GIR	293-313K, 1-1.2 bar, 900-1300 rpm
Kluytmans *et al*. (2003)	O_2	Water, electrolyte(sodium gluconate)+carbon particles	SAR GIR	298K, 500-1500 rpm

Nielsen *et al*. (2003)	O_2	Alcaligenes xylosoxidans+n-hexadecane	GSR	303 K, 200-800 rpm
Sardeing *et al*. (2004a)	O_2	Tap water	GSR	Ambient condition, 300-500 rpm
Kapic and Heindel (2006)	O_2	Water	GSR	298 K, 200-800 rpm
Martín *et al*. (2008a)	O_2	Deionized water	GSR	293 K, 180-430 rpm
Zhang *et al*. (2010)	CO_2	Water+n-heptane/dimethylbenzene/ isoamyl alcohol	GSR	293 K, 0.2 bar, 250-650 rpm
Ngo and Schumpe (2012a, b)	CO_2, O_2	Water+n-heptane/n-dodecane/n-hexadecane	SAR	298 K, 1000 rpm
Sauid *et al*. (2013)	O_2	Xanthan gum solution+palm oil	GSR	303 K, 400-800 rpm
Zokaei-Kadijani *et al*. (2013)	O_2	Acidthiobacillus ferrooxidans	GSR	298 K, 400-600 rpm
de Lamotte *et al*. (2017)	O_2	Tap water	SAR	293 K, 300 rpm

From the above table, it is clear that the volumetric mass transfer coefficient for gas absorption depends on stirred reactor configuration, stirrer speed, temperature, type of gas and solution or emulsion characteristics (viscosity, density and interfacial tension).

2.2 Chemical Absorption

2.2.1 Introduction

The knowledge of the liquid-side mass transfer coefficient k_L, the specific interfacial area a, and the gas holdup ε, are of considerable importance for design and scale-up of gas-liquid contactors (Stegeman *et al*. 1995). Kawase and Moo-Young. (1992) and Vázquez *et al.* (2000) observed that the variation in absorption rate is mainly due to variation in specific interfacial area, as the liquid-side mass transfer coefficient is not as changeable. Therefore, to understand the mass transfer mechanism, it is important to evaluate the specific interfacial area.

The kind of contact devices, the physical and chemical properties of gas-liquid systems and the operating conditions may affect the value of interfacial area. The experimental methods for specific interfacial area determination can be classified as physical methods and chemical methods.

Physical methods are based on the separate measurements of gas holdup and bubble diameter, *e.g.*, optical detectors (Schweitzer *et al.*, 2001), conductivity sensors (Bińi *et al.*, 2001), gas disengagement (Lee *et al.*, 1999) or video imaging (Akita and Yoshida, 1974; Luewisutthichat *et al.*, 1997). Light transmission technique was the first attempt to measure a in gas-liquid systems (Vermeulen *et al.*, 1955) and then this method was extended for organic liquids and water by Calderbank (1958). According to Cents *et al.* (2001) these techniques can be inaccurate because of difficulty to use laser and photographic methods in the cloudy liquids and also due to complex calibration.

The chemical methods are based on measuring the gas or liquid phase conversion for a chemical reaction of known kinetics. Unfortunately, the chemical methods can only be used for certain gas-liquid systems with specific physico-chemical properties (Oyevaar and Westerterp, 1989; Vázquez *et al.*, 2000). O_2/sodium sulfite, O_2/sodium dithionite and CO_2/aqueous NaOH are typical examples of chemical reaction systems.

2.2.2 An overview of the chemical absorption method

Chemical reaction between the dissolved gas and a reactant in the liquid phase may increase the gas absorption rate. In the liquid, an irreversible reaction takes place between a gas component *A* and reactant *B*:

$$A + zB \rightarrow Products \tag{8}$$

It is assumed that this reaction is fast enough to occur entirely in the film so that the bulk concentration of component *A* is zero. Still, the concentration of *B* at the interface shall be practically the same as in the bulk liquid. The gas side resistance is negligible so that all resistance to mass transfer is confined to the liquid phase (Oyevaar and Westerterp, 1989).

The above reaction is *m*th order with respect to *A* and *n*th order with respect to *B* so that the local rate of reaction as follows:

$$r_A = k_{m,n} c_A^m c_B^n \tag{9}$$

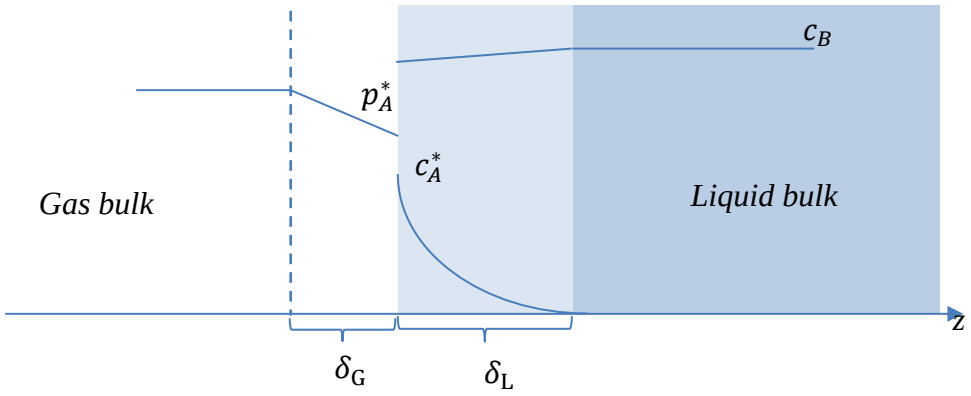

Fig. 3 Schematic of fast reaction.

Generally, the absorption rate of reactant *A* under these conditions is given by

$$R_A = a c_A^* \sqrt{\frac{2}{m+1} D_A k_{m,n} {c_A^*}^{m-1} {c_{B,0}}^n} \tag{10}$$

where

R_A = absorption rate, mol m^{-3} s^{-1}

a = specific interfacial area, m^{-1}

c_A^* = c_A in equilibrium with gas phase, mol m^{-3}

D_A = diffusivity of *A* in liquid phase, m^2 s^{-1}

k_{mn} = rate constant of m+n order reaction, (mol m^{-3})$^{1-(m+n)}$ s^{-1}

$c_{B,0}$ = bulk concentration of *B*, mol m^{-3}.

The rate equation can be simplified by introducing an absorption parameter K_m (Schumpe and Deckwer, 1980):

$$R_A = a K_m P_A^{(m+1)/2} \tag{11}$$

where

$$K_m = \sqrt{\frac{2}{m+1} \frac{D_A k_m}{(H)^{m+1}}} \tag{12}$$

$$k_m = k_{m,n} {c_{B,0}}^n \tag{13}$$

The k_m value is a function of catalyst ion concentration, pH and temperature.

The equations above are valid only at sufficiently high Hatta (Ha) number which means the reaction is fast and occurs in the film volume only:

$$Ha = \frac{\sqrt{\frac{2}{m+1} D_A k_m c_A^{*m-1}}}{k_\mathrm{L}} > 3 \tag{14}$$

Additionally, depletion of the liquid phase reactant towards the G/L interface has to be negligible. This is granted if the following condition holds:

$$Ha \ll 1 + \frac{D_B c_{B,0}}{z D_A c_A^*} \tag{15}$$

2.2.3 Sodium sulfite oxidation

The sodium sulfite oxidation is one of the standard and reliable methods for determining mass transfer characteristics in different gas-liquid contactors such as stirred vessels (Camacho *et al.*, 1991), bubble columns and packed bed reactors (Danckwerts and Rizvi, 1971; Onda *et al*., 1972).

This method, first presented by Cooper *et al.* (1944), is based on the reduction of sodium sulfite (*B*) to sulfate by dissolved oxygen (*A*):

$$O_2 + 2Na_2SO_3 \rightarrow 2Na_2SO_4 \tag{16}$$

The rate of reaction is given as

$$(-r_{O_2}) = k_{m,n}[O_2]^m[SO_3^{2-}]^n \tag{17}$$

The rate of this slow reaction can be increased by the addition of metallic ions like Co^{2+}, Fe^{2+} and Cu^{2+} which form complexes with the sulfite or sulfate ions present in the solution (Linek and Vacek, 1981). Cobalt sulfate ($CoSO_4$) has been mostly used in recent studies as the catalyst, because its action is more reproducible, effective and reliable than copper sulfate ($CuSO_4$) (de Waal and Okeson, 1966).

The sulfite ions oxidation sequence was originally developed by Bäckström (1934). For the reaction with cobaltous ions, a free radical chain mechanism is assumed according to

$$SO_3^{2-} + Co^{3+} \overset{k_1}{\rightarrow} Co^{2+} + \cdot SO_3^- \quad (18)$$

$$\cdot SO_3^- + O_2 \overset{k_2}{\rightarrow} \cdot SO_5^- \quad (19)$$

$$\cdot SO_5^- + SO_3^{2-} \overset{k_3}{\rightarrow} SO_5^{2-} + \cdot SO_3^- \quad (20)$$

$$SO_5^{2-} + SO_3^{2-} \overset{k4}{\rightarrow} 2SO_4^{2-} \quad (21)$$

The role of the catalytic cations is to separate an electron from sulfite ions, produce active centers and stabilize these radicals (Chen and Barron, 1972).

Although the kinetics of the uncatalyzed (Yagi and Inoue, 1962; Srivastava *et al.*, 1968; Hui and Palmer, 1990) and catalyzed (Sivaji and Murty, 1982; Zhao *et al*., 2005; Karatza *et al*., 2010) sodium sulfite oxidation has been studied widely during last decades, it is still not well understood. There is a disagreement on the order of reaction with respect to oxygen which changes with sulfite concentration and also with oxygen partial pressure. Sivaji and Murty (1982) found the catalyzed reaction is second order in oxygen when sulfite concentration is 0.39 M and first order when it is 0.15 M. According to Alper and Abu-sharkh (1988), the reaction is second order with respect to oxygen and is independent of sulfite concentration for the temperature range of 298-313 K and at atmospheric pressure. All in all, the catalyzed reaction is zero-order in sulfite when sulfite concentration is greater than 0.5 M, zero-order in oxygen when the sulfite concentration is 0.06 M, first-order when it is 0.25 M, and second-order when it is 0.25-1 M (Astarita *et al*., 1964; Vázquez *et al*., 2000). Nevertheless, advantages such as harmless and cheap chemicals have led to the frequent use of sulfite oxidation technique for determining specific interfacial area by chemical absorption.

2.3 Liquid-Liquid Systems

The great majority of industrial reactions are carried out in two or more phases, including gases, liquids and/or solids. The phases can be applied as the source or storage of reactants, catalyst for the reactions or improving mixing or transport processes in the reactor.

Liquid-liquid dispersions have been the objects of many investigations dealing with emulsification and multiphase reactions. As can be seen in Figure 4, in a liquid-liquid system, *i.e.*, oil-in-water emulsion, when the agitation of the stirrer starts with enough mixing energy, the dispersed phase is introduced into the continuous phase (Carlucci, 2010).

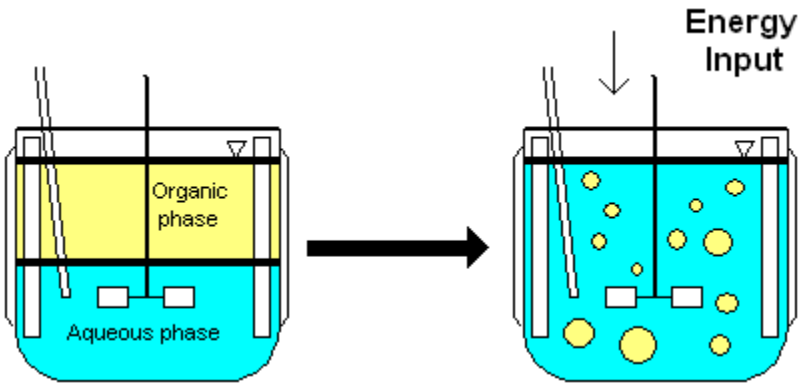

Fig. 4 Organic phase dispersion into media under agitation.

The drop breakage and coalescence of the dispersed phase during stirring plays an essential role in gas-liquid-liquid mass transfer enhancement in stirred tanks (Fig. 5). There have been different approaches based on these phenomena reported in the literature to explain the mass transfer mechanism.

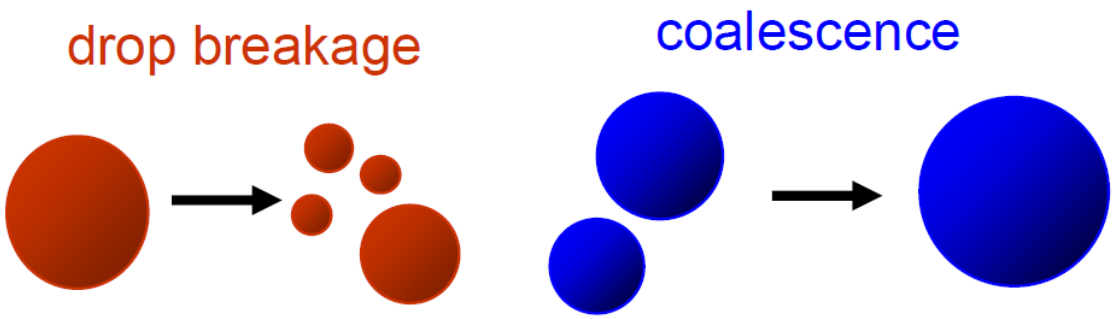

Fig. 5 Representation of drop breakage and coalescence.

In recent years, researchers attempted to understand and explain the mechanism of mass transfer from the gas phase to the liquid phase in order to reduce mass transfer barriers and improve mass transfer. By exploring the effect of some mass transfer enhancing agents, more insight into the mechanism of mass transfer may be obtained (Das *et al.*, 1985; Cents *et al.*, 2001; Ngo and Schumpe, 2012a, b). The presence of a third phase, either small solid particles (*e.g.*, activated carbon) or a second liquid phase (*e.g.*, organic solvent), dispersed in a gas-liquid system may enhance the mass transfer rate of gas into the continuous liquid phase (Rols *et al.*, 1990), retard it (Yoshida *et al.*, 1970) or have no effect (Cents *et al.*, 2001).

2.4 Stirred Tank Reactors

Stirred vessels are applied for dispersing solids, liquids and gases into liquids. The purpose of the stirrer in mass transfer operations is to disperse gas effectively in order to promote contact between gas and liquid phase.

2.4.1 Axial flow impellers

Axial flow impellers cause the fluid to flow parallel to the blade along the axis of the rotating shaft. They generate an up and down flow pattern, useful in blending two or more liquids. The axial flow impellers are introduced to replace radial flow impellers because

of lower power numbers which makes them ideal for better gas dispersion and improved axial mixing. McFarlane *et al*. (1995) discussed that the axial flow impellers provide high gas handling capacity and excellent top-to-bottom mixing over radial disc turbines which have traditionally been used for gas-liquid processes (Fig. 6).

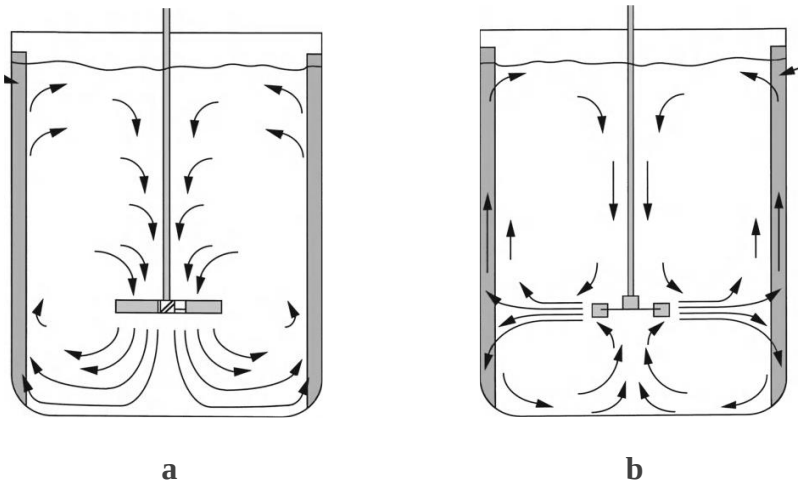

Fig. 6 Flow Pattern generated by (a) axial and (b) radial flow impellers (McFarlane *et al*., 1995).

2.4.2 Comparison of down- and up-pumping impeller

The axial flow impellers produce an excellent top to bottom motion. The pitched blade turbine (PBT) is the most popular axial flow impeller. Examples of down- and upward pitched blade impellers are shown in Fig. 7.

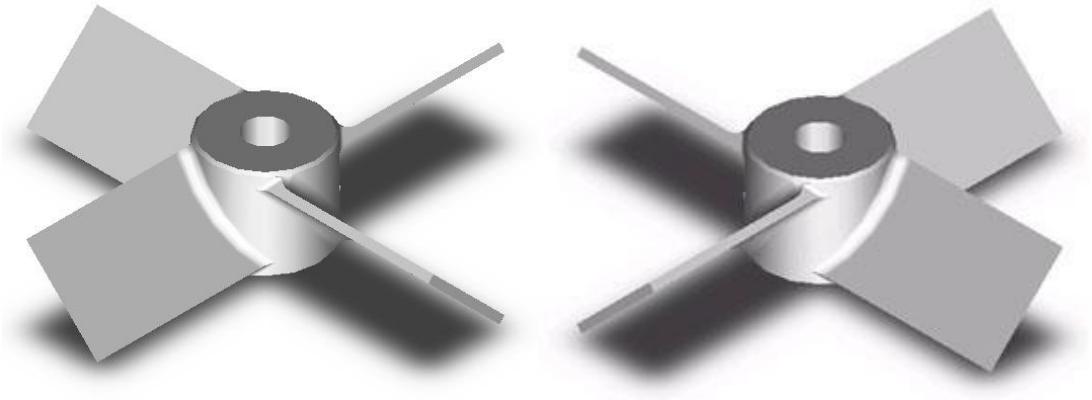

a **b**

Fig. 7 PBT axial flow impellers: a) downward; b) upward for clockwise motion.

- Down-pumping mode: The impeller is rotated so that the blades push the fluid down towards the bottom of the vessel.
- Up-pumping mode: The impeller will push fluid in an upward manner towards the top of the vessel.

The axial impellers in the up-pumping mode have shown better performance over the down-pumping axial flow impellers when aerated (Nienow, 1990; Sardeing *et al.*, 2004b). Sardeing *et al.* (2004b) evaluated the volumetric mass transfer coefficient and gas holdup for a down- and up-pumping pitched blade turbine and then compared with two radial impellers. Tap water was used as the working fluid and air was fed into the tank via a ring sparger. They concluded that the up-pumping turbines give superior performance in gas handling capacity, gas holdup capacity and gas–liquid mass transfer than down-pumping impellers. However, many think this to be paradoxical because intuitively the down-pumping mode appears to be more beneficial than the up-pumping mode for dispersing gas (Khopkar *et al.*, 2003).

Although the investigations of axial flow agitators have been focused on power characteristics, mixing times, turbulent flow patterns (Hari-Prajitno *et al.*, 1998; Jaworski and Dyster, 2001; Özcan-Taşkin and Wei, 2003) and their mass transfer potential under aeration (Sardeing *et al.*, 2004b), no studies have been carried out to compare the surface

aerated up- and down-pumping performance with respect to the mass transfer parameters and gas solubility for oil in water emulsions. In this work, based on the published data by Ngo and Schumpe (2012a), a comparison of the down-pumping with the up-pumping impeller is made.

2.5 Surfactants

2.5.1 Definition of surfactants

Surfactants (emulsifiers, wetting agents, tensides, detergents and etc.) are widely used active substances which are able to reduce the surface and the interfacial tension. Table 2 represents some applications of surfactants in the chemical industry.

Table 2

Summary of surfactant applications in the chemical industry (Schramm and Marangoni, 2000).

Gas/liquid systems	*Liquid/liquid systems*	*Liquid/solid systems*
Oil flotation process froth	Emulsion drilling fluids	Reservoir wettability modifiers
Gas-mobility control foams	Heavy oil pipeline emulsions	Tank/vessel sludge dispersants
Blocking and diverting foams	Fuel oil emulsions	Drilling mud dispersants

Amphiphilic or amphipathic substances consist of two parts: one part that exhibits a strong affinity for nonpolar media (hydrophobic group) and one part that has an attraction for polar media, particularly water (hydrophilic group). Because of its dual affinity, these molecules tend to migrate to interfaces so that the hydrophilic group is placed in water and the hydrophobic group lies in oil. They show superficial and interfacial activity and they lower the surface tension of a liquid and the interfacial tension between two liquids (Schramm and Marangoni, 2000).

2.5.2 Classification and application of surfactants

When water, oil and a surfactant come into contact, the surfactant adsorbs at the water-oil interface. The polar head group favours water, while the hydrophobic chain (or tail) favours oil (Mishra *et al*., 2009).

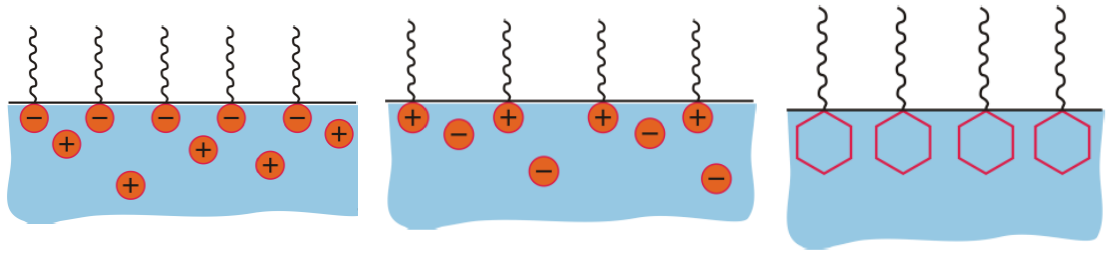

Fig. 8 Head and tail orientation of surfactants (Denkov and Tcholakova, 2010).

There are many kinds of surfactants, and they are classified by use, properties and chemical structure. The most accepted classification of surfactants is based on the nature of the polar head (hydrophilic) group, as illustrated in Figure 8 and Table 3.

Table 3

Surfactants classification (Schramm and Marangoni, 2000).

Class	***Name***	***structures***
Anionic	Na dodecyl sulfate	$CH_3(CH_2)_{11}SO_4^-Na^+$
	Na dodecyl benzene sulfonate	$CH_3(CH_2)_{11}C_6H_4SO_3^-Na^+$
Cationic	Laurylamine hydrochloride	$CH_3(CH_2)_{11}NH_3^+Cl^-$
	Cetyl trimethylammonium bromide	$CH_3(CH_2)_{15}N^+(CH_3)^3Br^-$
Nonionic	Polyoxyethylene alcohol	$C_nH_{2n+1}(OCH_2CH_2)_mOH$
	Alkylphenol ethoxylate	C_9H_{19}-C_6H_4-$(OCH_2CH_2)_nOH$

In general, surfactants have been classified based on their dissociation in water:

- ***Anionic surfactants*: negatively charged**

They are the earliest development and the largest group of surfactants for the household industry, *e.g*., laundering, dishwashing agents and shampoos, because of their excellent cleaning properties. They are also used as foaming agents, emulsifiers and stabilizers. The anionic groups mainly include alkyl sulfates, sulfonates or carboxylate (Morelli and Szajer, 2000).

- ***Cationic surfactants*: positively charged**

Because of their good bactericidal properties, cationic surfactants are widely used for sterilization and cleansing wounds or burns (Morelli and Szajer, 2000).

- ***Nonionic surfactants*: uncharged**

Hydrophilic groups do not ionize in the solution. They have wide application in drug delivery, petroleum, food, textile, glass industries and to produce nano-emulsions (Posocco *et al*., 2016).

2.5.3 Surfactant-stabilized oil/water emulsions

Surface tension plays an important role in mass transfer processes such as distillation, absorption and desorption. The mass transfer rate can be affected by interfacial tension gradient as a result of presence of surfactants. The addition of small amounts of surfactants can significantly decrease surface or interfacial tension between two immiscible liquids. Surfactants with hydrophilic and hydrophobic properties will tend to migrate towards the oil–water interface, even at low concentrations. The interfacial tension is reduced by accumulation at the interface of two liquids and coalescence of the dispersed phase is inhibited (Asgharpour *et al*., 2010). Above the critical micelle concentration (CMC) the surface tension remains almost constant (Rosu and Schumpe, 2006; García-Abuín *et al*., 2010).

2.6 Literature Review

Previous researchers on mass transfer into emulsions have reported rather contradictory results. Some investigations dealing with gas-liquid-liquid systems are briefly reviewed in the following section.

2.6.1 Effects of a dispersed liquid phase on oxygen transfer

One of the first attempts to study gas absorption into oil-in-water emulsion was made by Yoshida *et al*. (1970). They investigated the volumetric coefficient of oxygen transfer into water with the addition of kerosene, liquid paraffin, toluene or oleic acid as the dispersed phase in a bubble column and a gas-liquid agitator. They found that non-spreading ($S_{OW} < 0$) oil like n-paraffin and kerosene inhibit gas transfer, presumably, because of partial occupation of the bubble surface by beading oil droplets. In toluene- and oleic acid-water systems with positive spreading coefficient, $k_L a$ initially decreases and then increases. This sharp reduction might be attributed to increased liquid phase resistance due to spreading oil as a thin film on the gas-liquid interface. Linek and Beneš (1976) also used the spreading coefficient concept to explain some unusual mass transfer behavior.

Surprisingly, Hassan and Robinson (1977) reported air-to-aqueous phase $k_L a$ in a stirred tank increased in an emulsion with negative spreading coefficient (n-hexadecane) but decreased for positive spreading coefficient (n-dodecane).

The effect of soybean oil on oxygen transfer in a fermentor was evaluated by Rols and Goma (1991). They concluded that the cause of enhancement in oxygen transfer rate was the layering of the oil phase as a thin film at the gas liquid interface. Similar results were reported by Sauid *et al*. (2013) for palm oil in xanthan gum solutions in a stirred tank. They suggested that oil with high positive spreading coefficient (S = 38.3 mN/m) tends to spread on the bubble surface and lead to lower bubble size and higher interfacial area.

Mass transfer enhancement in a bubble column in the presence of seven different immiscible organic liquids dispersed as droplets was measured by Kundu *et al*. (2003).

Adittion of n-decane, dodecane and n-heptane significantly enhanced mass transfer whereas toluene, anisole and 2-ethyl-1-hexanol hindered mass transfer.

Ngo and Schumpe (2012b) found that $k_L a$ exhibits an initial rapid increase at very low oil fraction (n-dodecane and n-hexadecane) then decreases towards the phase inversion region. n-Heptane emulsions always showed higher $k_L a$ values compared to the pure water. They concluded that this increase might be caused by a bubble covering mechanism enabled by the high spreading coefficient.

Table 4

Reported effects of dispersed organic liquids on oxygen transfer.

Dispersed phase	φ_O,%	$S_{O/W}$[a]	k_La[b]	k_L	*Authors*
n-Paraffin	0-20	-	↘		Yoshida *et al*. (1970)
Kerosene					
Toluene		+	↘↗		
Oleic acid					
Oleic acid	0-100	+	↘↗	↘↗	Linek and Beneš (1976)
n-Alkanes		-	→↗	→↗	
n-Dodecane	0-10	+	↘↗		Hassan and Robinson (1977)
n-Hexadecane		-	↗→		
Soybean oil	0-30	+	↗↘		Rols and Goma (1991)
n-Decane	0-10		↗		Kundu *et al*. (2003)
n-Dodecane					
n-Heptane					
Toluene			↘		
Anisole					
2-Ethyl-1-hexanol					
n-Dodecane	0-60	+	↗↘		Ngo and Schumpe (2012b)
n-Hexadecane					
n-Heptane		+	↗		
Palm oil	0-50	+	↗↘		Sauid *et al*. (2013)

a) Spreading coefficient (cf. §3.3); b) Trend with increasing oil volume fraction.

2.6.2 Effects of a dispersed liquid phase on carbon dioxide transfer

This section is devoted to reviewing the literature on carbon dioxide absorption into different liquid-liquid systems.

Kierzkowska and Zarzycki (2000) used a mechanically agitated vessel to determine the volumetric mass transfer coefficient for CO_2 in toluene/water system. The oil fraction ranged from 1 to 20 vol% and the stirring rate varied from 400-600 min^{-1}. The experiments were carried out in semi batch condition under constant pressure in the reactor. They observed that k_La increased with increasing toluene volume fraction, presumably, due to gas-liquid interface covering by a toluene layer with higher gas solubility than the continuous phase.

Cents *et al*. (2001) measured k_La, the liquid side mass transfer coefficient k_L and the specific international area a simultaneously by the Danckwerts-plot technique. They applied toluene, n-dodecane, n-heptane and 1-octanol as dispersed phases. The initial decrease in k_La on the addition of four dispersed phases was observed. However, they discussed the initial effect should not be considered to make a comparison at higher oil phase fraction. They observed that the addition of toluene and 1-octanol the buffer solutions caused an increase in mass transfer rate while n-dodecane and n-heptane retarded mass transfer.

Zhang *et al*. (2010) studied the carbon dioxide mass transfer in the presence of n-heptane, dimethylbenzene and isoamyl alcohol (0-5%) in a stirred tank reactor. They observed that k_La increased up to a maximum at 3% oil volume fraction and then decreased. They claimed dispersed phase droplets accumulation on the water surface causing the liquid-side mass transfer coefficient and the gas-liquid interfacial area to decrease.

In contrast, Ngo and Schumpe (2012a), found that k_La exhibits an initial rapid increase at very low oil fraction (n-dodecane and n-hexadecane) and then decreases towards the phase inversion region. n-Heptane emulsions always showed higher k_La values compared to pure water. They concluded that this increase might be caused by a bubble covering mechanism enabled by the high spreading coefficient.

Table 5

Reported effects of dispersed organic liquids on carbon dioxide transfer.

Dispersed phase	φ_O,%	$S_{O/W}$[a]	k_La[b]	k_L[b]	a[b]	*Authors*
Toluene	0-20		↗			Kierzkowska and zarzycki (2000)
n-Heptane	0-40		↘	→	↘	Cents *et al*. (2001)
n-Dodecane			↗	↗	↘	
Toluene			↗	↗	↘	
1-Octanol			↗	↗	↘	
n-Heptane	0-5		↗↘	↗↘		Zhang *et al*. (2010)
Dimethylbenzene			↗↘	↗↘		
Isoamyl alcohol			↗↘	↗↘		
n-Dodecane	0-60	+	↗↘			Ngo and Schumpe (2012a)
n-Hexadecane		+	↗↘			
n-Heptane		+	↗			

a) Spreading coefficient (cf. §3.3); b) Trend with increasing oil volume fraction.

2.6.3 Effects of surfactants on mass transfer

Yoshida *et al*. (1970) showed that the addition of a small amount of Tween 85 causes an initial sharp decrease in overall volumetric mass transfer coefficient of oxygen in water in the agitated vessel. This was interpreted as a result of increasing liquid phase resistance due to accumulation of surfactants on the gas-liquid interface. In contrast, k_La at low volume fractions of kerosene in the presence of surfactant first increases and then decreases slightly with increasing fraction of kerosene.

Painmanakul *et al*. (2005) investigated the effect of an anionic surfactant (Sodium laurylsulfate) and a cationic surfactant (Lauryl dimethyl benzyl ammonium bromine) on the mass transfer parameters in a bubble column with a single orifice as gas sparger. They

found that the interfacial areas in surfactant solutions are larger than those in water and the volumetric- and liquid side mass transfer coefficients are smaller than those of water. They deduced that the presence of surfactant at the gas-liquid interface disturbs the mass transfer by modifying the liquid film thickness around the gas bubbles.

Gómez-Díaz *et al*. (2009) applied a photographic method and a slip velocity model in a bubble column reactor to study mass transfer parameters of carbon dioxide absorption in water. An initial increase in the liquid-side mass transfer coefficient was obtained at low decyltrimethylammonium bromide (DTABr) concentrations. This was attributed to interfacial turbulence in the liquid film due to surface tension gradients. They postulated that this behavior could be generalized for a great part of the surfactants of different types. Presence of a low concentration of surfactant caused a decreased in the value of the interfacial area.

Asgharpour *et al.* (2010) studied the absorption of oxygen in different emulsions with surfactants in a bubble column. They observed that k_La increases with increasing concentration of hydrocarbons. The presence of oil droplets in the liquid film around the gas bubbles was claimed to cause reduction of bubble coalescence. The presence of surfactant increased the mass transfer rate by increasing the coalescence-inhibiting tendency while the k_L values remained roughly constant.

Chen *et al*. (2013) used a fine bubble aeration system to study the effects of different surfactant types on oxygen absorption in an organic glass cube vessel. They compared the influence of four different anionic, cationic and nonionic surfactants on k_La, k_L and a. They observed that, with the addition of surfactants, the specific interfacial areas are larger than those in clean water while increase in the surfactant concentration leads to decrease in k_La and k_L.

Table 6

Effects of surface active agents on the mass transfer parameters reported in the literature.

Surfactants		k_La	k_L	a	*Authors*
Tween 85	Water / Water+kerosene	↘↗			Yoshida *et al*. (1976)
SDS[a] **LDBABr**[b]	Water	↘	↘	↗	Painmanakul *et al*. (2005)
DTABr	Water	↗	↗↘	↗	Gómez-Díaz *et al*. (2009)
SDS	Water / Water+n-tridecane	↗	→	↗	Asgharpour *et al*. (2010)
SDS **SDBS**[c] **CTAB**[d] **Tween 20**	Water	↘	↘	↗	Chen *et al*. (2013)

a) Sodium dodecyl sulfate; b) Lauryl dimethyl benzyl ammonium bromine; c) Sodium dodecyl benzene sulfonate; d) Dodecyltrimethylammonium bromide.

2.6.4 Mass transfer with chemical reaction

The reaction between CO_2 and aqueous alkanolamine solutions was introduced by Danckwerts and Sharma (1966) as a model system for the determination of mass transfer parameters. Vázquez *et al*. (2000) determined the interfacial area by different chemical methods: Danckwerts method for absorption of carbon dioxide in carbonate buffer solutions and sulfite or dithionite oxidation. They also studied the influence of the anionic surfactant SDS on interfacial area.

Most attempts have been made to observe the dependence of the specific interfacial area on the gas velocity in the bubble columns and stirred reactors. A few investigations have been presented in the literature on the effect of organic liquid phase fraction on the chemically determined specific interfacial area.

Mehta and Sharma (1971) observed an increase in interfacial area in a stirred vessel upon addition of 2-ethyl hexanol as an organic liquid into the NaOH solution. They concluded that the initial increase in interfacial area with increasing oil volume fraction could be due to CO_2 transfer to the aqueous phase through the organic droplets (series pathway) and/or reduced coalescence of gas bubbles by presence of small oil droplets.

An investigation was done by Das *et al*. (1985) to study the effect of toluene on the interfacial area in a stirred vessel. They used the chemical absorption of CO_2 in NaOH solution and physical methods such as bubble size and gas hold-up measurements. Although the methods showed different values, similar trends were observed: The interfacial area increased initially with increase in oil fraction up to a maximum value and then decreased.

Schumpe and Deckwer (1980) reviewed literature data for bubble column reactor comprehensively to compare interfacial area values $a_{\text{chem.}}$ obtained from sulfite oxidation and CO_2 absorption into alkali solutions. The interfacial area obtained from sulfite oxidation method showed higher value even for the same reactors. Generally, because of the diversity of the bubble sizes, the geometrical specific interfacial area $a_{\text{geo.}}$ is larger than $a_{\text{chem.}}$.

Cents *et al*. (2001) studied CO_2 chemical absorption into a carbonate buffer solution in the presence of dispersed organic liquids, using the Danckwerts-plot technique in order to determine the liquid side mass transfer coefficient and the interfacial area simultaneously. They observed that the addition of n-heptane and n-dodecane caused a reduction in mass transfer rate while the presence of toluene and 1-octanol enhanced mass transfer. The liquid side mass transfer coefficient remained constant when n-heptane and n-dodecane were added to the buffer solutions. The addition of toluene and 1-octanol caused an increase in k_L. The interfacial area decreased with the addition of dispersed organic liquids.

Reported results in the literature reveal that there is a lot of contradiction about the gas absorption mechanism in the presence of second immiscible liquid. By studying mass transfer parameters separately, more insight on the gas-liquid-liquid systems may be obtained.

Chapter 3

Emulsion Morphology and Phase Inversion

3.1 Viscosity

Bubble coalescence, mass transfer characteristics, liquid film behavior and hydrodynamic parameters are affected by liquid properties such as viscosity, density and surface tension. The influence of liquid properties on the boundary layer thickness, interfacial surface properties and liquid-phase mass transfer coefficient was studied by Worden and Bredwell (1998).

Viscosity has a strong effect on the bubble breakup and coalescence. Increasing viscosity leads to suppress the bubbles breakup and promote coalescence (Martín *et al.*, 2008b). Bigger bubbles have smaller specific interfacial area and increasing mass transfer resistance is offered by the liquid film with increasing viscosity. According to the reported results the liquid side mass transfer coefficient, the specific interfacial area and finally the volumetric mass transfer coefficient decrease as the viscosity increases (Fujasová, *et al.*, 2007; Linek *et al.*, 2004).

For emulsions, various models for calculating mixture viscosity were suggested (Taylor, 1932; Vermeulen *et al*., 1955; Laity and Trebal, 1957; Barnea and Mizrahi, 1976; Bedeaux, 1983). The Vermeulen *et al*. (1955) expression was found in good agreement with reported experimental results (Guilinger *et al*., 1988). In this study, the Vermeulen (1955) relation (Eq. 22) was used for calculating the viscosities of the two types of dispersions, water continuous and oil continuous.

$$\mu_m = \frac{\mu_{cont.}}{1-\varphi_{disp.}}\left(1+\frac{1.5\varphi_{disp.}\mu_{disp.}}{\mu_{disp.}+\mu_{cont.}}\right) \tag{22}$$

where

μ_m = mixture viscosity, Pa s

$\varphi_{disp.}$ = dispersed phase volume fraction, -

$\mu_{disp.}$ = dispersed phase viscosity, Pa s

$\mu_{cont.}$ = continuous phase viscosity, Pa s.

Figure 9 illustrates the viscosity variation based on the oil volume fraction in n-hexadecane, n-dodecane and n-heptane emulsions.

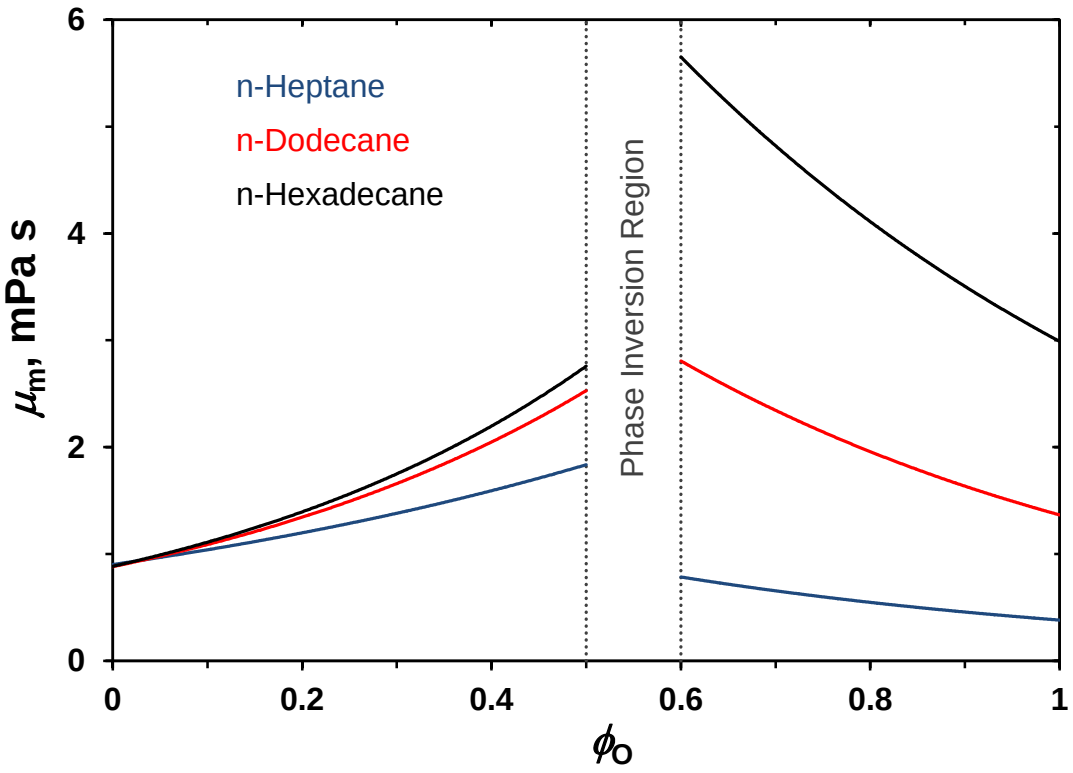

Fig. 9 Viscosity as function of oil volume fraction (Eq. 22).

For all emulsion systems, the viscosity increases with an increase in the dispersed phase volume fraction. For n-hexadecane and n-heptane, the emulsion viscosity changes drastically upon phase inversion.

Some other relations suggested in the literature imply stronger effects of the dispersed phase volume fraction. These models are compared to the Vermeulen *et al*. (1955) relation in Figure 10.

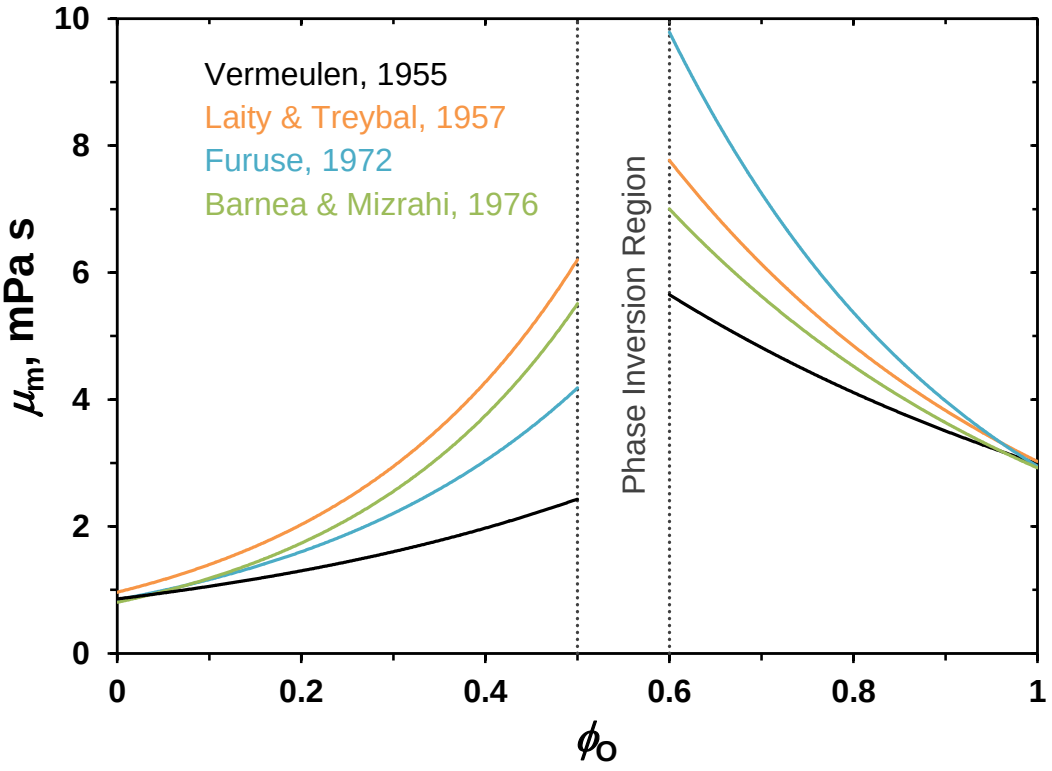

Fig. 10 Comparison of viscosity models for n-hexadecane emulsions (Vermeulen *et al*., 1955; Laity and Treybal, 1957; Furuse, 1972; Barnea and Mizrahi, 1976).

3.2 Phase Inversion

Two types of dispersions can be distinguished: oil-in-water (O/W) where oil drops form the dispersed phase in water as the continuous phase and water-in-oil (W/O) where oil is the continuous phase.

Phase inversion refers to a complex phenomenon when an interchange occurs between the dispersed and the continuous liquid phase. Under steady-state conditions the droplet

distribution in an O/W dispersion follows a dynamic balance between drop breakup and coalescence. An increase of the oil phase volume fraction increases both the coalescence and the drop breakup rate as more oil drops pass through the impeller region. With increasing oil fraction, the coalescence rate increases faster than the breakup rate and the droplets will grow in size. At very high dispersed phase fraction, the coalescence rate overwhelms the breakup rate, leads to phase inversion and another dynamic equilibrium of breakage and coalescence of the water droplets (Hu *et al*., 2005).

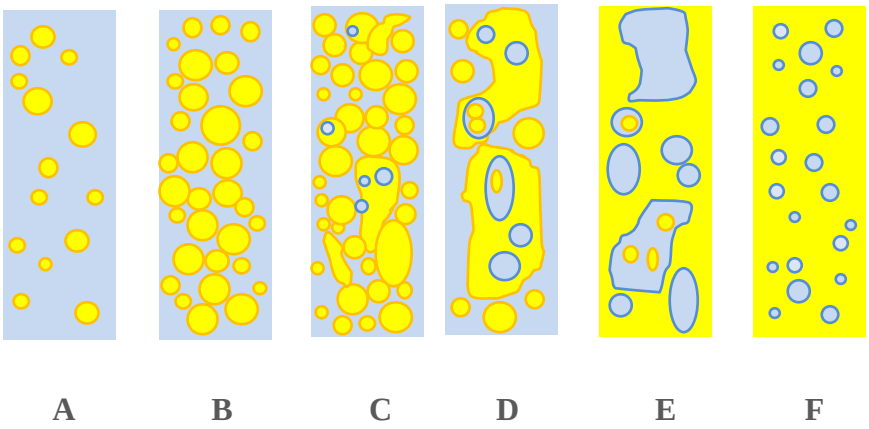

Fig. 11 Transition of oil-in-water to water-in-oil emulsion (Hu and Angeli, 2006).

A schematic diagram of the transition O/W to W/O is shown in Figure 11. In the O/W dispersion at low oil fractions, there are small spherical oil droplets in the water continuous phase (graph A). As the volume fraction of oil increases, the droplets will be more closely packed, tend to coalesce and form larger drops (graph B and C). With further increase of the dispersed oil fraction, the phase change from oil-in-water to water-in-oil will take place within the transitional region (graph D and E). After complete phase inversion, a water-in-oil dispersion is formed (graph F).

The evolution of Sauter mean diameter during an inversion from O/W to W/O is illustrated in Figure 12 by Vaessen (1996). They detected the phase inversion region for hexane-in-water emulsions in the stirred vessel at the speed of 1500 rpm. From this figure, it can be observed that with increasing dispersed phase volume fraction the Sauter mean diameter first goes up and drops dramatically at the inversion point.

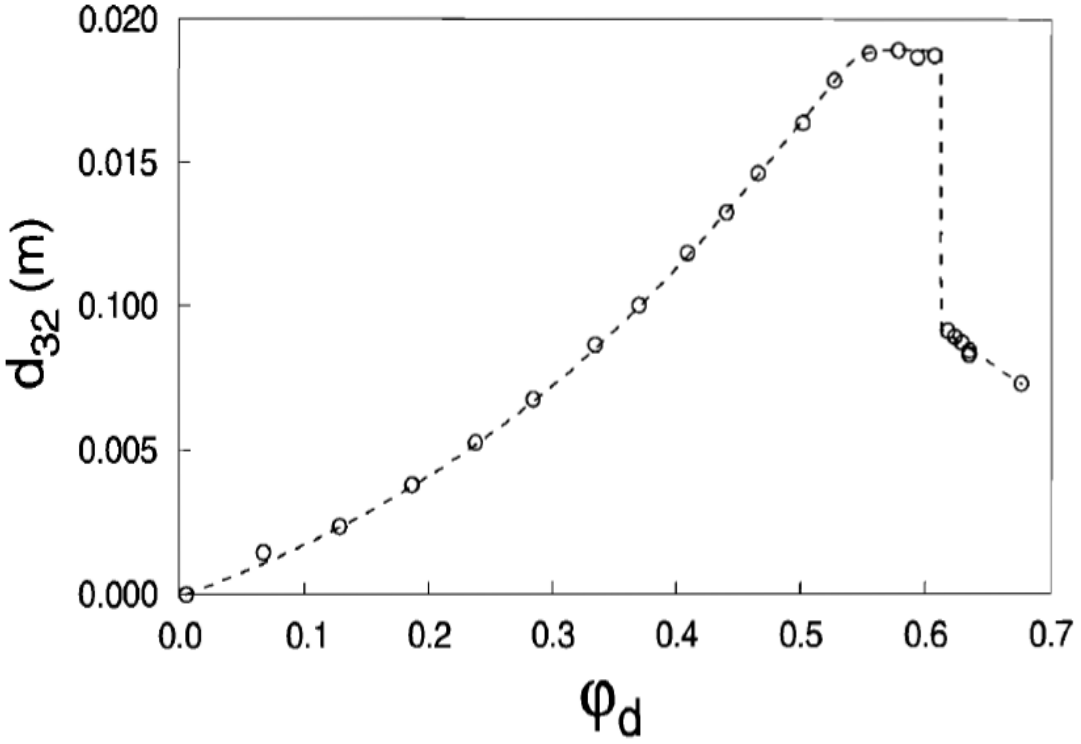

Fig. 12 Evolution of Sauter mean droplet diameter for hexane/water emulsion in the stirred vessel (Vaessen, 1996).

Previous experimental results have shown the following features of phase inversion (Vaessen, 1996):

- The phase inversion is dependent on the vessel geometry, impeller type, position and degree of agitation.
- The phase inversion is dependent on the density, the interfacial tension and the viscosities of the phases.

The phase inversion mechanism is not well understood and has been investigated for the past several decades.

3.2.1 Identifying phase inversion region

Several techniques are used to detect and monitor phase inversion from O/W to W/O emulsions:

- **Conductivity:** One of the most popular methods to detect and monitor phase inversion is the electrical conductivity of the emulsion. An electrolyte such as sodium chloride, only soluble in the aqueous phase, is added to the emulsion. When an oil in water emulsion inverts to a water in oil emulsion, the conductivity decreases rapidly since the new continuous phase is not conductive (Hu and Angeli, 2006; Ngo and Schumpe, 2012a).
- **Viscosity:** The emulsion viscosity increases with increasing volume fraction of the dispersed phase. When the phase inversion occurs, a sharp change in emulsion viscosity is observed (Tyrode *et al*., 2005).
- **Light scattering:** this technique has been used to monitor the size distribution of the droplets in emulsions (Pizzino *et al*., 2009).

We did not study phase inversion in our experiments, but refer to the measurements of Ngo and Schumpe (2012a) in the same systems.

3.3 Cohesion, Adhesion and Spreading Coefficient

The interfacial tension between organic liquids and water is an important parameter in determining the mass transfer characteristics.

A compilation of surface and interfacial tensions measured by different authors is listed in Table 7-9.

Table 7

Summary of surface tension values for organic liquid at 25˚C.

	$\gamma_{O/G}$ (mN/m)			
n-alkane	Hirasaki (1993)	Demond and Linder (1993)	Kundu *et al*. (2003[a])	Ngo and Schumpe (2012a)
n-Heptane	19.7	16.66	20.30	19.8
n-Dodecane	25.1	24.91	25.41	24.6
n-Hexadecane	27.3	26.95	-	26.7

a) at 20 ˚C.

Table 8

Summary of air-saturated water surface tension values at 25˚C.

	$\gamma_{W/G}$[a] (mN/m)		
n-alkane	Demond and Linder (1993)	Kundu *et al*. (2003[b])	Ngo and Schumpe (2012a)
n-Heptane	72.59	65	71.8
n-Dodecane	72.74	71	68.2
n-Hexadecane	71.83	-	71.2

a) Air-saturated aqueous phase; b) at 20 ˚C.

Table 9

Summary of interfacial tension values for organic liquids at 25˚C.

	$\gamma_{O/W}$ (mN/m)		
n-alkane	Demond and Linder (1993)	Zeppieri *et al*. (2001)	Ngo and Schumpe (2012a)
n-Heptane	50.2	50.71	40.8
n-Dodecane	52.8	52.55	41.4
n-Hexadecane	53.3	-	42.9

The work required to separate the two liquids, which are brought in contact, to give clean surfaces of individual liquids is defined as $W_{O/W}$:

$$W_{O/W} = \gamma_{O/G} + \gamma_{W/G} - \gamma_{O/W} \quad (23)$$

where

$\gamma_{O/G}$ = surface tension of oil, N m^{-1}

$\gamma_{W/G}$ = surface tension of water, N m^{-1}

$\gamma_{O/W}$ = interfacial tension of oil and water, N m^{-1}.

This is known as the work of adhesion between two immiscible liquids or as Dupré's equation (Davies and Rideal, 1961). The work of cohesion for a single liquid (*e.g*., oil) is

$$W_O = 2\gamma_{O/G} \quad (24)$$

The initial spreading of the oil over the clean surface of water can be related to the work of adhesion and cohesion by subtracting equation (24) from (23),

$$S_{O/W} = \gamma_{W/G} - (\gamma_{O/W} + \gamma_{O/G}) \tag{25}$$

It is necessary to calculate the spreading coefficient $S_{O/W}$, in order to determine whether an organic liquid will form a thin film on the water surface or a droplet lens.

The oil spreading on the water occurs only if oil molecules adhere to the water molecules more strongly than they cohere to themselves ($S_{O/W} \geq 0$). Then the organic liquid will spread as a thin film on the bubble surface and act like surfactants to lower the surface tension, and thereby increase the specific interfacial area of the gas dispersion and, hence, possibly increase $k_L a$. On the other hand, if $S_{O/W}$ is negative, the organic liquid tends to form floating distinct droplets that may partially block the surface area effective for gas transfer at the interface, thus reducing the mass transfer rate as a consequence of reducing the rate of surface renewal (Pinho and Alves, 2010).

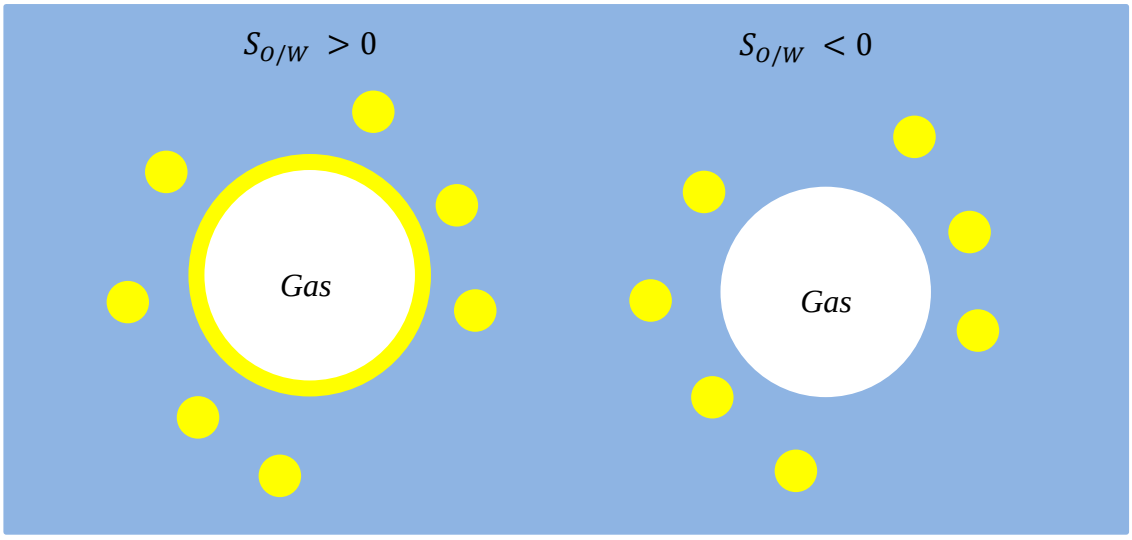

Fig. 13 Effect of spreading coefficient on the mass transfer of gas into oil-in-water emulsion: ● aqueous phase; ● dispersed oil phase.

Although interfacial properties and the spreading coefficient have been taken into account in determination of the volumetric mass transfer coefficient (Fig. 13), an extensive review of gas transfer into oil-in-water systems (Dumont and Delmas, 2003) reveals that, because of the lack of information of oil distribution near the gas-liquid interface and contradictory reported spreading coefficient values, it is not possible to interpret the mass transfer behavior only through the interfacial properties and further investigations are needed (Table 10).

Table 10

Summary of spreading coefficient values for organic liquid at 25˚C.

n-alkane	Rols *et al.* (1990)	Hassan and Robinson (1977[a])	Oliveira *et al.* (1999)	Drelich and Miller (2000)	Pinho and Alves (2010)	Ngo and Schumpe (2012a)
n-Heptane				+1.3	+1.2 to +2.3	+11.8
n-Dodecane	+0.6	-2.6	+3.7	-6.1	-5.3 to -5.9	+2.0
n-Hexadecane		-9.3		-8.5		+2.2

a) at 20 ˚C.

Drelich and Miller (2000) studied the spreading of low viscosity n-alkanes (pentane, heptane, dodecane and hexadecane) on the water surface using a Kodak high-speed video system. They found that when a small hydrocarbon droplet was placed on the water surface, dodecane and hexadecane (with negative spreading coefficients) remained as droplets on the surface, whereas pentane and heptane (with positive spreading coefficients) spread immediately on the water surface. Their results are shown in Figure 14. It is evident that heptane is more likely to spread on the surface than the other organic liquids.

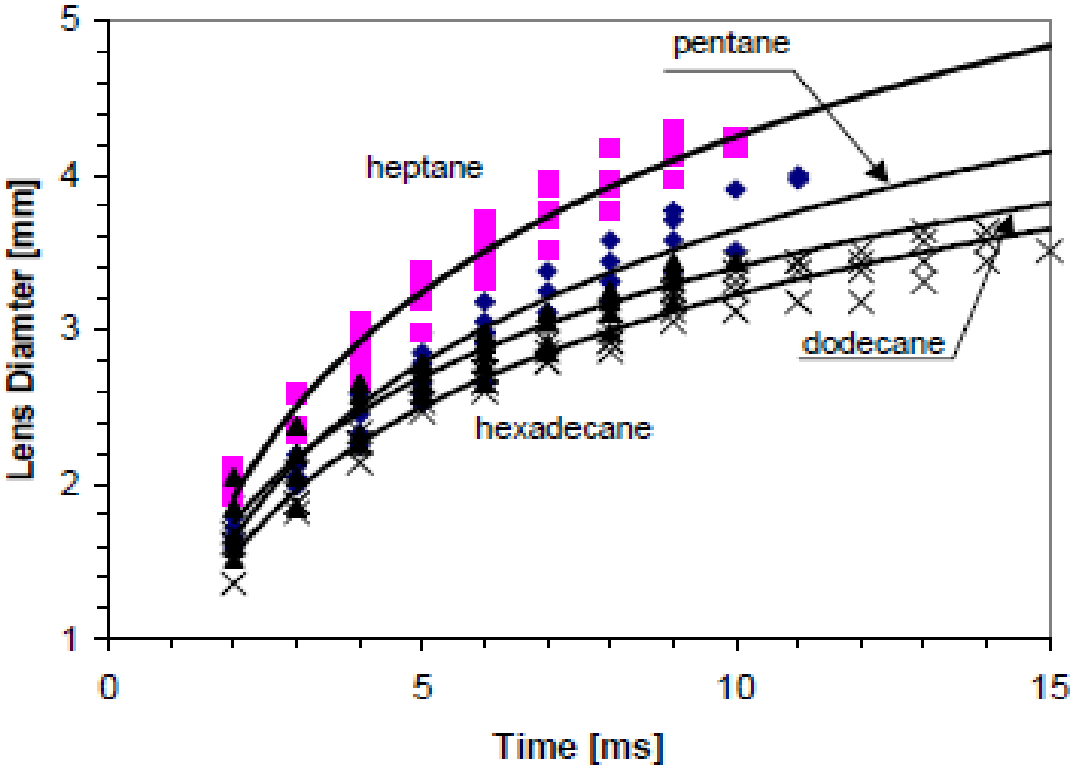

Fig. 14 Spreading kinetics for different n-alkanes (Drelich and Miller, 2000).

For spreading oils ($S_{O/W} > 0$), Yoshida *et al*. (1970) concluded that the initial rapid decrease in $k_L a$ for oxygen absorption in the toluene/water emulsions in an agitated vessel might be attributable to spreading oil film on the gas-liquid interface which means increasing specific interfacial area but decreasing liquid side mass transfer coefficient. In contrast, Ngo and Schumpe (2012a, b) reported an increase in $k_L a$ at low n-dodecane concentrations for both oxygen and carbon dioxide absorption. According to them, the initial increase may be due to shuttle mechanism (Fig. 15).

For negative spreading coefficients ($S_{O/W} < 0$), Hassan and Robinson (1977) found that the oxygen transfer was reduced in the case of n-dodecane whereas the addition of n-hexadecane gave an enhancement of oxygen transfer. However, they were not able to interpret these contrary results (Fig. 15).

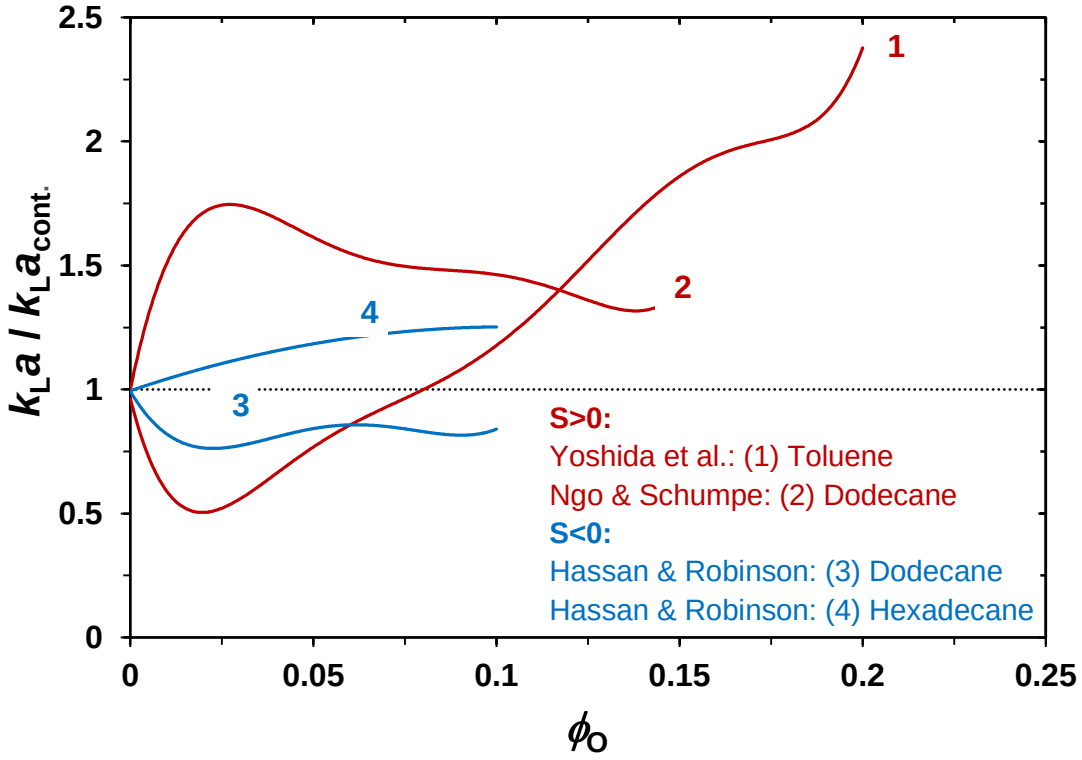

Fig. 15 The discrepancy of the spreading coefficient effect on $k_L a$.

It is obvious that the spreading coefficient for oil-in-water emulsions cannot provide a clear explanation of unusual variations in the mass transfer characteristics upon addition of second immiscible phase.

3.4 Gas-liquid Mass Transfer Pathway

Gas-liquid-liquid mass transfer can be assumed to be a limiting step since the droplet size of the dispersed liquid is much smaller than the bubble size (Ngo and Schumpe, 2012a). The liquid phases are close to equilibrium, then. Different pathways may exist for gas-liquid mass transfer

3.4.1 Oil-in-water emulsions

When a gas bubble comes into contact with a liquid-liquid dispersion, different interactions and possible mass transfer pathway might occur:

- $S_{O/W} > 0$
    - Oil spreads around the bubble totally or partially and forms a thin film.
        - Serial transfer path: gas → oil → water
        - Parallel transfer path: gas → oil
          gas → water
- $S_{O/W} < 0$
    - Beading oil droplets cover the bubble surface partially.
        - Serial transfer path: gas → water → oil

The schematic diagram of the three possible pathways are depicted in Figure 16.

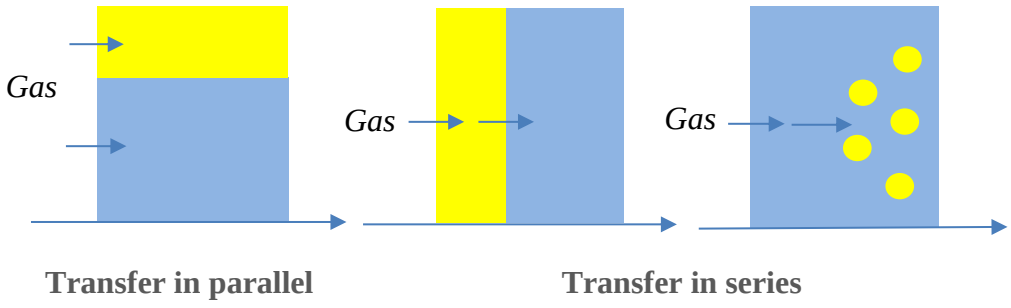

Fig. 16 Possible mass transfer pathway for O/W emulsions;
●aqueous phase; ●dispersed oil phase.

The most probable mass transfer path for spreading oil where there is a direct contact between gas and oil, $S_{O/W} > 0$, is parallel transport (Yoshida *et al*., 1970; Hassan and Robinson, 1977; Rols *et al*., 1990)**.** Linek and Beneš (1976) studied absorption of oxygen and argon into different type of emulsions in an agitated vessel. They observed in O/W

emulsions with positive spreading coefficient, k_L initially decreased and then increased with increasing oil volume fraction. k_L remained constant in emulsions with positive spreading coefficient; so they suggested there is no direct contact between gas and dispersed oil and the transfer path is gas → water → oil.

3.4.1 Water-in-oil emulsions

A little data has been published so far on the effect of aqueous dispersed phase (W/O) on the mass transfer coefficient considering possible pathways (Linek and Beneš, 1976; Ngo and Schumpe, 2012a). Whatever the spreading coefficient, two mass transfer pathways might be considered for W/O emulsions:

- No direct contact between gas and dispersed aqueous phase.
  - Serial transfer path: gas → oil → water
- Gas is in direct contact with both the dispersed aqueous phase and oil continuous phase.
  - Parallel transfer path: gas → oil
    gas → water

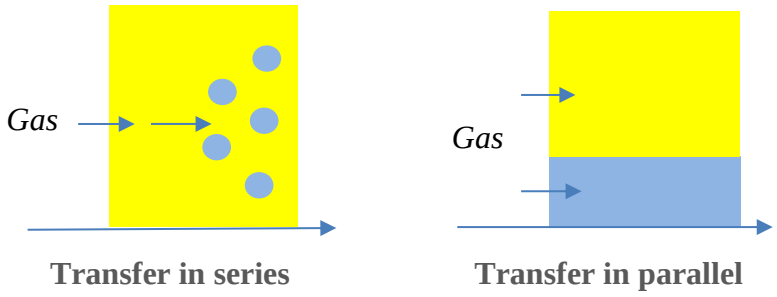

Fig. 17 Possible mass transfer pathway for W/O emulsions; ●dispersed aqueous phase; ●oil phase.

Based on the investigation of Linek and Beneš (1976), the mass transfer coefficient increased with increasing oil volume fraction in W/O emulsions. They discussed the parallel pathway is more probable than gas transfer in series as the mass transfer coefficient showed a strong increase with increasing oil volume fraction.

3.5 Enhancement Factor

In physical gas absorption into emulsions, the effect of the dispersed phase on the mass transfer rate is often represented by an enhancement factor *E*. This factor is defined as the ratio of the absorption flux in the presence of the dispersed liquid to that in the pure continuous phase at the same hydrodynamic conditions and the same driving force (Dumont and Delmas, 2003):

$$E = \frac{(N_A)_{(\varphi_{disp.}\neq 0)}}{(N_A)_{(\varphi_{disp.}=0)}} = \frac{k_L a_{(\varphi_{disp.}\neq 0)}}{k_L a_{(\varphi_{disp.}=0)}} \tag{26}$$

3.6 Shuttle Mechanism

In the literature several mechanisms have been proposed to explain gas absorption enhancement.

A shuttle- or grazing mechanism was proposed by Bruining *et al*. (1986). The mechanism is based on the absorbed gas being transferred to the continuous phase outside the boundary layer by loaded dispersed phase droplets (Fig. 18). In this mechanism, in order to achieve significant enhancement of mass transfer in the presence of second immiscible phase, the droplet size should be small compared to the mass transfer film thickness in the liquid (Bruining *et al*., 1986).

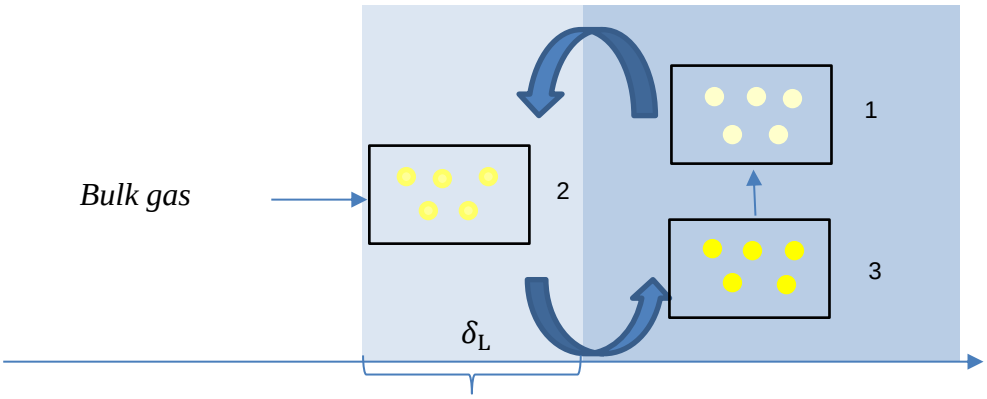

Fig. 18 Shuttle mechanism: ● aqueous phase; ● dispersed oil phase.

A theoretical enhancement factor can be also calculated for the shuttle effect (Bruining *et al.*, 1986):

$$E_{shuttleeffect} = \sqrt{1 + \varphi_{disp.}(m_R - 1)} \tag{27}$$

where m_R is the ratio of the gas solubility in the organic phase to that in the aqueous phase.

3.7 Bubble Covering Mechanism

In contrast to the shuttle mechanism, the bubble covering or coalescence-redispersion mechanism has rarely been considered due to lack of information concerning interface properties and bubble-oil droplet interaction. This mechanism was proposed by Rols *et al.* (1990) for positive spreading coefficients which cause an oil layer on the bubble surface. There is gas-to-oil transfer and, after oil redispersion into droplets, oil-to-water transfer. Figure 19 illustrates the steps of the bubble covering mechanism.

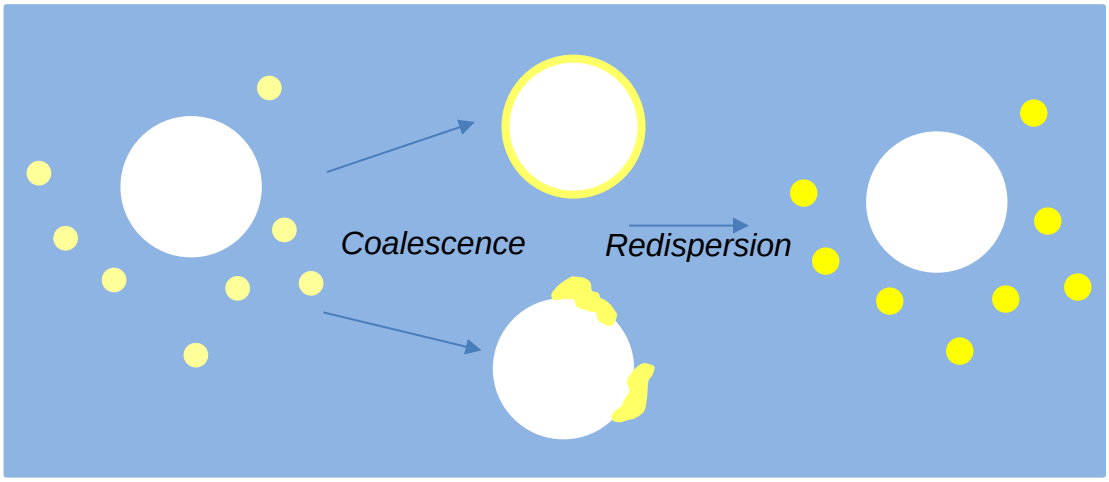

Fig. 19 Bubble-covering mechanism: ● aqueous phase; ● dispersed oil phase.

Van Ede *et al.* (1995) assumed a direct contact between gas and organic liquids. Thus the gas transfer to aqueous continuous phase and dispersed organic liquid phase was assumed to be in parallel. They calculated a maximum enhancement factor by the film theory:

$$E_{max}^{filmtheory} = 1 + \varphi_{disp.}\left(m_{\mathrm{R}}\frac{D_{A,O}}{D_{A,W}} - 1\right) \tag{28}$$

However, Dumont and Delmas (2003) discussed that experimental enhancement factors showed lower values than E_{max}.

Chapter 4

Material and Methods

4.1 Physical Absorption

4.1.1 Experimental set-up

A scheme of the experimental apparatus and a photo are given on Figure 20 and 21, respectively. The mechanically agitated vessel, made of glass, had an effective volume of 1940 ml, 100 mm inner diameter and 210 mm total height. Four equally spaced baffles with a width of 10 mm served to ensure sufficient mixing and prevent vortex formation within the reactor. To adjust the temperature, ethylene glycol solution was circulated through the jacket of the reactor by means of a thermostat.

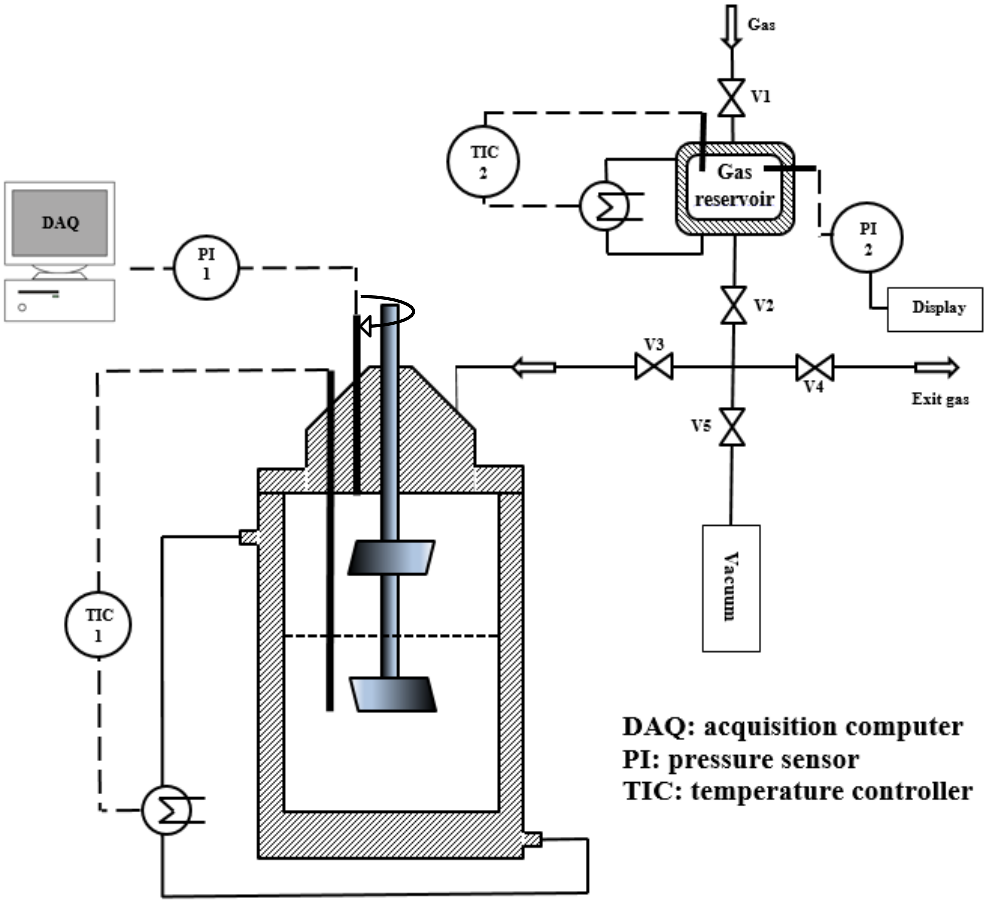

Fig. 20 Scheme of the experimental setup.

Fig. 21 Photo of the experimental setup.

The dispersions inside the reactor were agitated with a 4-blade 45˚ pitched blade turbine (PBT) operating in the down-pumping mode. The diameter of the impeller was 1/2 of the inner diameter of the vessel and placed 30 mm above the bottom of the reactor (Fig. 22). The rotational speed of the impeller was 1000 rpm in all experiments. Mixing was adequate to disperse the oil in the aqueous phase and entrain gas from the top. A second impeller was installed at the top to ensure mixing in the gas phase.

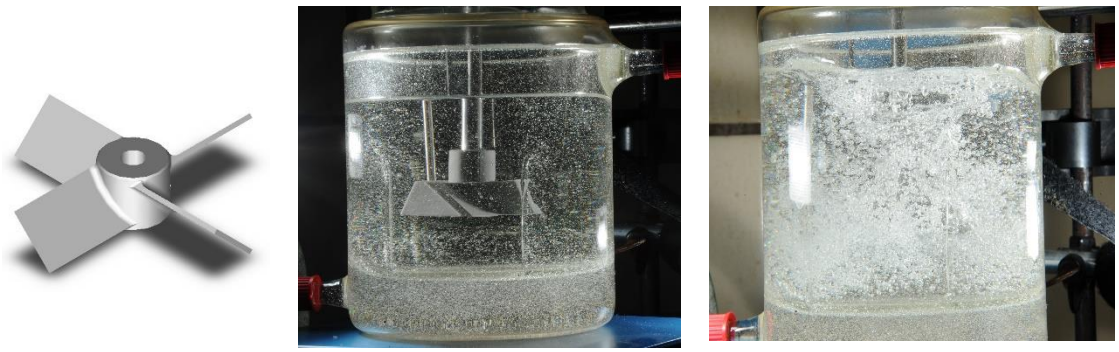

Fig. 22 Four-blade 45˚ pitched blade impeller and gas entertainment at 1000 rpm.

The liquid in the amount of 700 ml (80 mm height) added for each experiment was heated to 25±0.1˚C and kept at this temperature by a thermostat (Model F32, JULABO). The temperature was measured with a temperature sensor (Pt 100, JULABO). The operating pressure in the reactor was measured with a pressure sensor (Model E, HONEYWELL), installed on the lid of the reactor. The characteristics of the reactor are summarized in Table 11.

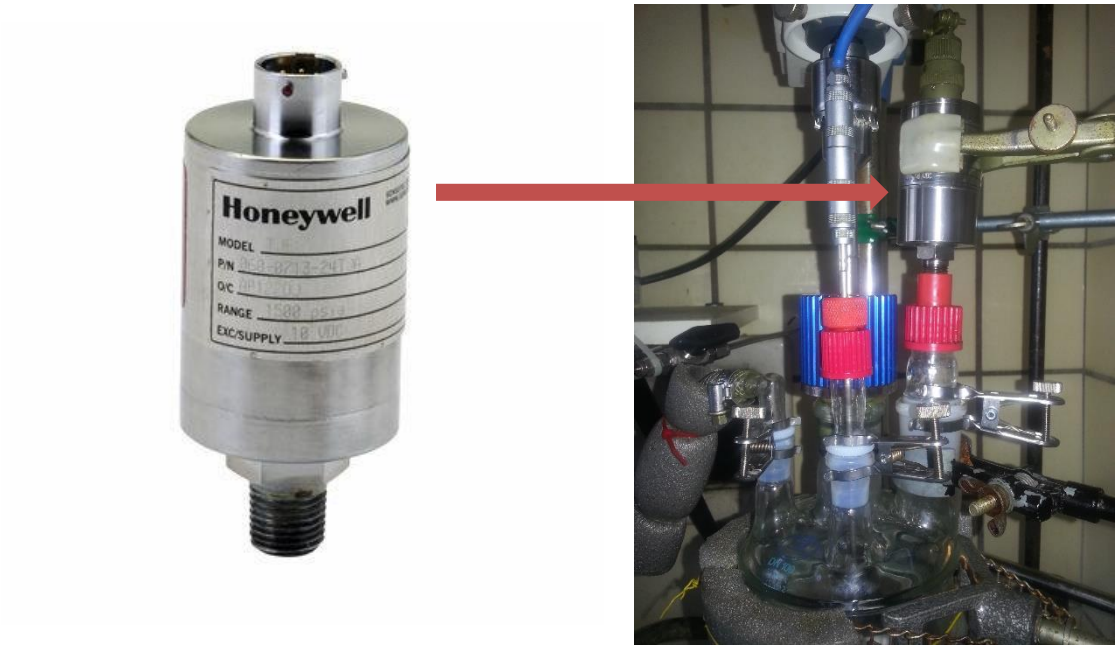

a **b**

Fig. 23 a) Pressure sensor used, b) Installation of the sensor.

Table 11

Characteristics of the reactor and stirrer.

Characterize	
Total volume	1940 ml
Liquid volume	700 ml
Internal diameter	100 mm
Total height	21mm
Number of baffles	4
Baffles width	10 mm
Off-bottom clearance of lower impeller (for liquid phase)	30 mm
Off-bottom clearance of upper impeller (for gas phase)	140 mm
Type of impeller	45˚ Pitched-blade turbine
Diameter of impeller	50mm
Impeller blade width	4mm
Impeller blade height	18mm
Number of blades	4
Stirrer shaft diameter	8 mm

4.1.2 Chemical material

***Gas*:** the gas used to carry out the physical absorption experiments was 99.999% pure carbon dioxide (CO_2).

- Henry constant (*H*): 2980.1 Pa m^{-3} mol^{-1} (Vázquez *et al*., 1997).
- Diffusion coefficient in water (*D*): 1.97×10^{-9} m^2 s^{-1} (Vázquez *et al*., 1997).

***Liquids*:** Double-distilled water or aqueous solutions of sodium dodecyl sulfate (SDS) were taken as the aqueous phase and three different organic liquids, n-heptane (Sigma Aldrich), n-dodecane and n-hexadecane (Merck) with purity ≥ 99%, were used as the oil phase. Some relevant properties for the liquids used in this work are given in Table 12.

Table 12

Physical properties of liquids at 25˚C (Lide, 2003).

Liquid	***Formula***	***Vapor Pressure*** kPa	***Viscosity*** mPa s	***Density*** kg m^{-3}
Water	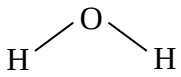	3.17	0.890	997
Heptane	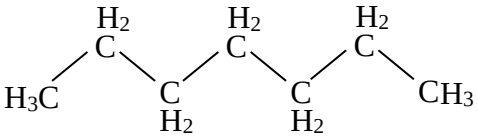	6.09	0.387	679.5
Dodecane	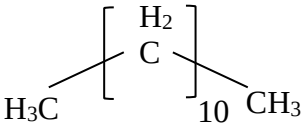	0.02	1.383	749.5
Hexadecane	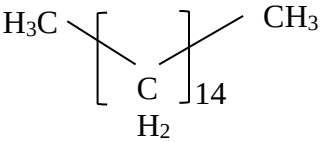	~0	3.032	770.1

***Surfactant*:** The anionic surfactant sodium dodecyl sulfate (SDS) with the chemical formula of $C_{12}H_{25}SO_4Na$ was applied in the present work, supplied by Merck KGaA with a purity of 99%. The concentration of SDS was kept constant with respect to the aqueous

phase (0.22 g L^{-1}), while the oil volume fraction ranged from 0 to 100%. The concentration of the surfactant was well below the critical micelle concentration (CMC) of 1.9 g L^{-1} (Painmanakul *et al*., 2005) in order to avoid foam formation at the surface during the absorption process (Fig. 24).

a **b**

Fig. 24 Photo of O/W emulsion of n-hexadecane ($\varphi_O = 10\%$);
a) before and b) during agitation.

It can be assumed that the density and viscosity of surfactant dilute aqueous solutions are equal to those of water (Painmanakul *et al.*, 2005). Also Gómez-Díaz *et al*. (2007) showed that low concentrations of surfactant have no effect on the viscosity. The diffusivity and solubility of CO_2 were also equal to their values for pure water (Vázquez *et al*., 1997).

4.1.3 Surface tension

Liquid-air surface tensions and liquid-oil interfacial tensions reported in this work were measured with the Ring method using the tensiometer K11 (KRÜSS) at 25˚C (Table 13 and 14). The apparatus was calibrated with distilled water.

Table 13

Surface and interfacial tensions for current study at 25˚C.

n-alkane	$\gamma_{W/G}$[a]	$\gamma_{O/G}$	$\gamma_{O/W}$	$S_{O/W}$
		mN m^{-1}		
n-Heptane	71.6	19.8	49.0	+1.4
n-Dodecane	72.1	24.8	40.7	+5.59
n-Hexadecane	72.1	27.1	41.0	+4.0

a) Oil-saturated water.

Table 14

Surface and interfacial tensions in the presence of SDS (0.22 g L^{-1}) at 25˚C.

n-alkane	$\gamma_{W/G}$[a]	$\gamma_{O/G}$	$\gamma_{O/W}$	$S_{O/W}$
		mN m^{-1}		
n-Heptane	66.1	19.8	34.2	+12.1
n-Hexadecane	66.4	27.1	22.6	+16.7

a) Oil-saturated aqueous phase.

4.1.4 Pressure drop technique for CO_2 absorption

Reactor temperature and pressure were recorded using a data acquisition system. The reactor was operated batchwise with respect to both gas and liquid. For all absorption experiments the initial pressure (P_i) was about 1.6 bar.

***Degassing*:** Before starting the absorption experiment, the emulsion with desired oil volume fraction (0-100 vol.%) in the reactor was heated to 25±0.1˚C and then degassed under stirring (Fig. 20):

- V3, V5 and V6 were opened.
- V2 and V4 were closed.

The liquid losses during degassing treatment were determined using a cold trap with liquid nitrogen as the coolant. The losses were negligible for n-dodecane and n-hexadecane. The n-heptane loss was about 2.5 ml. The volume losses were compensated by adding 2.5 ml n-heptane before each measurement.

***Pressurizing*:** After degassing, when the temperature equilibrium was established and the liquid surface had become stable, pure CO_2 was injected slowly into the head space of the reactor (Fig. 20):

- V3, V5 and V6 were closed.
- V2 was opened.

***Absorption*:** When the CO_2 pressure had reached the set value (P_i) and the pressure was constant after thermal equilibration, the absorption process was initiated by switching on the stirrer. The subsequent pressure decrease in the reactor was recorded until the saturated pressure was reached (P_f).

***Reactor cleaning*:** Before and after a set of experiments, the reactor was treated with acetone and double-distilled water at least thrice and then dried. In the case of using SDS, in addition, the apparatus was further cleaned with a 1:1 mixture of acetone and ethanol to do away with the surfactant remnants.

Figure 25 shows the absorption process versus time for 5% oil volume fraction of n-dodecane/water emulsion for two different runs. The total pressure drop is used to calculate the gas solubility and the overall volumetric mass transfer coefficient is evaluated based on the pressure-time curve. All the experiments were repeated at least 6 times. The difficulties in keeping the initial pressure consistently at the same value for all experiments caused the small difference between the two curves in Figure 25.

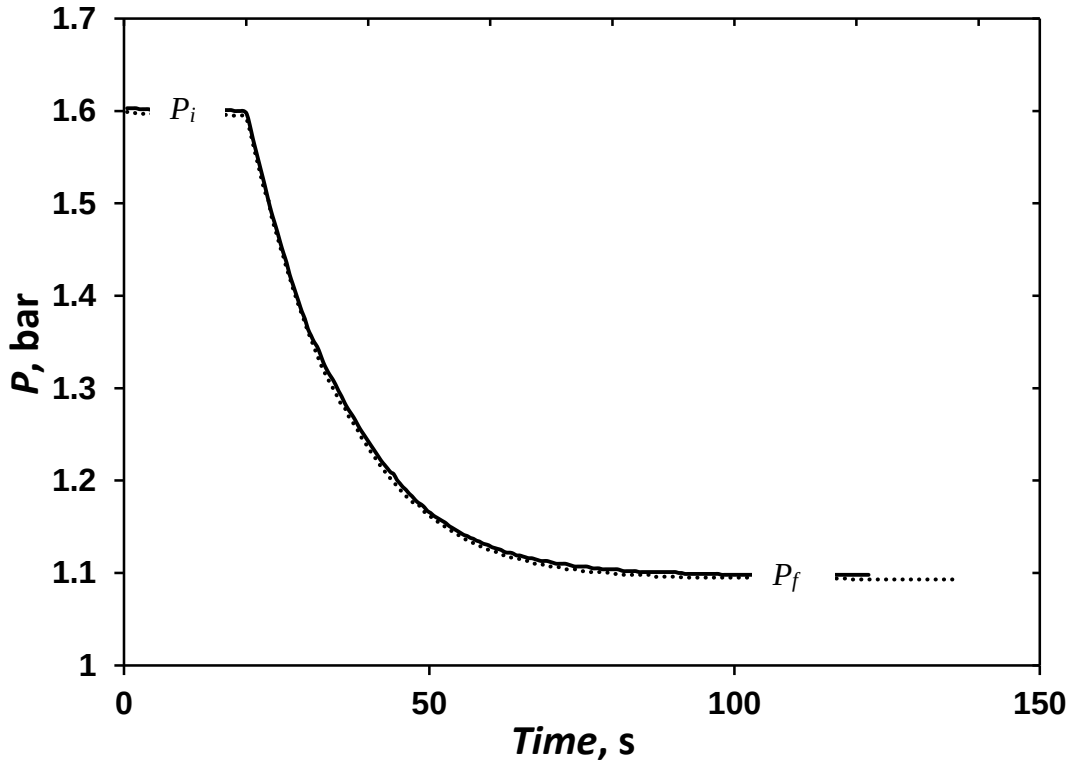

Fig. 25 CO_2 absorption into n-dodecane emulsion ($\varphi_O = 5\%$).

The reported k_La values were the mean values of at least 6 determinations and the mean relative standard deviations for k_La were less than 5% for all experiments.

The pressure decline curve for the experiments with and without SDS have been shown in Figure 26. It is evident that the addition of soluble surfactant has slightly changed the mass transfer rate of CO_2 into the emulsions.

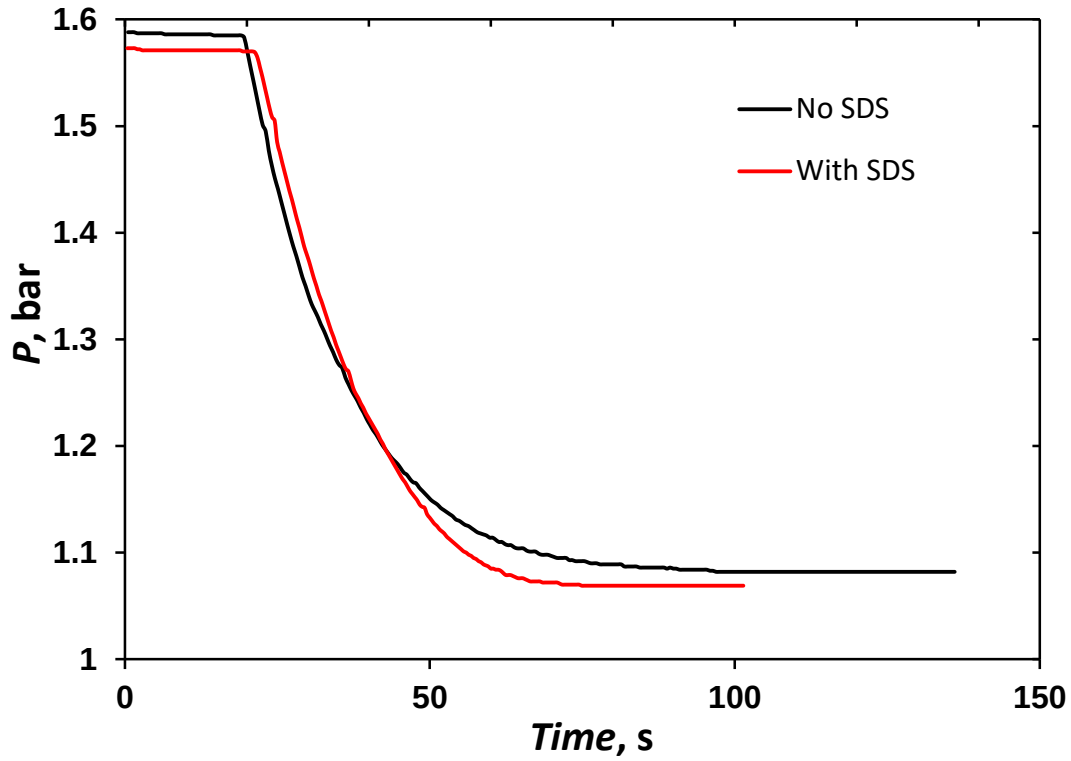

Fig. 26 CO_2 absorption into n-hexadecane emulsion in the presence and the absence of SDS ($\varphi_O = 5\%$).

4.1.5 Data analysis

4.1.5.1 $k_L a$ evaluation

For the calculation of the volumetric liquid-phase mass transfer coefficient a pseudo-homogeneous model was used (Ngo and Schumpe, 2012a). The following assumptions were made:

- The liquid phases are completely mixed throughout the tank.
- The concentration of dissolved gas in the both dispersed and continuous phases was always at equilibrium within the mass transfer zone which implies liquid-liquid mass transfer resistances are neglected.

Albal *et al*. (1988) showed that the absorption rate can be calculated from the change in total pressure *P* according to

$$-\frac{dN_G}{dt} = \frac{V_G}{RT} \cdot \frac{dP}{dt} \tag{29}$$

$$\frac{dN_G}{dt} = V_L k_L a(c^* - c_L) \tag{30}$$

where

R = Gas constant, Pa m^3 mol^{-1} K^{-1}

T = temperature, K

V_G = volume of gas, m^3

V_L = volume of liquid, m^3.

From above equations, it follows that

$$-\frac{dP}{dt} = \frac{V_L RT}{V_G} k_L a(c_L^* - c_L) \tag{31}$$

The bulk concentration of the dissolved gas c_L in the liquid can be expressed as

$$c_L = \frac{V_G}{V_L RT}(P_i - P) \tag{32}$$

where

P_i = initial total pressure, Pa.

According to Henry's law:

$$c_L^* = \frac{(P - p_W - p_O)}{H} \tag{33}$$

where p_W is partial pressure of water and p_O is partial pressure of oil.

Substitution of Eqs. 32 and 33 into Eq. (31) gives

$$-\frac{dP}{dt} = k_L a \left[\frac{V_L RT}{HV_G}(P - p_W - p_O) - (P_i - P)\right] \tag{34}$$

At equilibrium, the final pressure is P_f and the final concentration of the dissolved gas $c_{L,eq}^*$ can be calculated from Eq. (32)

$$c_{L,eq}^* = \frac{V_G}{V_L RT}\left(P_i - P_f\right) \tag{35}$$

Also,

$$c_{L,eq}^* = \frac{(P - p_W - p_O)}{H} \tag{36}$$

From Eqs. (35) and (36) and simplifying, we obtain

$$\frac{\left(P_i - P_f\right)}{(P - p_W - p_O)} = \frac{V_L RT}{HV_G} \tag{37}$$

Combining Eqs. (37) and (34) gives

$$-\frac{dP}{dt} = k_L a \left[\frac{(P_i - P_f)}{(P - p_W - p_O)} (P - p_W - p_O) - (P_i - P) \right] \tag{38}$$

Integration of Eq. (38) will give

$$-\frac{P_f - p_W - p_O}{P_i - p_W - p_O} \cdot \ln(P - P_f) = k_L a \cdot t + const. \tag{39}$$

The volumetric mass transfer coefficient can then be evaluated based on the above relation.

Thus, the dependence of the left-hand side of equation 39 versus time is a straight line with a slope representing the value of $k_L a$. An example of $k_L a$ determination is presented in Figure 27.

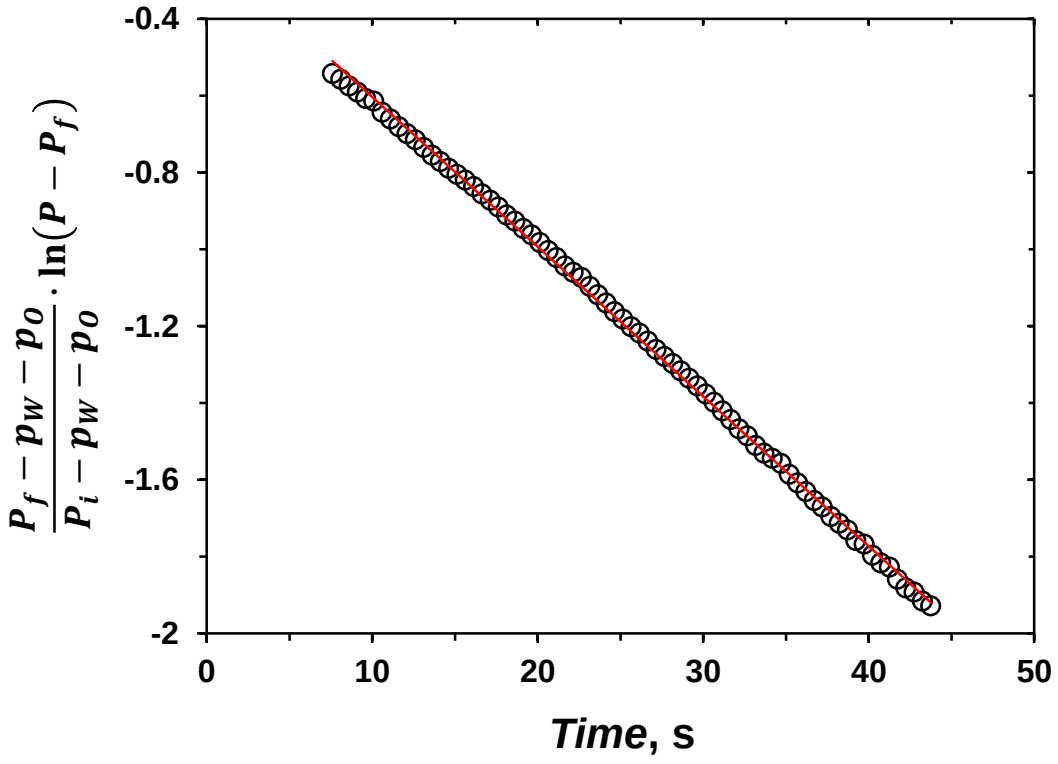

Fig. 27 Linearization of Eq. 39,
(15% hexadecane/water; $k_L a$ = 0.039 s^{-1}).

For determination of $k_L a$, the data at 15% to 90% saturation was used in order to exclude the initial re-emulsification phase as well as the final phase with low driving force (Ngo and Schumpe, 2012b).

4.1.5.2 Gas solubility evaluation

Carbon dioxide dissolves in water according to:

$$CO_2(g) \leftrightarrow CO_2(l) \tag{40}$$

Upon dissolution in water, the following equilibrium is established:

$$CO_2(l) + H_2O(l) \leftrightarrow H^+ + HCO_3^- \tag{41}$$

Carbon dioxide is more soluble in water than other gases such as nitrogen, oxygen, argon, neon, hydrogen and helium (Weiss, 1974). For instance, its solubility is about 26 times higher than that of oxygen (Kordac and Linke, 2008). However, carbon dioxide solubility in aqueous solutions depends on composition, temperature and pH (Wang *et al*., 2010). The solubility of carbon dioxide in aqueous systems has been reported by several investigators (Carrol *et al*., 1991; Kiepe *et al*., 2002); limited data is available on systems involving CO_2 and organic liquid emulsions.

The overall gas solubility (c^*) in the emulsion at a partial pressure of 101325 Pa can be determined from the total pressure change (Ngo and Schumpe, 2012a):

$$c^* = \frac{V_G}{V_L} \cdot \frac{(P_i - P_f)}{RT} \cdot \frac{101325}{P_f - p_W - p_O} \tag{42}$$

4.2 Chemical Absorption

4.2.1 Experimental set-up

The intrinsic sulfite oxidation experiments were carried out in the stirred reactor at the stirring speed 1000 rpm also used for physical absorption. After adding 700 ml mixture of 0.8 M sodium sulfite solution and oil into the reactor, the temperature was adjusted to 25˚C and air was charged during agitation. Three samples (1 ml) were taken at about 10 minutes intervals and analyzed for the sulfite concentration by iodometric titration (cf. 4.2.3).

To characterize the absorption kinetics, sulfite solution from the same batch (without oil) was placed into a stirred vessel with a flat surface (Fig. 28). After adding 1000 ml solution into the beaker, a magnetic stirrer was started at low stirring speed (70 rpm). A flat gas-liquid interface was maintained which ensured a known interfacial area and enabled the evaluation of the K_2 value (Eq. 46) as suggested by Schumpe and Deckwer (1980). The experiments were conducted for a time of approximately 10 hours. Samples were taken at about one hour intervals and analyzed for the sulfite concentration.

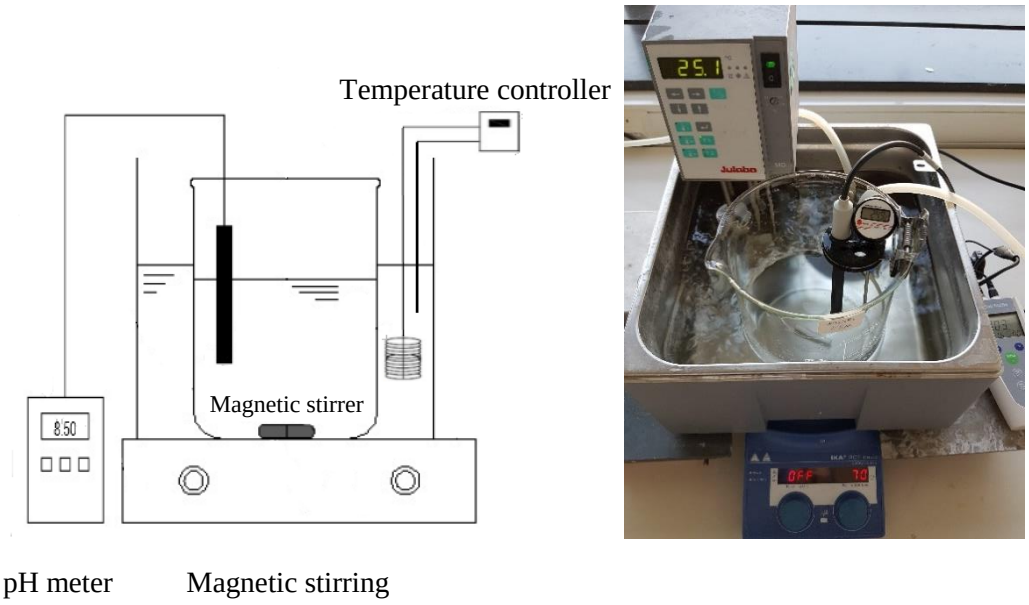

Fig. 28 Magnetic stirring setup used.

4.2.2 Chemical material

***Gas*:** The source of oxygen was air at room temperature and pressure.

***Liquids*:**

- Chemicals for interfacial areas investigation, such as sodium sulfite (Na_2SO_3, 97% purity) and cobalt (II) sulfate heptahydrate ($CoSO_4.7H_2O$, ≥99% purity) were purchased from Merck. Aqueous sodium sulfite solution was the continuous phase and n-hexadecane (Merck, with purity ≥ 99%) was the dispersed oil phase.
- Chemicals for iodometric titration, such as potassium iodide (KI, ≥99.5% purity), iodine (I_2, ≥99.8% purity) and the indicator starch solution (1% in H_2O) were procured from Merck. Sodium thiosulfate ($Na_2S_2O_3$, 99% purity) and sodium carbonate (Na_2CO_3, ≥99.95% purity) were purchased from Sigma-Aldrich.

4.2.3 Sodium sulfite oxidation for oxygen absorption

Prepared sulfite solution with catalyst was placed in the stirring vessel and in the stirred reactor, in the latter case, with the desired oil volume fraction. The pH and temperature were measured continuously. Samples of oil-free sulfite solution were taken from both vessels and the concentration decrease was measured iodimetrically. 1 ml of the solution was added to an excess of 0.1 N iodine standard solution. The solution was then back-titrated with 0.1 N sodium thiosulfate standard solution. Upon addition a few drops of 1% starch indicator solution, a dark blue color appeared. The sodium thiosulfate solution was added dropwise, till the end point of titration which was detected by a color change from dark blue to colorless. Therefore, the remaining amount of sulfite can be determined. The above procedure was repeated 3 times and the sulfite concentration was determined by conventional titrimetric calculations. The measurements were carried in the sulfite concentration range of about 0.8-0.5 M.

4.2.4 Data analysis

4.2.4.1 Interfacial area evaluation

A solution of 0.8 M sodium sulfite catalyzed by cobaltous sulfate (0.5×10^{-3} M) was prepared. The pH was adjusted to ~8.5 adding concentrated sulfuric acid in order to avoid forming cobalt precipitate. No significant variation in the pH was observed during experiments. Some authors have shown that the reaction is second order (m = 2) with respect to oxygen at 25˚C and air at atmospheric pressure (Sivaji and Murty, 1982; Alper *et al.*, 1988). The same assumption was made since the partial pressure of oxygen in the present work was 0.21 bar. It was attempted to keep liquid properties and conditions practically the same for all runs.

The sulfite concentration was measured by iodometric back-titration. Therefore, the oxygen absorption rate was calculated based on the stoichiometry of the reaction (Eq. 16). The interfacial area a_{aq} (referred to the volume of the aqueous phase) can be determined by equation 43:

$$R_{O_2} = 0.5\left(\frac{\Delta c_{SO_3^{2-}}}{\Delta t}\right) = a_{aq}K_2\left(x_{O_2}P\right)^{3/2} \tag{43}$$

The interfacial area referred to the total liquid volume is given by:

$$a = \varphi_{cont.}.\, a_{aq} \tag{44}$$

where

x_{O_2} = oxygen mole fraction (0.209)

P = total pressure, Pa

$\varphi_{cont.}$ = volume fraction of continuous phase (sulfite solution).

The overall absorption coefficient K_2 can be determined either based on the sulfite oxidation in a stirring vessel with a known flat interface (Schumpe and Deckwer, 1980) or it can be calculated from available correlations.

- ***Experimental determination of K_2***

The absorption rate equation can be written as

$$R_{O_2} = 0.5\, R_{SO_3^{-2}} \tag{45}$$

$$R_{O_2} = 0.5\left(\frac{\Delta c_{SO_3^{2-}}}{\Delta t}\right) = a_S K_2 (x_{O_2} P)^{3/2} \tag{46}$$

where a_S is the specific surface area in the stirred vessel with flat interface.

$$a_S = \frac{A_S}{V_{S,L}} = \frac{(\pi/4)0.152^2\ m^2}{10^{-3}\ m^3} = 18.14\ \text{m}^{-1} \tag{47}$$

where

$V_{S,L}$ = volume of liquid, m^3

A_S = beaker surface area, m^2.

Therefore, the actual K_2 values can be obtained from equation 46.

- ***Estimation of K_2 based on literature correlations***

The overall absorption rate for pseudo-second order reaction is given by

$$K_2 = \sqrt{\frac{2}{3}\frac{D_{O_2} k_2}{H^3}} \tag{48}$$

The diffusivity of oxygen in the sodium sulfite solution was calculated by the Wilke-Chang (1955) equation

$$D_{O_2} = 7.4 \times 10^{-8} \frac{(XM_S)^{1/2}T}{\mu_s V_{O_2}^{0.6}} = 1.6 \times 10^{-9} \text{ m}^2 \text{ s}^{-1} \quad (49)$$

where

X = association parameter (2.26) (Reid *et al*., 1977),

M_s = molecular weight of solvent (18 g mol^{-1})

T = temperature (298.15 K)

μ_s = viscosity of solution (1.26 mPa s) (Schumpe *et al*., 1986)

V_{O_2} = molar volume of oxygen at normal boiling point (25.6 cm^3 g^{-1} mol^{-1}).

The second order rate k_2 was obtained by the Linek and Tvrdik (1971) correlation

$$k_2 = 1.44 \times 10^{10} c_{CoSO_4} \left[\frac{pH - 7.9 + 0.04t}{0.6 + 0.04t}\right]^2 exp\left\{-8.45 \times 10^3 \left(\frac{1}{T} - \frac{1}{293}\right)\right\} \quad (50)$$

$$= 2.04 \times 10^7 \text{ m}^3 \text{ kmol}^{-1} \text{ s}^{-1}$$

where

c_{CoSO_4} = catalyst concentration (0.5×10^{-3} kmol m^{-3})

t = temperature (25˚C).

Oxygen solubility in sodium sulfite solution can be calculated from the following equation which Schumpe (1993) suggested for mixed electrolyte solutions:

$$\log(H/H_o) = \sum (h_i + h_G)c_i \quad (51)$$

where

H_o = Henry's constant for pure water (79.8×10^6 Pa m^3 $kmol^{-1}$) (Wilhelm *et al*., 1977)

h_i = ion-specific parameter, m^3 $kmol^{-1}$

(Na^+: 0.1143, SO_3^{-2}: 0.1270, SO_4^{-2}: 0.1117) (Weisenberger and Schumpe, 1996)

h_G = gas-specific parameter, m^3 $kmol^{-1}$ (≡0 for oxygen)

c_i = concentration of ion i, kmol m^{-3},

Therefore, Henry's constant for oxygen at 298.15 K is $H = 153\times10^6$ Pa m^3 $kmol^{-1}$.

Using above equations gave the value of $K_2 = 7.79 \times 10^{-14}$ kmol m^{-2} s^{-1} $Pa^{-1.5}$.

Chapter 5

Results and Discussion

5.1 Physical Absorption

5.1.1 Carbon dioxide solubility in emulsions

Usually physical gas solubility in oils is significantly higher than that in water. The ratio of the CO_2 solubility in the organic phase to that in the aqueous phase

$$m_R = \frac{c_o^*}{c_w^*} \tag{52}$$

determined in this study are listed in Table 15.

Table 15

Solubility ratio of CO_2 in organic liquids used in the experiments at 25ºC.

n-alkane	**n-Heptane**	**n-Dodecane**	**n-Hexadecane**
$\boldsymbol{m_R}$	1.70	1.67	1.42

The physical properties of organic liquids have important effect on the gas solubility. As can be seen in this Table, the CO_2 solubility is deceased by increasing the carbon number.

The effects of the dispersed phase volume fraction and the addition of SDS (0.22 g L^{-1}) on the carbon dioxide solubility are illustrated in Figures 29 and 30. The mean relative standard deviation of the measured solubility values was less than 1%.

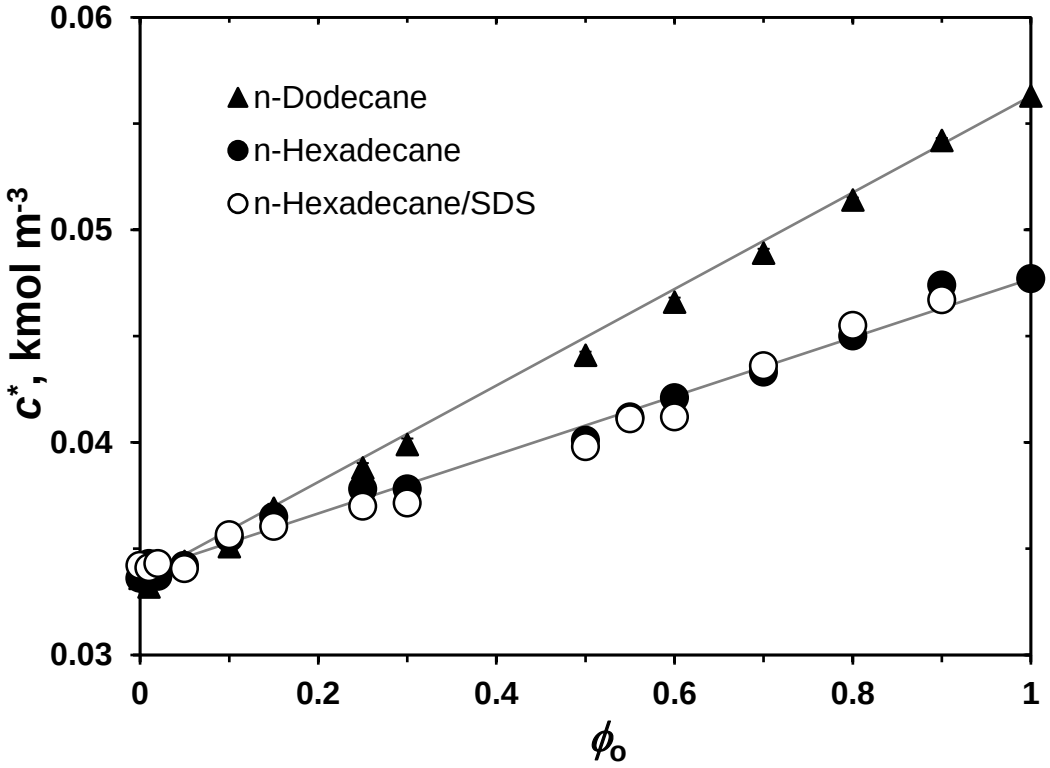

Fig. 29 CO_2 solubility in n-hexadecane/ and n-dodecane/water emulsions.

The overall solubility of carbon dioxide in the emulsions varies linearly with the oil volume fraction for both n-hexadecane and n-dodecane. The carbon dioxide solubility in pure water is in good agreement with Schumpe *et al*. (1982), 3.39×10^{-2} kmol/m^3. SDS has no significant effect due to its low concentration in the liquid phase.

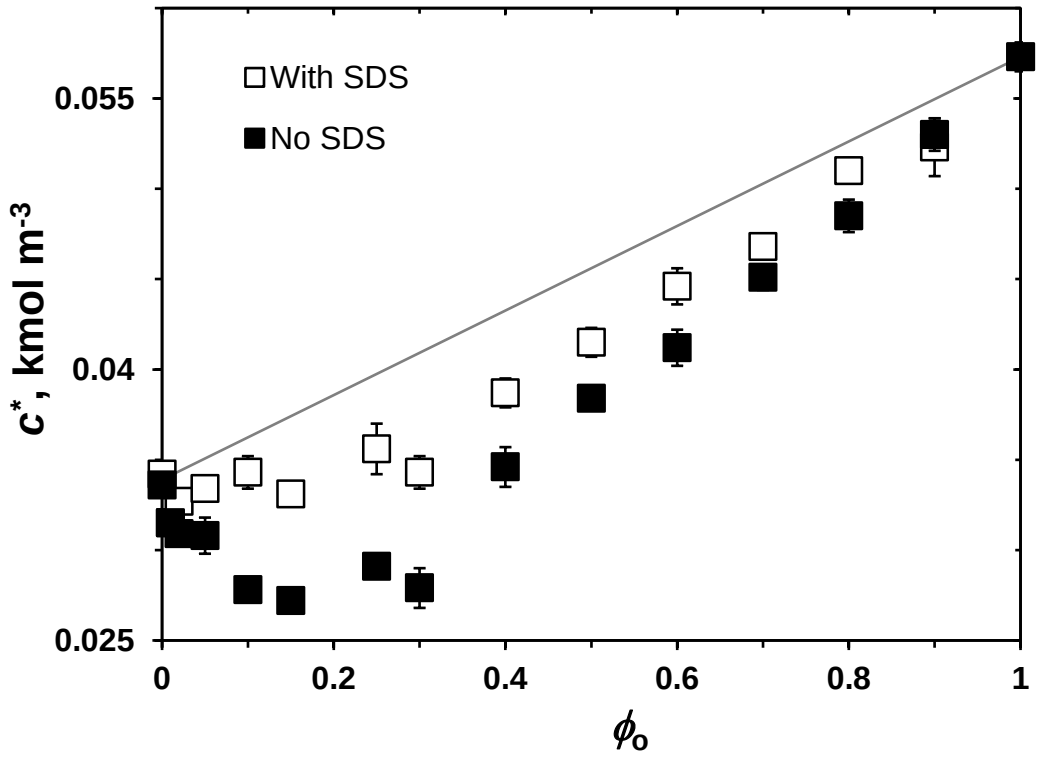

Fig. 30 CO_2 solubility in n-heptane/water emulsions.

Although, it is evident from Figure 30 that the presence of the anionic surfactant SDS has no significant effect on the CO_2 solubility in n-hexadecane emulsions, the addition of SDS affects the CO_2 solubility in n-heptane emulsions. Both curves (with and without SDS) deviate from linear interpolation, but the deviation is smaller in the presence of SDS. Ngo and Schumpe (2012a) also observed lower values as compared to the linear trend.

In the following section, n-heptane emulsions show unexpected trends also for mass transfer.

5.1.2 Carbon dioxide transfer into emulsions

5.1.2.1 Oil volume fraction and viscosity effect on k_La

Figures 31-33 indicate the effect of the oil volume fraction and viscosity, respectively, on the volumetric mass transfer coefficient for three different organic liquids.

At very low oil fractions, k_La for all three oils increases with increasing oil volume fraction until it reaches a maximum value at 1-2%. As the gas solubility in the dispersed organic phase is higher than that in water ($m_R > 1$), the initial increase might indicate an additional mass transfer mechanism at the gas/water interface caused by organic droplets with high gas solubility.

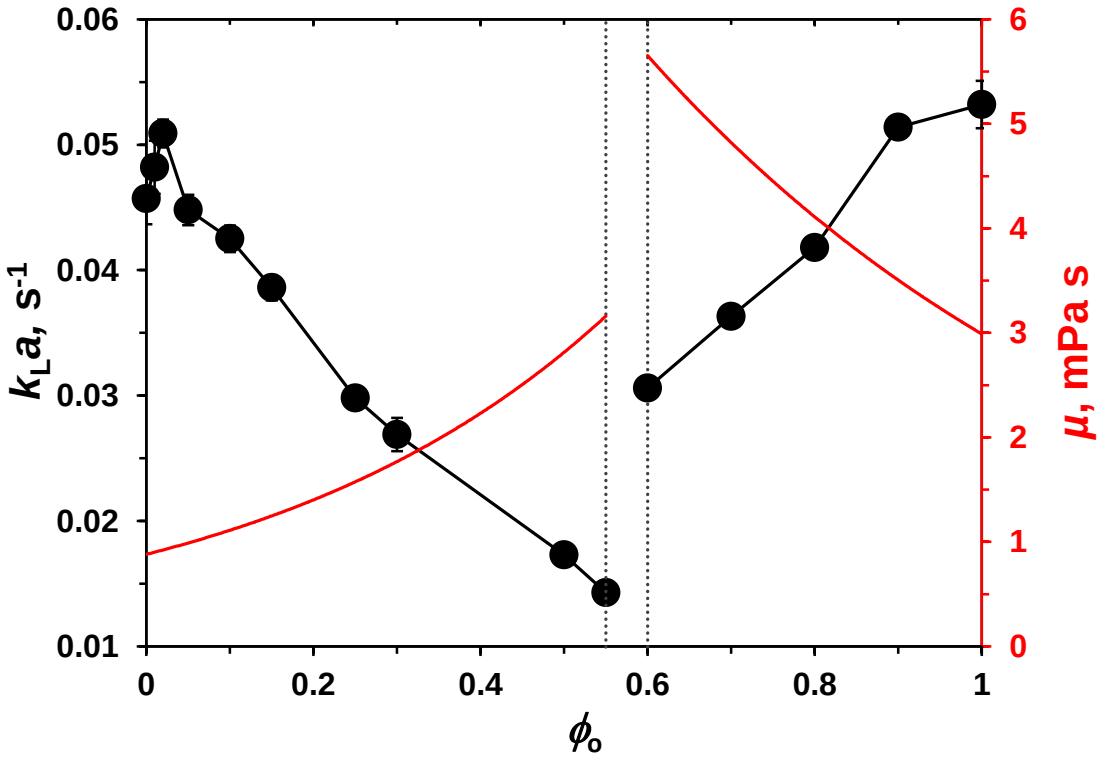

Fig. 31 Effect of n-hexadecane volume fraction and emulsion viscosity on k_La (… phase inversion).

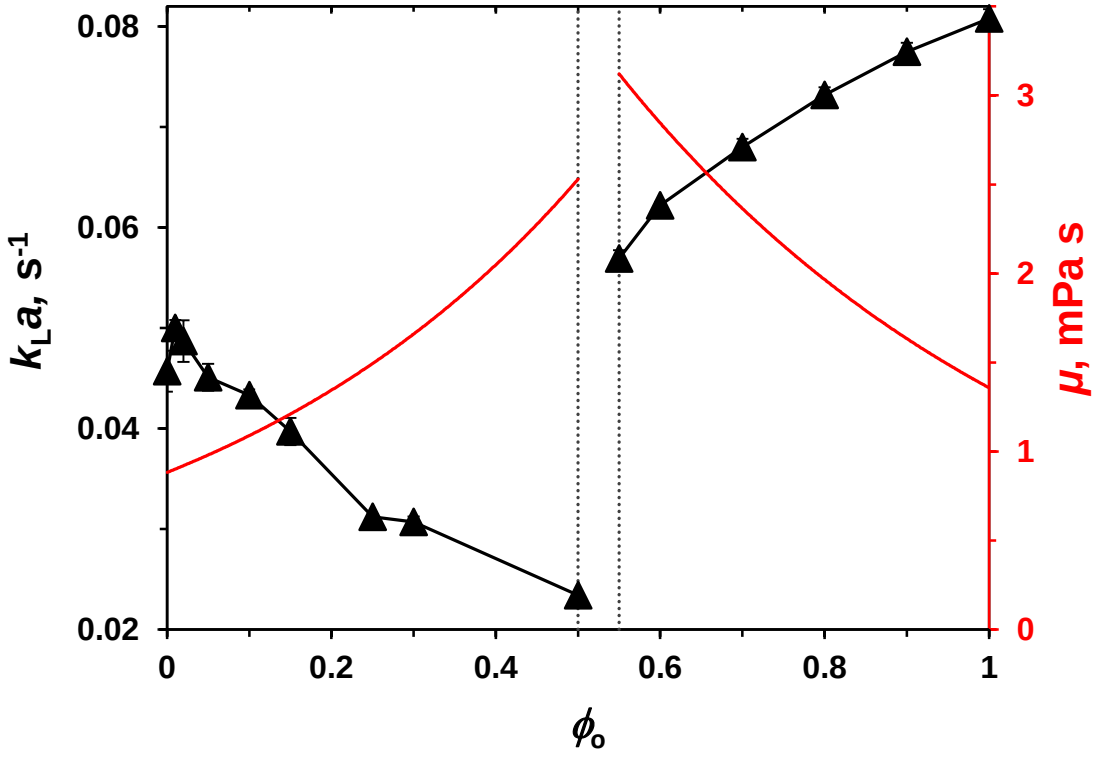

Fig. 32 Effect of n-dodecane volume fraction and emulsion viscosity on k_La (... phase inversion).

Considering the presence of small oil droplets in the mass transfer film and rapid exchange of gas between the dispersed oil and continuous aqueous phase, the shuttle mechanism could result in the additional transport mechanism (cf. Chapter 3). The effect was observed by several authors (Hassan and Robinson, 1977; Cents *et al.*, 2001; Zhang *et al.*, 2010). Ngo and Schumpe (2012b) reported relative oxygen solubilities of 7.7 and 6.5 for n-dodecane, and n-hexadecane, respectively. Then, the effect should be stronger for oxygen than for carbon dioxide but the k_La maxima were similar as for CO_2.

At higher oil fractions, the mass transfer rate decreases towards the phase inversion region, because of a considerable increase of the viscosity (Fig. 31 and 32).

The influence of the addition of n-heptane on k_La is presented in Figure 33. The behavior of n-heptane emulsions appears to be anomalous. With increasing oil volume fraction,

k_La first increases, passes through a maximum, then decreases to a minimum at 10% oil volume fraction and increases again.

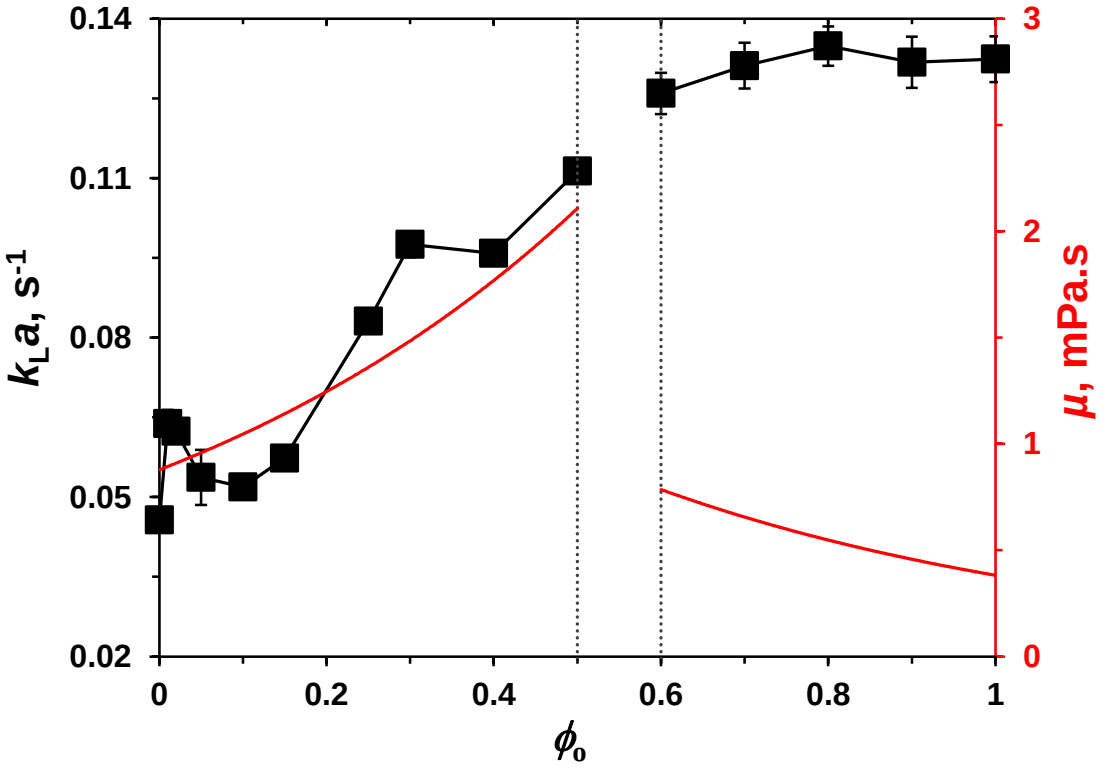

Fig. 33 Effect of n-heptane volume fraction and emulsion viscosity on k_La (... phase inversion).

Up to 10% volume fraction the behavior is similar to the other systems but then k_La strongly increases up to phase inversion. Similar behavior had been previously observed for toluene-in-water in an agitated vessel by Yoshida *et al*. (1970). The tendency of n-heptane to spread as a thin film on the gas bubble surface could be the reason. Lower surface tension of n-heptane might lead to higher interfacial area. This is in good agreement with the conclusion of Drelich and Miller (2000). They found n-heptane spreads spontaneously at the water surface while n-dodecane and n-hexadecane never tend to form a thin film on the surface, but rather remain as lenslike drops due to their negative spreading coefficients (Table 10).

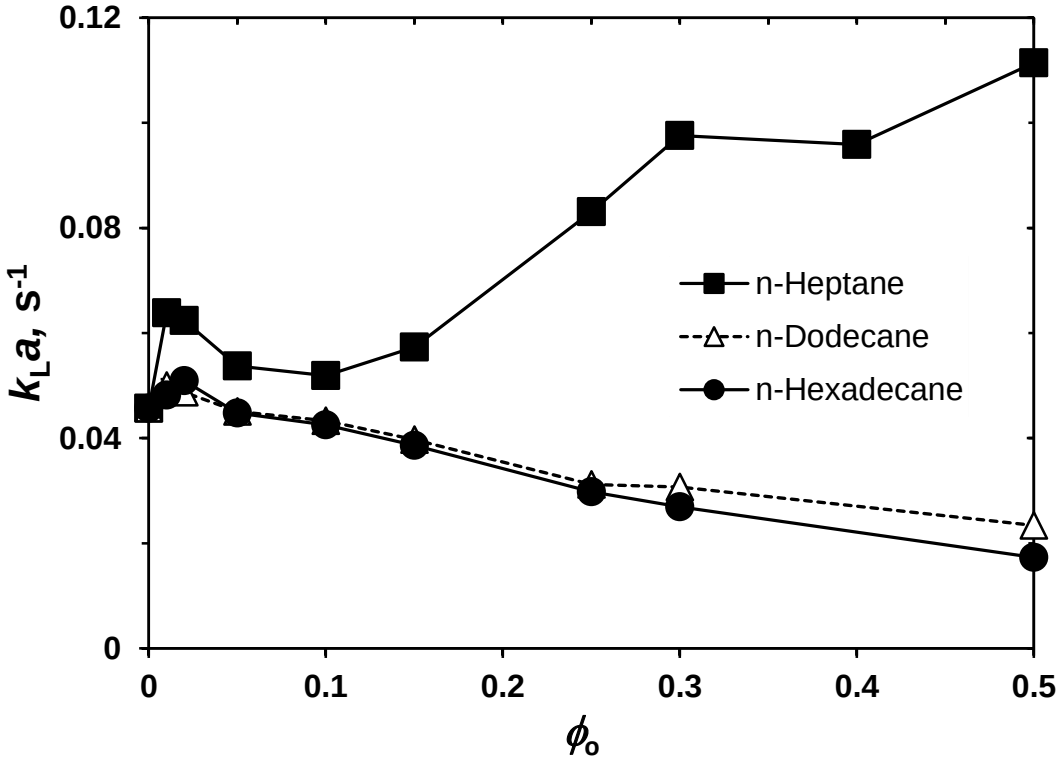

Fig. 34 Dissimilarity between n-heptane/water and other emulsions.

After phase inversion, in W/O emulsions, k_La is reduced by increasing the volume fraction of the dispersed aqueous phase. Such behavior has been previously observed for argon mass transfer into oleic acid emulsion by Linek and Beneš (1976). According to these authors, a parallel transfer of gas to both the continuous and the dispersed phase is the only possible pathway for gas absorption in W/O emulsions with either negative or positive spreading coefficient. They discussed that gas in the W/O emulsions is in direct contact with both the dispersed phase and the continuous liquid phase. The other possible pathway is gas transfer in series. In this case, the gas is not in the direct contact with the aqueous phase. They rejected this mechanism as the increase in the mass transfer coefficient could not be only due to the presence of oil around the bubbles. In contrast, Ngo and Schumpe (2012a) reported an increase in k_La for n-heptane and n-dodecane with decreasing water content. They used an endoscopic photographic technique in order to find any explanation for such strange behavior, *e.g.*, multiple emulsions of oil in water in oil droplets (O/W/O) which might been formed just before phase inversion from W/O to

O/W (Pal, 1993; Perazzo *et al*., 2015) (Fig. 35a). No multiple emulsion was detected by Ngo and Schumpe (2012a) (Fig. 35b) so that they were not able to give an explanation for the surprising trends.

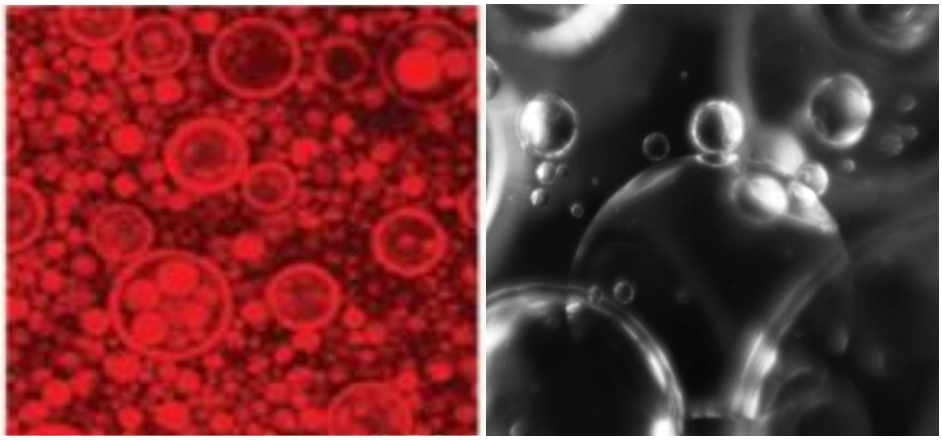

a **b**

Fig. 35 a) Multiple toluene/water emulsion (φ_O =50%) (Besnard *et al*., 2013); b) n-dodecane/water emulsion (φ_O =70%) (Ngo and Schumpe, 2012a).

Unfortunately, there is a lack of reported results in the literature regarding gas absorption rate in W/O emulsions.

The absorption rate in both O/W and W/O emulsions is dominated by oil viscosity:

$$\mu_{Hexadecane} > \mu_{Dodecane} > \mu_{Heptane} \implies k_L a_{Hexadecane} < k_L a_{Dodecane} < k_L a_{Heptane}$$

5.1.2.2 Surfactant effect on $k_L a$

The volumetric mass transfer coefficient values in the presence of surfactant depend on the type of surfactant and its concentration (Vázquez *et al*., 1997; Álvarez *et al*., 2000; Chen *et al*., 2013). High specific interfacial area plays a major role at low surfactant concentration while mass transfer resistance gains increasing significance at higher concentration (Kadic and Heidel, 2010).

The variation of the volumetric mass transfer coefficient in the presence of SDS for n-heptane and n-hexadecane systems is shown in Figure 36. There still is a maximum at very low oil fraction but the general trend is a decrease towards the phase inversion region due to viscosity effect in O/W and W/O emulsions.

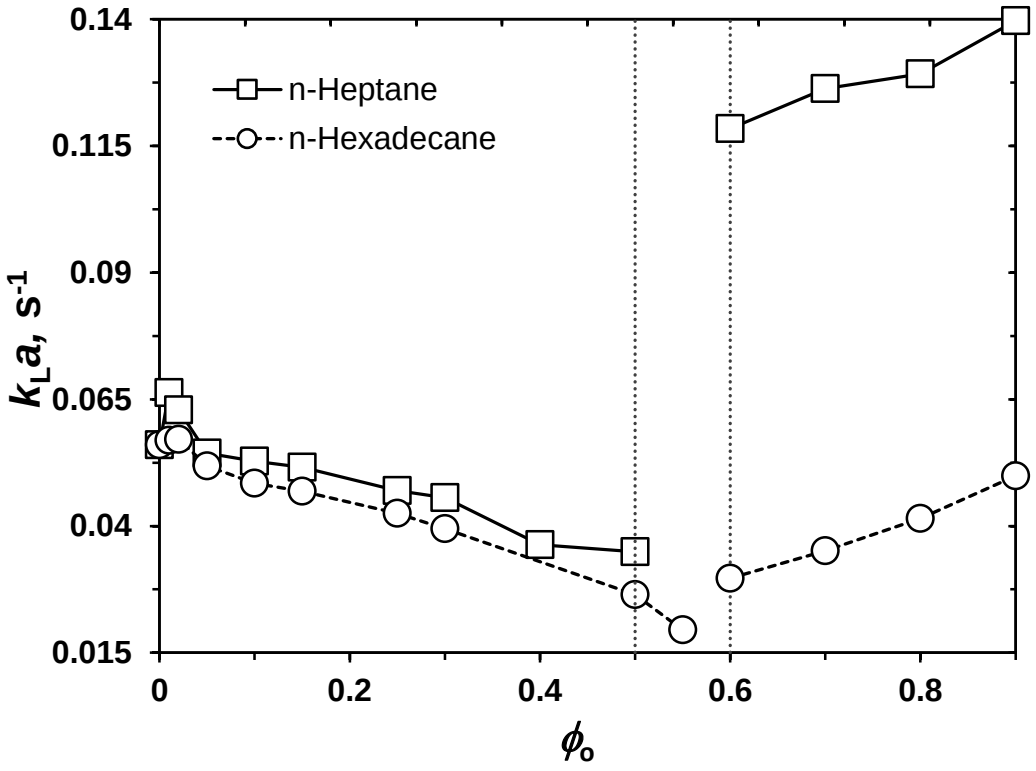

Fig. 36 Surfactant effect on $k_L a$
(... phase inversion).

Figures 37 and 38 compare the $k_L a$ values for carbon dioxide with and without surfactant for n-heptane/ and n-hexadecane/water emulsions, respectively.

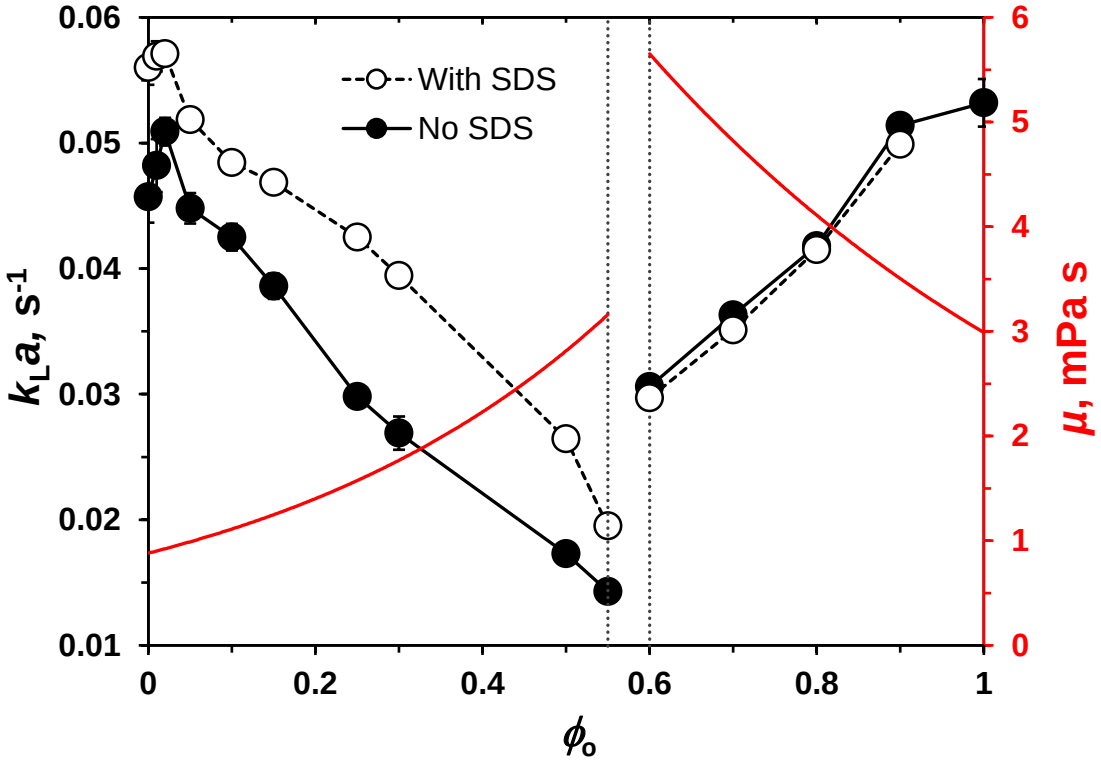

Fig. 37 Surfactant effect on k_La in n-hexadecane/water emulsion (... phase inversion).

It is not surprising that the volumetric mass transfer coefficient of carbon dioxide in O/W emulsion shows higher values in the presence of SDS because of the surfactant's ability to form a layer at the gas/liquid interface. The rate of bubble coalescence and hence the mean bubble size is reduced.

When a surfactant is added to emulsions, it tends to migrate to the oil-water interface where it acts to decrease the interfacial tension (Table 14). At the G/L interface the interfacial area increases by bubble coalescence inhibition. It can be concluded that the interfacial area is large enough to offset any liquid side mass transfer coefficient decrease so that k_La is larger with the use of SDS. Also, the soluble surfactants like SDS add no measurable resistance to the mass transfer passage through the gas-liquid interface (Springer and Pigford, 1970; Hanwright *et al*., 2005; Farajzadeh *et al*., 2007; Preziosi *et al*., 2013).

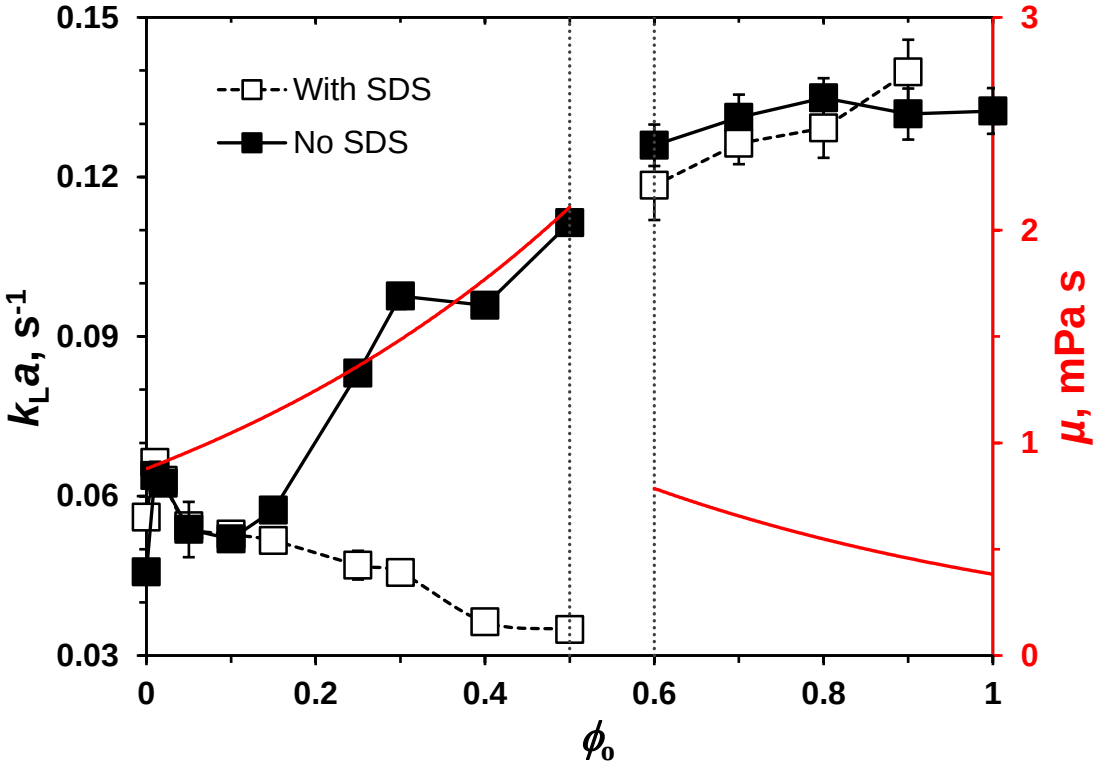

Fig. 38 Surfactant effect on k_La in n-heptane/water emulsion (... phase inversion).

Although surfactant-free n-heptane-in-water (O/W) emulsions showed strange behavior, the addition of SDS retards the mass transfer rate and induces the same oil volume fraction effect as for the two other alkanes.

In W/O emulsions, the surfactant has no significant effect on the mass transfer rate as it is located on the liquid/liquid interface and the bubbles are in contact with the pure organic liquid.

5.1.3 Oil volume fraction effect on the enhancement factor

The physicaal enhancement factors E (ratio of k_La to that the pure continuous phase) were calculated from Equation 26 and are presented in the following figures (Fig. 39 and Fig. 40).

The oil volume fraction effects on the enhancement factor are similar for n-hexadecane and n-dodecane. It first increases up to a maximum value of 1.11, 1.02 and 1.09 for n-hexadecane without and with SDS and for n-dodecane, respectively. A rapid decrease is found with increasing oil volume fraction towards the phase inversion.

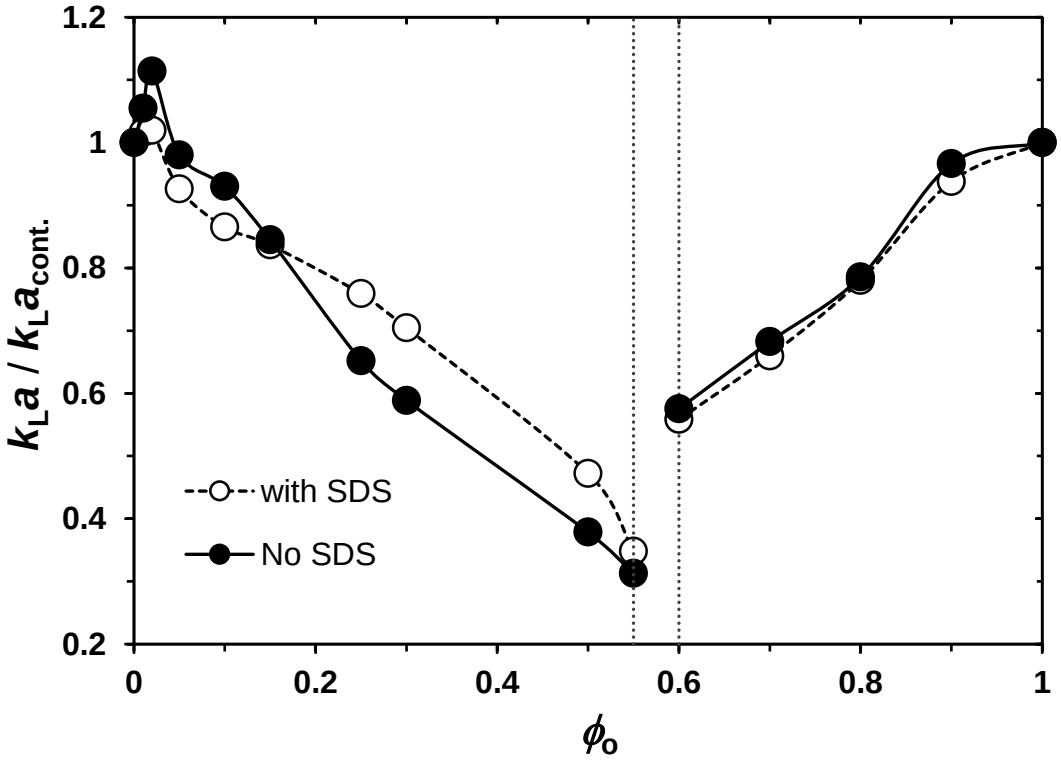

Fig. 39 Enhancement factor for n-hexadecane/water emulsions.

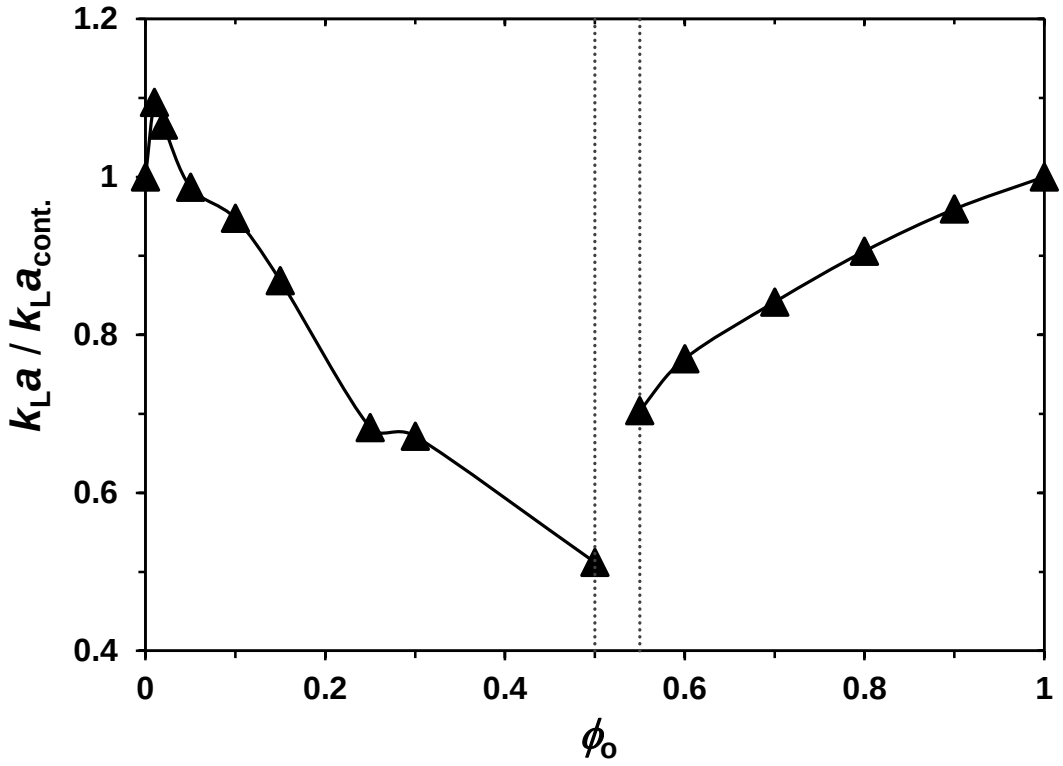

Fig. 40 Enhancement factor for n-dodecane/water emulsions.

For n-heptane-in-water emulsions without surfactant, mass transfer enhancement was observed at any oil volume fraction up to the phase inversion region (Fig. 41). We conclude that n-heptane forms a very thin layer on the bubble surface.

Addition of the ionic surfactant SDS reduces the mass transfer rate, probably by inhibiting spreading of n-heptane on the bubble surface. This finding supports the explanation of Ngo and Schumpe (2012a), *i.e.*, the bubble covering mechanism.

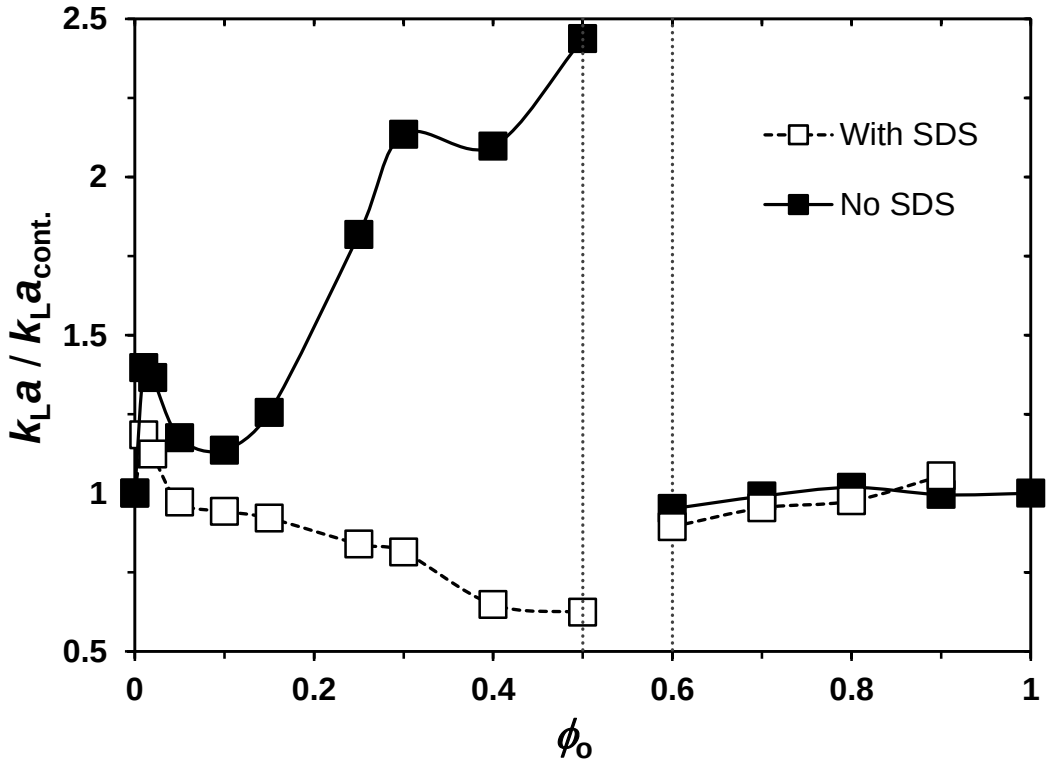

Fig. 41 Enhancement factor for n-heptane/water emulsions.

In W/O emulsions, as expected, the enhancement factor decreases towards the phase inversion region with increasing dispersed water fraction for all systems studied.

5.1.4 Down- vs. up-pumping impellers

5.1.4.1 Carbon dioxide mass transfer coefficient

Volumetric mass transfer coefficients for the UPBI and DPBI are compared in Figures 42-44.

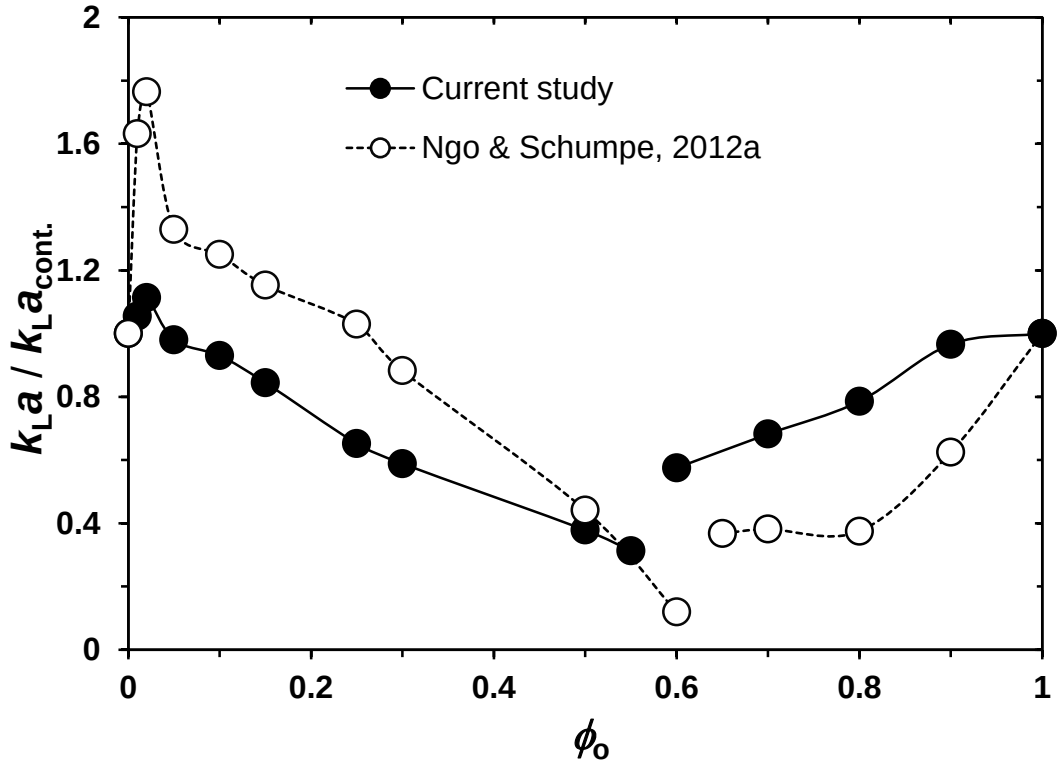

Fig. 42 Comparison of k_La values in n-hexadecane/water emulsions for a down- and an up-pumping impeller.

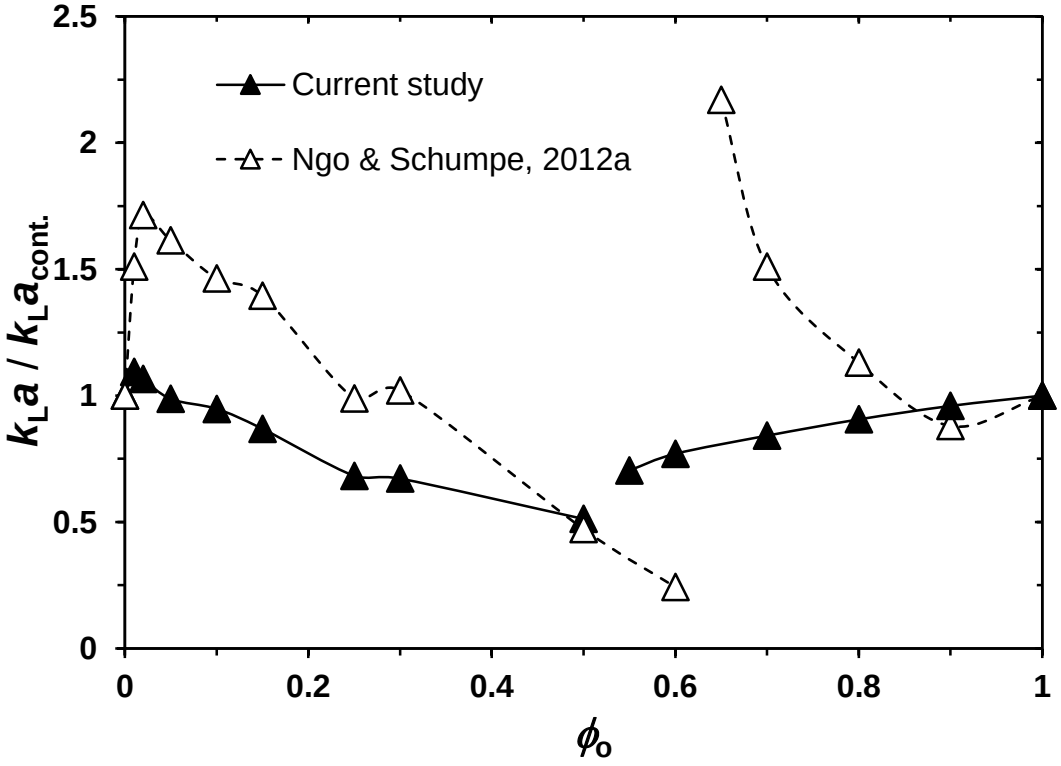

Fig. 43 Comparison of k_La values in n-dodecane/water emulsions for a down- and an up-pumping impeller.

For oil-in-water emulsions of n-dodecane and n-hexadecane, similar trends was observed by Ngo and Schumpe, 2012a.

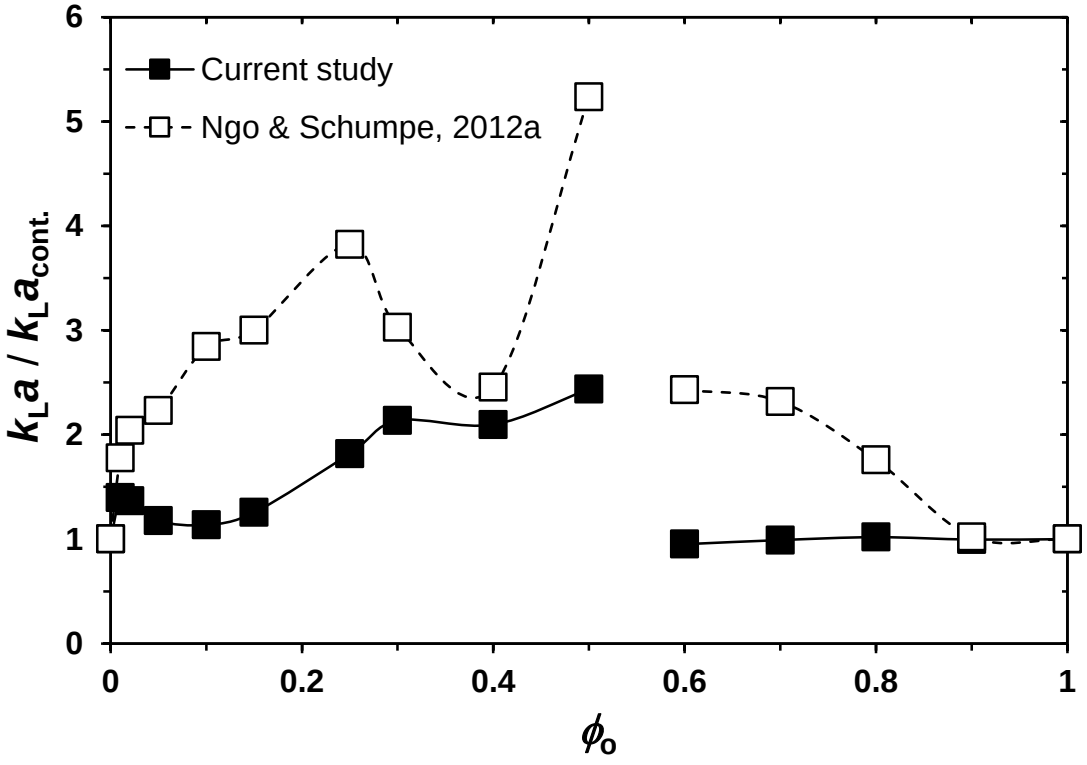

Fig. 44 Comparison of k_La values in n-heptane/water emulsion for a down- and an up-pumping impeller.

Ngo and Schumpe (2012a), observed a surprising increase in k_La, for both n-dodecane and n-heptane, from 100% oil volume fraction down to the phase inversion region. However, our results for the DPBI show a reduction with increasing W/O emulsion viscosity, as expected.

Generally, the volumetric mass transfer coefficients for UPBI are higher than that of the down-pumping impeller. This could be explained by the fact that in the down-pumping mode only one circulation loop is produced and the mixing in the upper part of the tank is very poor while UPBI produces two circulation loops in the lower and upper part of the tank resulting better circulation and mixing (Mishra *et al*., 1998; Aubin *et al*., 2001).

Furthermore, Sardeing *et al*. (2004b) argued that the UPBI generated the stronger lower circulation loop which keeps the gas bubbles in the lower half of the tank for a long time, resulting in improved mass transfer (Fig. 45).

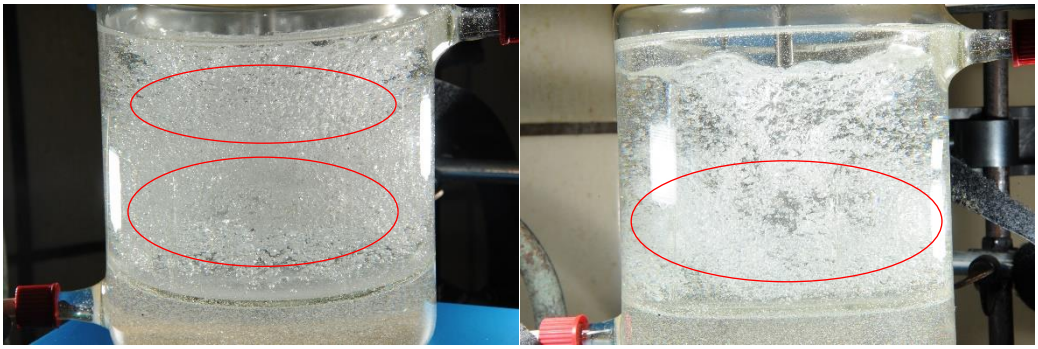

a **b**

Fig. 45 Flow pattern for a) downward and b) upward pumping impellers at 1000 rpm.

5.1.5 Volumetric mass transfer coefficient as a function of viscosity

From the literature overview it can be concluded that several dimensional correlations have been proposed for the calculation of $k_L a$ in stirred vessels for different liquids. $k_L a$ can be predicted as follows:

$$k_L a \propto C\, V_s^a\, N^b\, \mu^c \tag{53}$$

The exponent values (a, b and c) change for different authors, also being influenced by the tank configurations (stirrer types and diameter), liquid properties (density, viscosity and surface tension) and operational conditions (stirrer speed and gas superficial velocity) (Yagi and Yoshida, 1975; García-Ochoa and Gómez, 2004). Also the presence of surfactant could affect interfacial area and mass transfer coefficient values.

Figures 46 and 47 are log-log-plots of $k_L a$ (related to the $k_L a$ value in the pure continuous phase) against relative viscosity (related to the viscosity of the pure continuous phase) for

the O/W and the W/O emulsions, respectively. In O/W emulsions all systems (except for SDS-free n-heptane) follow the same trend (Fig. 46):

$$k_L a \propto \mu^{-0.72} \tag{54}$$

It is clear that the anionic surfactant SDS can eliminate the high absorption rate in n-heptane/water and induces the normal viscosity effect like all other systems. It was suggested by Ngo and Schumpe (2012a) that the high absorption rate in the absence of SDS is due to the bubble covering mechanism. Our results can be considered as an indirect proof of the oil spreading effect. Presence of the ionic surfactant on the gas/water interface might disturb heptane spreading and change the mass transfer pathway from serial transport (gas→oil→water) or parallel transport (gas→oil and gas→water) to the same serial transport (gas→water→oil) as with the other oils.

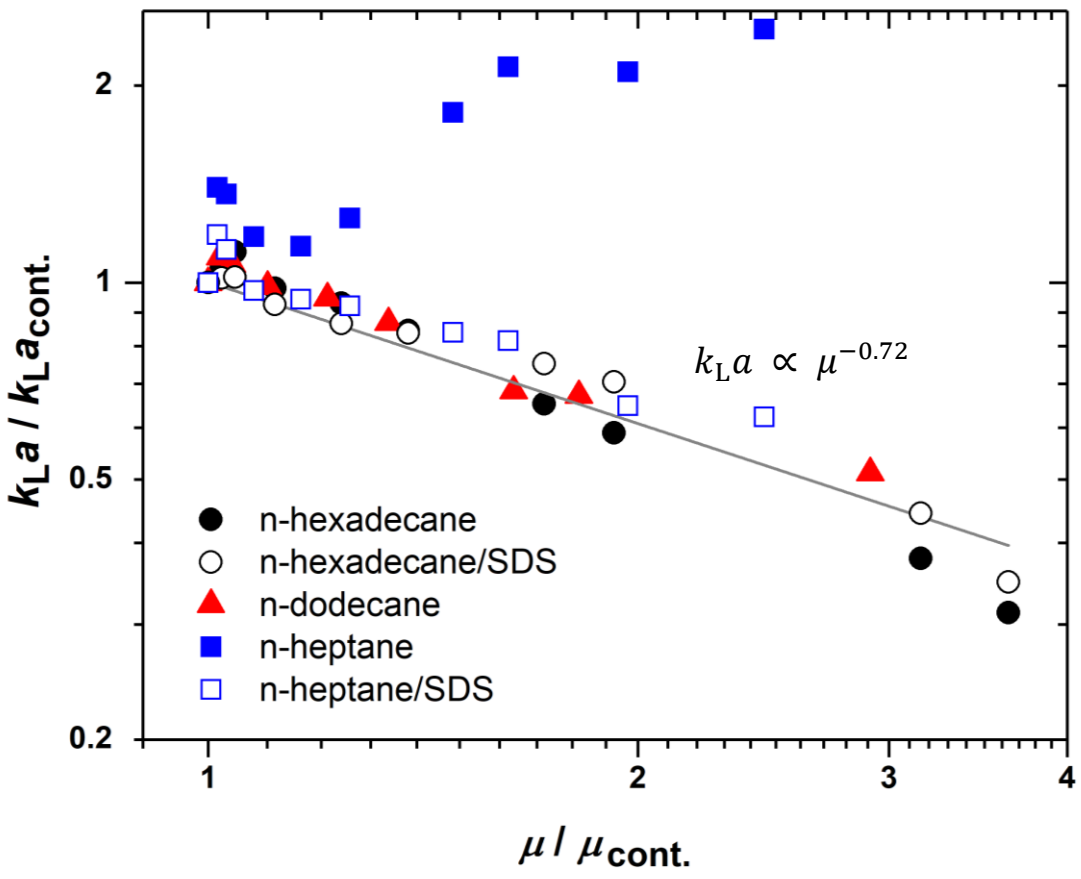

Fig. 46 Viscosity effect on $k_L a$ in oil-in-water emulsions.

In water-in-oil systems, the volumetric mass transfer coefficient sinks with increasing viscosity but this effect is specific to the oil (Fig. 47). Addition of surfactant has no effect on the mass transfer rate since SDS is located at the liquid-liquid interface and there is no direct contact with the gas.

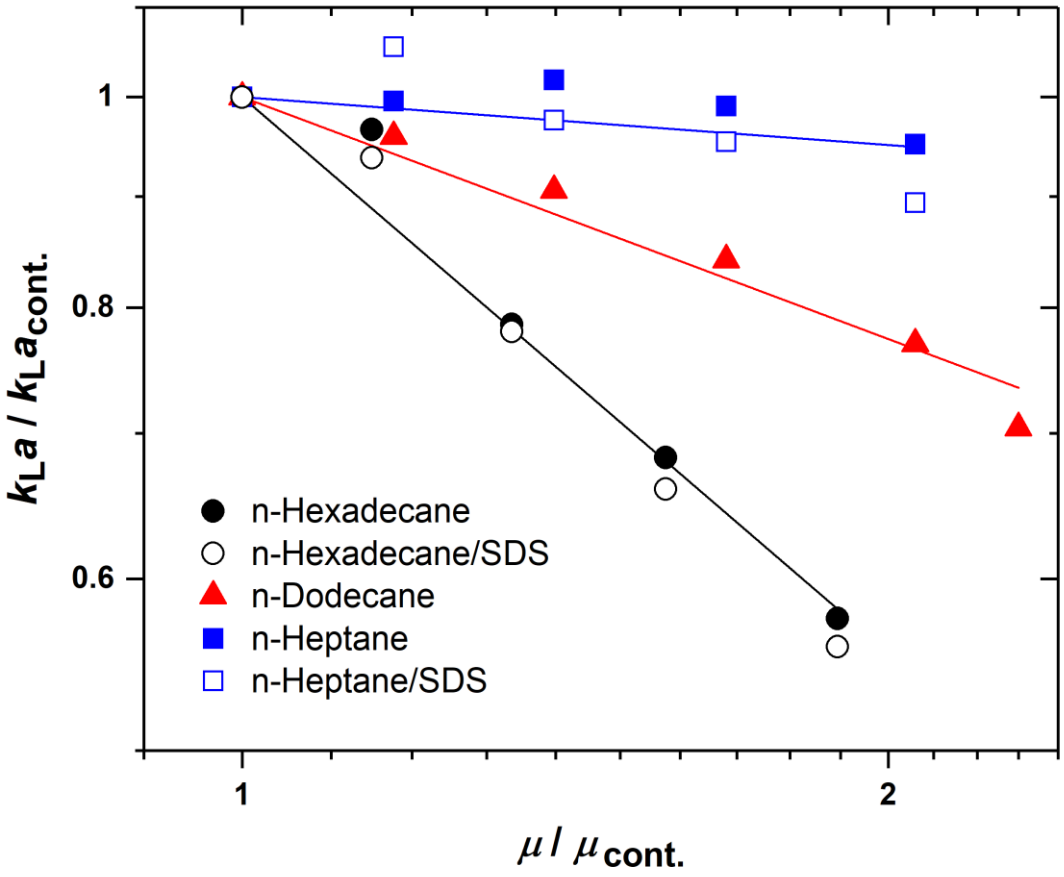

Fig. 47 Viscosity effect on k_La in water-in-oil emulsions.

There are quite different trends for the three organic liquids. In addition to the viscosity effect of the dispersed aqueous phase, there are specific effects of the continuous organic liquid. These effects are smaller than observed by Ngo and Schumpe (2012a) in the up-pumping mode but the order of the k_La values is the same (n-heptane > n-dodecane > n-hexadecane). When k_La is correlated with the power-law (Equation 53), it shows dependence to $(\mu/\mu_{cont.})^c$ with the exponent value -0.04 (n-heptane), -0.40 (n-dodecane)

and -0.82 (n-hexadecane). The results of Ngo and Schumpe (2012a) show much more variation and cannot be correlated to the emulsion viscosity (Fig. 48)

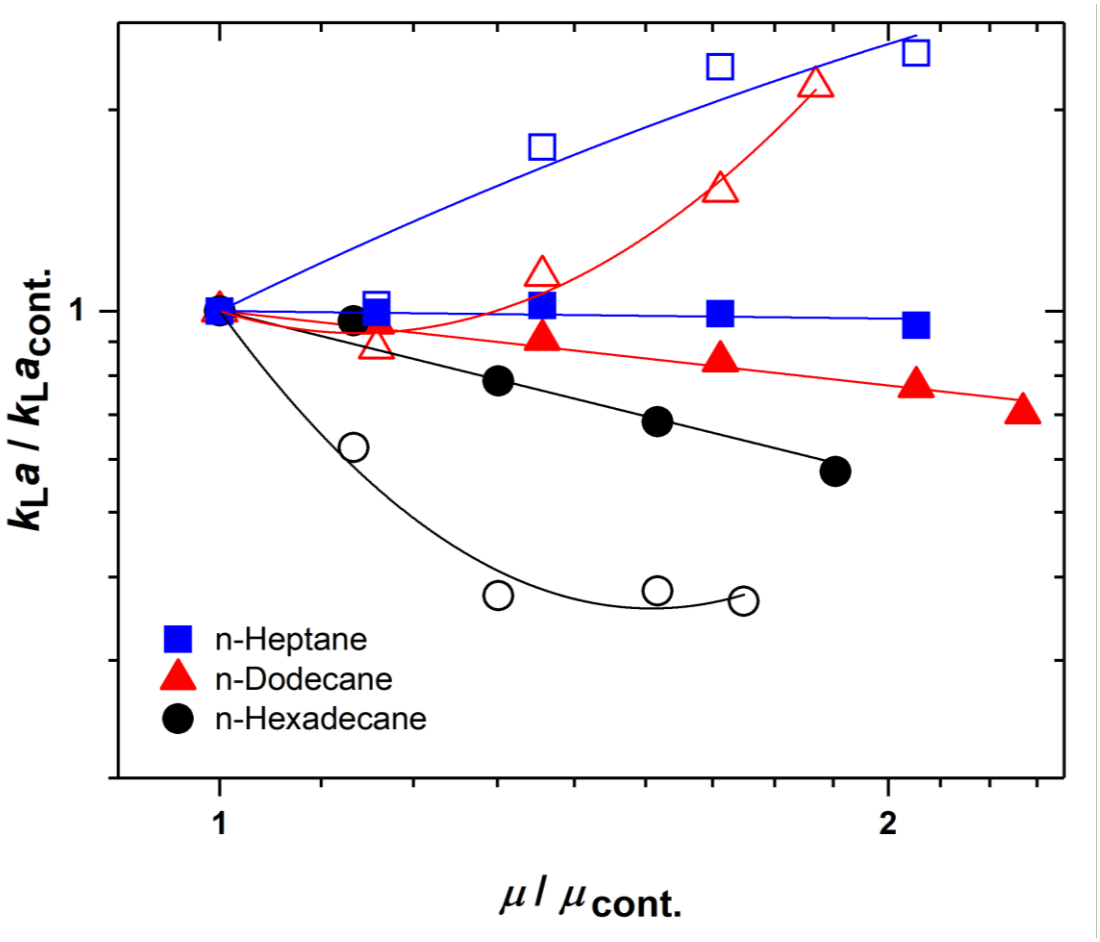

Fig. 48 Viscosity effect on k_La in water-in-oil emulsions for a down-pumping impeller (this study, filled symbols) and an up-pumping impeller (Ngo and Schumpe, 2012a, open symbols).

Various investigations have been carried out to measure the influence of the viscosity on the mass transfer coefficient and different values have been reported in the literature. For instance, Yagi and Yoshida (1975) reported the exponent value of -0.4, Nocentini *et al*. (1992) proposed an exponent of -0.25 for low-viscosity liquids and -0.375 for high viscosity liquids, García-Ochoa and Gómez (2004) found it ranging from -0.5 to -0.9.

5.2 Chemical Absorption

Figure 49 represents the decrease of sulfite concentration in the stirred reactor for various n-hexadecane volume fractions and the much slower decrease in the beaker with plane interface. Essentially, the ratio of the slopes reflects the ratio of the specific interfacial areas.

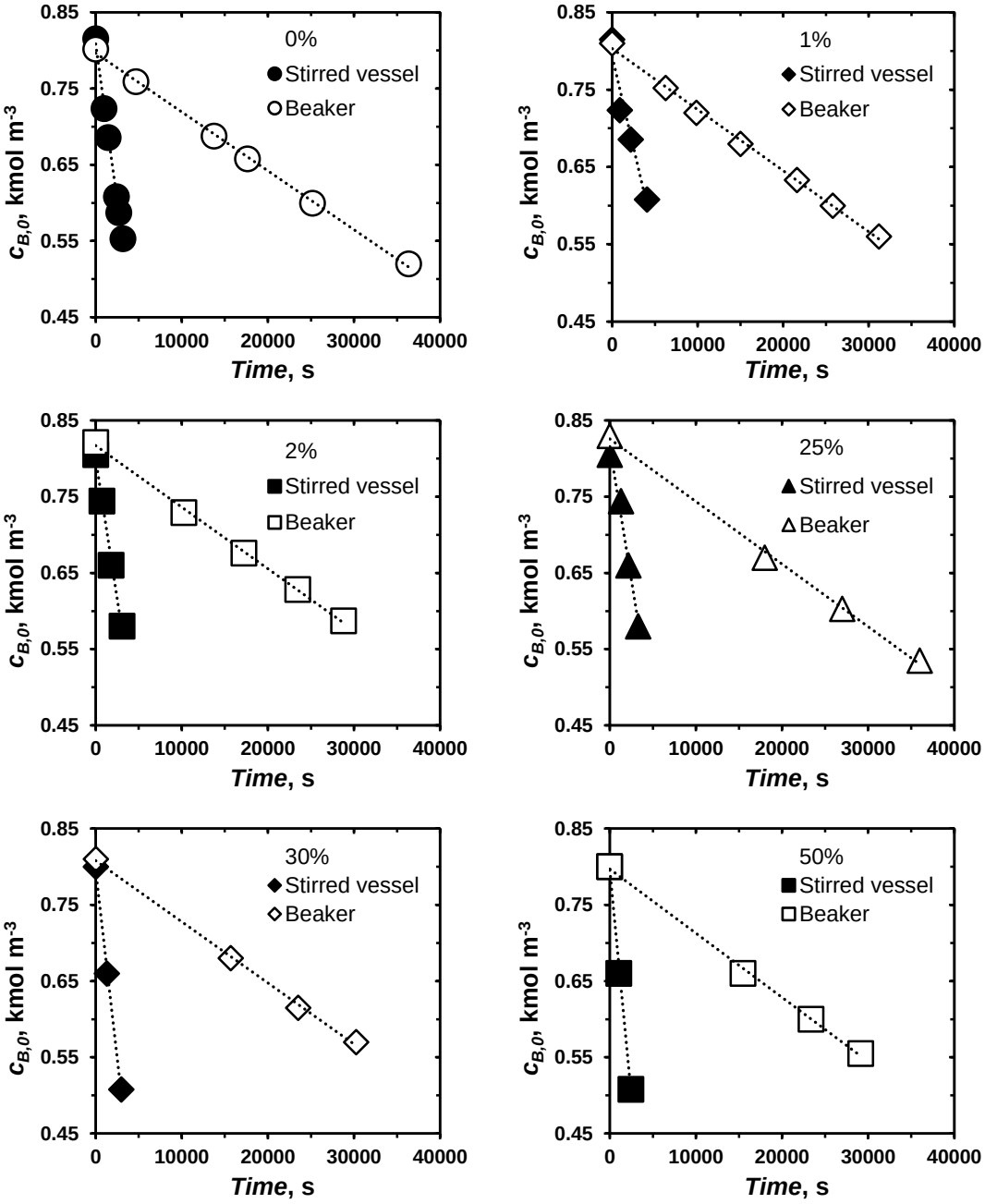

Fig. 49 Variation of the sulfite concentration in the vessel with flat interface (no oil) and in the stirred vessel with desired oil fraction.

For the runs in the vessel with flat interface, the decrease of the sodium sulfite concentration is compared in Figure 50. There is a slight curvature, *i.e.*, the oxidation rate decreases very slightly, probably, due to the effect of increasing pH value. Ignoring this trend, the slopes of straight line fits for different runs are very similar (Table 16). The value of the absorption parameter K_2 (defined in Eq. 48) is slightly but systematically lower than the value calculated based on literature data. This underlines the advantage of the experimental approach.

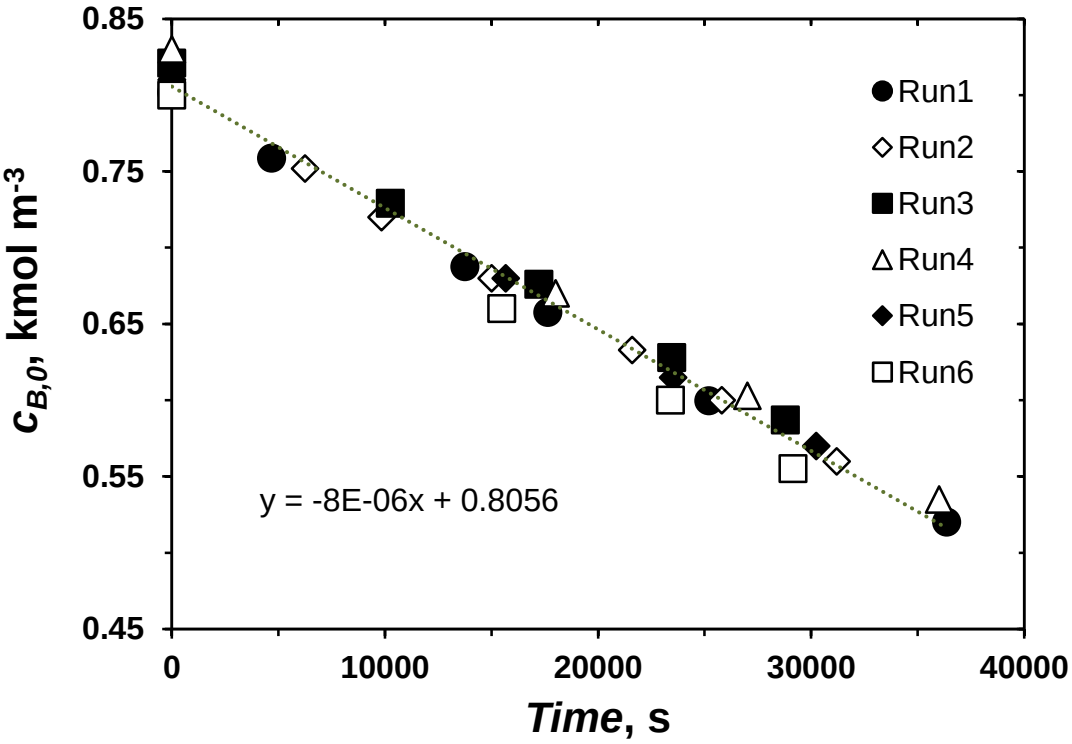

Fig. 50 Variation of the sulfite concentration in the vessel with flat interface (same symbols as in Fig. 49).

Table 16

Comparison of the overall absorption coefficients experimentally determined and calculated from Eq. 48.

K_2	$K_{2,calc.}$	*Difference%*
kmol m^{-2} s^{-1} $Pa^{-1.5}$		
7.50×10^{-14}	7.79×10^{-14}	3.8

The time-course of the sulfite concentration in the stirred vessel is shown in Figure 51 for various oil fractions. The oxygen is absorbed in the dispersed organic phase physically and in the continuous aqueous phase chemically. There might be a parallel pathway if the dispersed droplets can be in direct contact with the gas phase. The effect of volume fraction of the dispersed organic phase on sulfite oxidation is quite clear from this figure: It shows that at higher oil volume fraction the fall in sulfite concentration becomes steeper. This is expected even for the same absorption rate since the sulfite loading decreases with increasing oil fraction.

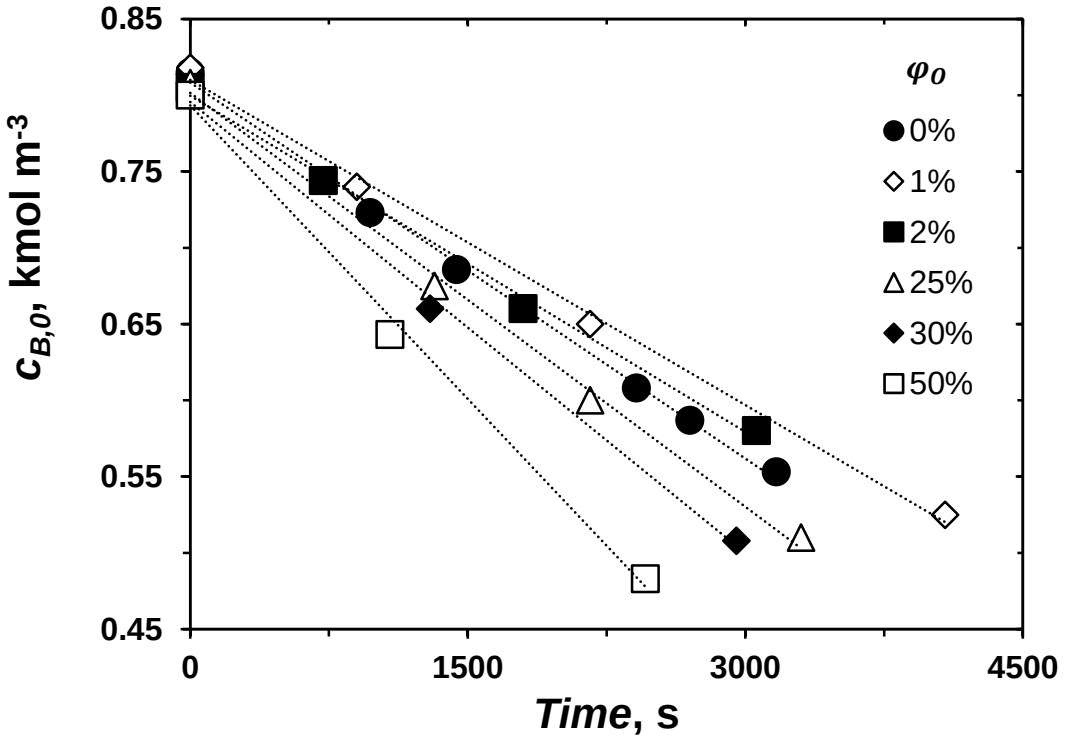

Fig. 51 Time-course of the sodium sulfite concentration in the stirred vessel with n-hexadecane emulsions.

The effect of oil volume fraction and viscosity on the interfacial area values are represented in Figures 52 and 53, respectively. A reduction in interfacial area with increasing oil volume fraction is observed in the figures. This can be attributed to increasing bubble coalescence rate. The viscosity effect on interfacial area was also observed by Vázquez *et al*. (2000) and Yoshimoto *et al*. (2007). It is particularly interesting that there is a clear drop in interfacial area at very low oil fractions of 1–2% where $k_L a$ showed a maximum. It may be concluded that the $k_L a$ maximum is not caused by coalescence hindering. The shuttle mechanism is still a possible mechanism since it may not be effective due to smaller effective film thickness in the absorption regime of fast chemical reaction. Assuming a k_L value of 0.032 cm s^{-1} (Schumpe *et al*., 1986), the Hatta number was about 5.2 and with a diffusion coefficient of 1.6×10^{-5} cm^2 s^{-1} (Eq. 49) the effective film thickness (Eq. 55) was:

$$\delta_{eff} = \frac{D_{O_2}}{Ha\, k_L} = 9.6 \times 10^{-5} \text{ cm} \qquad (55)$$

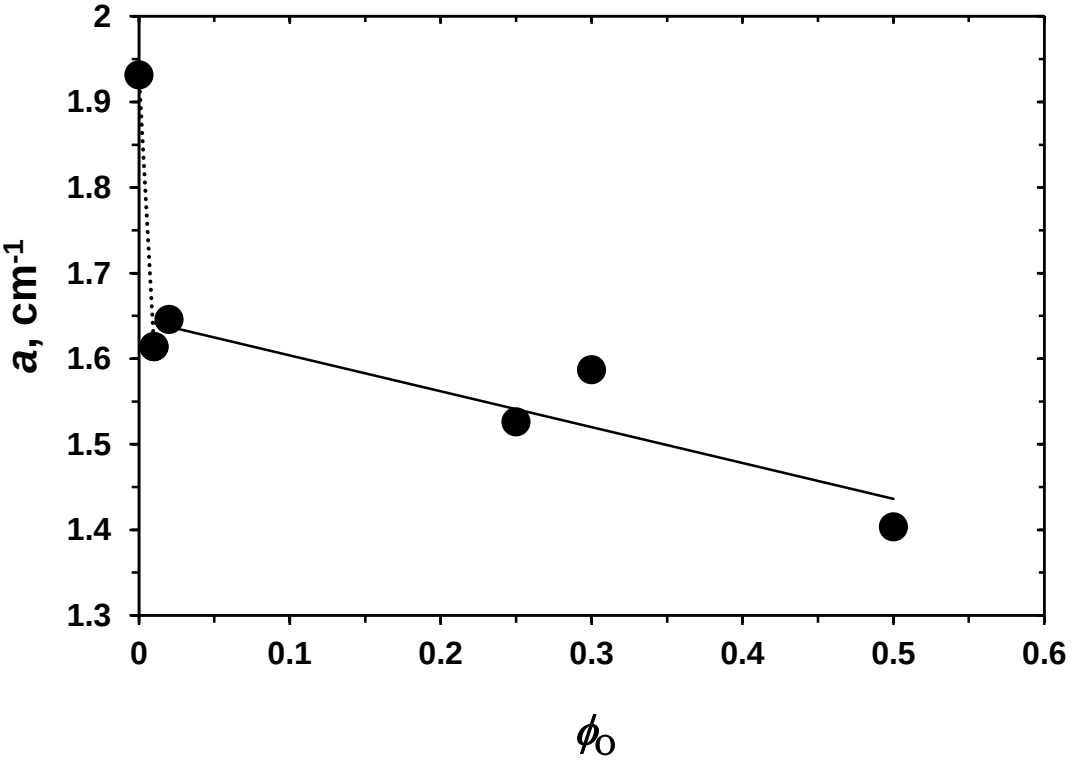

Fig. 52 Effect of n-hexadecane volume fraction on the interfacial area.

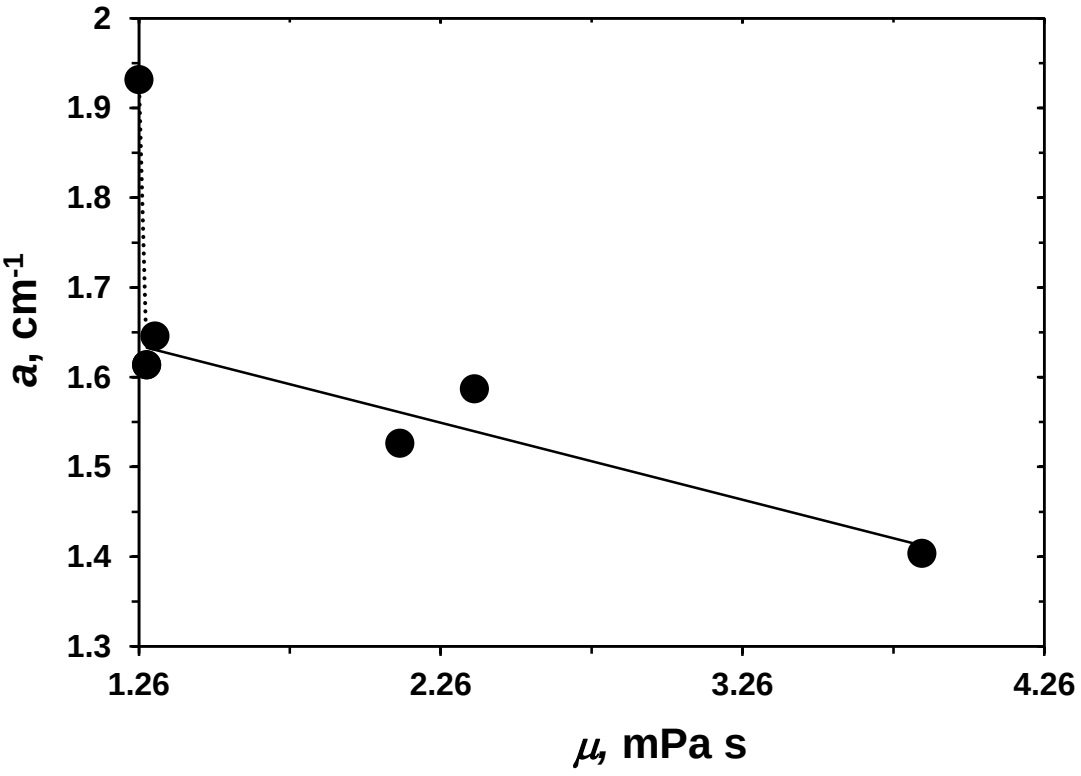

Fig. 53 Effect of viscosity on the interfacial area.

The decrease in interfacial area in the presence of organic liquids was also observed by Cents *et al*. (2001). Except for low oil volume fraction this reduction reflects our results obtained from physical absorption. It can be considered that the variation of overall volumetric mass transfer coefficient is due to alteration of specific interfacial area since increasing viscosity promotes bubble coalescence. However, the reduction in interfacial area is less effective on the $k_L a$ decrease; this indicates an additional effect on k_L.

This research was done with the objective to understand the underlying mass transfer phenomena in gas-liquid-liquid systems. It should be pointed out that for interpreting $k_L a$ values it is essential to separate the interfacial area and the liquid side mass transfer coefficient. $k_L a$ values to be compared with the specific interfacial areas determined by sulfite oxidation could be measured by physical absorption of pure oxygen in sodium sulfate solutions in the presence of oil. Specifically in the case of n-heptane this might

have improved the understanding of the spreading coefficient. Unfortunately, the experiments came to a sudden stop when the laboratory was closed because of insufficient fire hazard precautions in the building.

Chapter 6

Conclusions

The volumetric mass transfer coefficient $k_L a$ and the solubility of carbon dioxide was determined by physical absorption in a surface-aerated stirred vessel at a high stirring speed (1000 rpm). The experiments were carried out for three different n-alkanes (n-heptane, n-dodecane and n-hexadecane) at 0–100% oil volume fraction. Additionally, the effect of the anionic surfactant sodium dodecyl sulfate (SDS) was studied at 0.22 g L^{-1} in the aqueous phase. Some preliminary experiments were performed to determine the specific interfacial area in O/W emulsions of n-hexadecane by cobalt-catalyzed sulfite oxidation.

For n-hexadecane and n-heptane, the solubility of carbon dioxide varied linearly with the oil volume fraction. Addition of SDS had no significant effect on the gas solubility in n-hexadecane emulsions. For n-heptane emulsions, the gas solubility deviated from linear interpolation but addition of SDS reduced the deviation. This reflects some of the trends observed for mass transfer.

The volumetric mass transfer coefficient $k_L a$ showed a maximum at oil volume fractions of 1–2%, for all organic liquids studied. At the same low n-hexadecane loadings, the specific interfacial area determined by sulfite oxidation dropped from the value in oil-free sulfite solutions. This excludes a coalescence hindering effect of the oil often suggested in the literature. An additional transport mechanism (shuttle effect) could still be an explanation as this would be less effective at the smaller effective film thickness in the absorption regime of fast chemical reaction (Ha ≈ 5.2).

Upon further increase in oil fraction, for all O/W emulsions (except surfactant-free n-heptane), $k_L a$ decreased towards the phase inversion region because of the viscosity effect. This trend can be uniformly correlated with emulsion viscosity to the power of -0.72. The decrease in interfacial area is less strong; this indicates an additional effect on k_L.

Different from the other oils, the addition of n-heptane increased $k_L a$ even up to the phase inversion region. This trend had been observed previously and was tentatively attributed to bubble covering by oil spreading. In this study, addition of the ionic surfactant SDS

eliminated the high mass transfer rates in n-heptane emulsions and induced the same viscosity effect as in the other W/O emulsions. This indicates that spreading of n-heptane on the bubble surface is indeed the mechanism causing the high absorption rates.

In W/O emulsions, $k_L a$ decreased with increasing dispersed water volume fraction for all emulsions studied. The trends cannot be uniformly correlated to the volume fraction or the viscosity, respectively, but depend on the oil. SDS had no effect on $k_L a$ in W/O emulsions as it accumulates at the oil/water interface without having contact to the gas bubbles.

Higher mass transfer rate was observed by Ngo and Schumpe (2012a) in the up-pumping mode. Up-pumping pitched blade impeller induces two strong circulation loops, one in the upper part of the tank and one in the lower part while down pumping pitched blade impeller produces only one circulation loop in the lower half of the tank. Due to two circulation loops, the gas bubbles are forced down into the liquids for longer time resulting in higher volumetric mass transfer coefficient.

Further sulfite oxidation experiments, in comparison with physical absorption into emulsions with sodium sulfate solutions as the aqueous phase, had been planned and might have enabled more insight. Unfortunately, the experiments came to a sudden stop when the laboratory was closed.

Appendix A: $k_L a$ values for different oil/water emulsions at 25˚C

Table A1

$k_L a$ values for n-heptane/water emulsions.

φ_O	0	0.01	0.02	0.05	0.1	0.15	0.25	0.3	0.4	0.5	0.6	0.7	0.8	0.9	1
$k_L a$, s^{-1}	0.046	0.064	0.062	0.054	0.052	0.057	0.083	0.098	0.096	0.111	0.126	0.131	0.135	0.132	0.132
Stdev.%	0.14	0.26	0.17	0.52	0.12	0.22	0.14	0.24	0.15	0.23	0.39	0.43	0.37	0.48	0.43

Table A2

$k_L a$ values for n-dodecane/water emulsions.

φ_O	0	0.01	0.02	0.05	0.1	0.15	0.25	0.3	0.5	0.55	0.6	0.7	0.8	0.9	1
$k_L a$, s^{-1}	0.046	0.050	0.049	0.045	0.043	0.04	0.031	0.031	0.023	0.057	0.062	0.068	0.073	0.078	0.081
Stdev.%	0.20	0.08	0.21	0.13	0.06	0.13	0.03	0.06	0.03	0.08	0.04	0.08	0.07	0.09	0.09

Table A3

$k_L a$ values for n-hexadecane/water emulsions.

φ_O	0	0.01	0.02	0.05	0.1	0.15	0.25	0.3	0.5	0.55	0.6	0.7	0.8	0.9	1
$k_L a$, s^{-1}	0.046	0.048	0.051	0.045	0.043	0.039	0.030	0.027	0.017	0.014	0.031	0.036	0.042	0.051	0.053
Stdev.%	0.20	0.21	0.11	0.12	0.11	0.10	0.04	0.13	0.01	0.01	0.05	0.07	0.05	0.07	0.19

Table A4

$k_L a$ values for n-heptane /water emulsions in the presence of surfactant (0.22 g L^{-1} SDS).

φ_O	0	0.01	0.02	0.05	0.1	0.15	0.25	0.3	0.4	0.5	0.6	0.7	0.8	0.9	1
$k_L a$, s^{-1}	0.056	0.066	0.063	0.054	0.053	0.052	0.047	0.046	0.036	0.035	0.118	0.126	0.129	0.140	-
Stdev.%	0.2	0.18	0.08	0.12	0.20	0.13	0.27	0.16	0.06	0.08	0.65	0.39	0.56	0.61	-

Table A5

$k_L a$ values for n-hexadecane /water emulsions in the presence of surfactant (0.22 g L^{-1} SDS).

φ_O	0	0.01	0.02	0.05	0.1	0.15	0.25	0.3	0.5	0.55	0.6	0.7	0.8	0.9	1
$k_L a$, s^{-1}	0.056	0.057	0.057	0.052	0.048	0.047	0.043	0.039	0.026	0.02	0.03	0.035	0.042	0.05	-
Stdev.%	0.14	0.12	0.09	0.09	0.09	0.07	0.07	0.05	0.03	0.03	0.05	0.04	0.04	0.07	-

Appendix B: Comparison of $k_L a / k_L a_{cont.}$ values for down- and up-pumping impeller

Table B1

$k_L a$ values for n-heptane/water emulsions.

φ_O	0	0.01	0.02	0.05	0.1	0.15	0.25	0.3	0.4	0.5	0.6	0.7	0.8	0.9	1
DPBI	1.00	1.40	1.37	1.18	1.14	1.25	1.82	2.14	2.10	2.44	0.95	0.99	1.02	1.00	1.00
UPBI	1.00	1.78	2.04	2.23	2.84	3.00	3.82	3.03	2.46	5.24	2.43	2.32	1.76	1.02	1.00

Table B2

$k_L a$ values for n-dodecane/water emulsions.

φ_O	0	0.01	0.02	0.05	0.1	0.15	0.25	0.3	0.5	0.55	0.6	0.7	0.8	0.9	1
DPBI	1.00	1.09	1.07	0.99	0.95	0.87	0.68	0.67	0.51	0.70	0.77	0.84	0.91	0.96	1.00
UPBI	1.00	1.51	1.71	1.61	1.46	1.40	0.99	1.02	0.47	0.24	2.17	1.51	1.13	0.88	1.00

Table B3

$k_L a$ values for n-hexadecane/water emulsions.

φ_O	0	0.01	0.02	0.05	0.1	0.15	0.25	0.3	0.5	0.55	0.6	0.7	0.8	0.9	1
DPBI	1.00	1.05	1.11	0.98	0.93	0.84	0.65	0.59	0.38	0.31	0.58	0.68	0.79	0.97	1.00
UPBI	1.00	1.63	1.76	1.33	1.25	1.15	1.03	0.88	0.44	0.12	0.37	0.38	0.38	0.63	1.00

References

Aubin J., Mavros P., Fletcher D. F., Bertrand J., Xuereb C. (2001). "Effects of axial agitator configuration (up-pumping, down-pumping, reverse rotation) on flow patterns generated in stirred vessels." *Trans IChemE*, 79: 845-856.

Akita K., Yoshida F. (1974). "Bubble size, interfacial area, and liquid-phase mass transfer coefficient in bubble columns." *Industrial and Engineering Chemistry, Process Design and Development* 13(1): 84–91.

Albal R. S., Shah Y. T., Schumpe A., Carr N. L. (1988). "Mass transfer in multiphase agitated contactors." *The Chemical Engineering Journal*, 27(2): 61–80.

Alper E., Abu-Sharkh B. (1988). "Kinetics of absorption of oxygen into aqueous sodium sulfite: order in oxygen." *AIChE Journal*, 34(8): 1384–1386.

Álvarez E., Sanjurjo B., Cancela A., Navaza J. M. (2000). "Mass transfer and influence of physical properties of solutions in a bubble column." *Trans IChemE*, 78: 889-893.

Asgharpour M., Mehrnia M. R., Mostoufi N. (2010). "Effect of surface contaminants on oxygen transfer in bubble column reactors." *Biochemical Engineering Journal* 49(3): 351–360.

Astarita G., Marruci G., Gioia F. (1964). "The influence of carbonation ratio and total amine concentration on carbon dioxide absorption in aqueous monoethanolamine solutions." *Chemical Engineering Science*, 19(2): 95-103.

Barnea E., Mizrahi J. (1976). "On the ″effective″ viscosity of liquid–liquid dispersions." *Industrial and Engineering Chemistry Research Fundamentals*, 15(2): 120–125.

Bäckström H. L. J. (1934). "Der Kettenmechanismus bei der Autoxydation von Aldehyden." *Zeitschrift für physikalishe Chemie (B)*, 25(1-2): 99-121.

Bedeaux D. (1983). "The effective shear viscosity in two-phase flow for arbitrary volume fractions." *Chemical Physics Letters*, 94(3): 324–326.

Besnard L., Marchal F., Paredes J. F., Daillant J., Pantoustier N., Perrin P., Guenoun P. (2013). "Multiple emulsions controlled by stimuli-responsive." *Advanced Materials*, 25: 2844-2848.

Bińa. K., Duczmal B., Machniewski P. (2001). "Hydrodynamics and ozone mass transfer in a tall bubble column." *Chemical Engineering Science*, 56: 6233-6240.

Bird R. B., Stewart W. E., Lightfoot E. N. (2002). "Transport phenomena" *New York: John Wiley and Sons, 2nd edition*.

Bruining W. J., Joosten G. E. H., Beenackers A. A. C. M., Hofman H. (1986). "Enhancement of gas-liquid dispersed second mass transfer liquid phase." 41(7): 1873–1877.

Camacho F., Molina E., Valdés F., Andujar J. M. (1991). "Influence of operating and physical variables on interfacial area determination." *AIChE Journal*, 37(8): 1196–1204.

Calderbank P. H. (1958). "Physical rate processes in industrial fermentation. Part I: the interfacial area in gas–liquid contacting with mechanical agitation." *Transactions of the Institution of Chemical Engineers*, 36: 443–463.

Carlucci G. (2010). "Drop size distributions in stirred liquid/liquid systems influence of the dispersed phase." *Technische Universität Berlin*.

Carrol J. J., Slupsky J. D., Mather A. E. (1991). "The solubility of carbon dioxide in water at low pressure." *Journal of physical and chemical Reference Data*, 20(6): 1201-1209.

Cents A. H. G., Brilman D. W. F., Versteeg G. F. (2001). "Gas absorption in an agitated gas-liquid-liquid system." *Chemical Engineering Science*, 56(3): 1075–1083.

Chen T. I., Barron H. C. (1972). "Some Aspects of the Homogeneous Kinetics of Sulfite Oxidation." *Industrial and Engineering Chemistry Fundamentals*, 11(4): 466–470.

Chen X., Liu G., Fan H., Li M., Luo T., Qi L., Wang H. (2013). "Effects of surfactant contamination on oxygen mass transfer in fine bubble aeration process." *Korean Journal of Chemical Engineering*, 30(9): 1741–1746.

Cooper C. M., Fernstrom G. A., Miller S. A. (1944). "Performance of agitated gas-liquid contactors correction." *Industrial and Engineering Chemistry*, 36(9): 504-509.

Danckwerts P. V. (1955). "Gas absorption accompanied by chemical reaction." *AIChE Journal*, 1: 456-463.

Danckwerts P. V., Rizvi S. F. (1971). "The design of gas absorbers Part II: Effective interfacial areas for several types of packing." *Insights Into Chemical Engineering*, 49: 135-138.

Danckwerts P. V., Sharma M. M. (1966). "Absorption of carbon dioxide into solutions of alkalis and amines." *The Chemical Engineer*, 244–280.

Das T. R., Bandopadhyay A., Parthasarathy R., Kumar R. (1985). "Gas-liquid interfacial area in stirred vessels: the effect of an immiscible liquid phase." *Chemical Engineering Science*, 40(2): 209–214.

Davies J. T., Rideal E. K. (1961). "Interfacial phenomena." *Academic Press Inc, London*.

Demond A. H., Lindner A. S. (1993). "Estimation of interfacial tension between organic liquids and water." *Environmental Science & Technology*, 27(12): 2318-2331.

Denkov N. D., Tcholakova S. (2010). "Surfactants–classification, surfactants features and applications applications features." *Sofia University, Sofia, Bulgaria*.

Drelich J., Miller J. D. (2000). "Spreading Kinetics for Low Viscosity N-Alkanes on a Water Surface as Recorded by the High-Speed Video System." *Annales Universitatis Mariae Curie-Sklodowska Lublin-Polonia*, 54: 105–115.

Dumont E., Delmas H. (2003). "Mass transfer enhancement of gas absorption in oil-in-water systems: A Review." *Chemical Engineering and Processing: Process Intensification*, 42(6): 419–438.

Farajzadeh R., Barati A., Deli H. A., Bruining J., Zitha P. L. J. (2007). "Mass transfer of CO_2 into water and surfactant solutions."*Journal of Petroleum Science and Technology*, 1-10.

Fujasová M., Linek V., Moucha T. (2007). "Mass transfer correlations for multiple-impeller gas-liquid contactors. analysis of the effect of axial dispersion in gas and liquid phases on 'local' k_La values measured by the dynamic pressure method in individual stages of the vessel." *Chemical Engineering Science*, 62(6): 1650–1669.

Furuse H. (1972). "Viscosity of concentrated solution." *Japanese Journal of Applied Physics*, 11(10): 1537-1541.

García-Ochoa F., Gómez E. (2004). "Mass transfer coefficient in stirred tank reactors for xanthan gum solutions." *Chemical Engineering Science*, 59: 2489–2501.

García-Abuín A., Gómez-Díaz D., Navaza J. M., Sanjurjo B. (2010). "Effect of surfactant nature upon absorption in a bubble column." *Chemical Engineering Science*, 65(15): 4484–4490.

Gómez-Díaz D., Navaza J. M., Sanjurjo B. (2009). "Mass-transfer enhancement or reduction by surfactant presence at a gas-liquid interface." *Industrial and Engineering Chemistry Research*, 48(5): 2671–2677.

Gómez-Díaz D., Navaza J. M., Sanjurjo B. (2007). "Density, kinematic viscosity, speed of sound, and surface tension of hexyl, octyl, and decyl trimethyl ammonium bromide aqueous solutions." *Journal of Chemical and Engineering Data*, 52(3): 889–891.

Guilinger T. R., Grislingas A. K., Erga O. (1988). "Phase inversion behaviour of water–kerosene dispersions." *Industrial and Engineering Chemistry Research*, 27(6): 978–982.

Hari-Prajitno D., Mishra V. P., Takenaka K., Bujalski W., Nienow A., McKemmie J. (1998). "Gas-liquid mixing studies with multiple up- and down-pumping hydrofoil impellers: power characteristics and mixing time." *The Canadian Journal of Chemical Engineering*, 76(6): 1056–1068.

Hanwright J., Zhou J., Evans G. M., Galvin K. P. (2005). "Influence of surfactants on gas bubble stability." *Langmuir*, 21: 4912-4920

Hassan I. T. M., Robinson C. W. (1977). "Oxygen transfer in mechanically agitated aqueous systems containing dispersed hydrocarbon." *Biotechnology and Bioengineering*, 19(5): 661–682.

Hichri H., Accary A., Puaux J. P., Andrieu J. (1992). "Gas-liquid mass-transfer coefficients in a slurry batch reactor equipped with a self-gas-inducing agitator." *American Chemical Society*, 31(8): 1864-1867.

Higbie R. (1935). "The rate of absorption of a pure gas into a still liquid during short periods of exposure." *Transactions of the Americam Institute of Chemical Engineers*, 35: 365-389.

Hirasaki G. J. (1993). "Structural interactions in the wetting and spreading of van der Waals fluids." *Journal of Adhesion Science and Technology*, 7(3): 285-322.

Hsu Y. C., Peng R. Y., Huang C. J. (1997). "Onset of gas induction, power consumption, gas holdup and mass transfer in a new gas-induced reactor." *Chemical Engineering Science*, 52(21-22): 3883–3891.

Hsu Y. C., Chen T. Y., Chen J. H., Lay C. W. (2002). "Ozone transfer into water in a gas-inducing reactor." *Industrial & Engineering Chemistry Research*, 41(1): 120–127.

Hu B., Angeli P. (2006). "Phase inversion and associated phenomena in oil-water vertical pipeline flow." *The Canadian Journal of Chemical Engineering*, 84: 94–107.

Hu B., Angeli P., Matar O. K., Hewitt G. F. (2005). "Prediction of phase inversion in agitated vessels using a two-region model." *Chemical Engineering Science*, 60(13): 3487–3495.

Hui P. K., Palmer H. J. (1990). "Uncatalyzed oxidation of aqueous sodium sulfite and its ability to simulate bacterial respiration." *Biotechnology and Bioengineering*, 37: 392-396.

Inga J. R., Morsi B. I. (1997). "Effect of catalyst loading on gasliquid mass transfer in a slurry reactor: A statistical experimental approach." *The Canadian Journal of Chemical Engineering*, 75(5): 872–881.

Jaworski Z., Dyster K. N. (2001). "The effect of size, location and pumping direction of pitched blade turbine impellers on flow patterns: LDA measurments and CFD predictions." *Trans IChemE*, 79(A): 887–894.

Kadic E., Heindel T. J. (2010). "Mixing consideration in stirred tank bioreactors when using fluid property altering microorganisms." *8th International conference on Nanochannels, Microchannels, and Minichannels*, Montreal, Canada.

Kapic A., Heindel T. J. (2006). "Correlating gas-liquid mass transfer in a stirred-tank reactor." *Trans IChemE*, 84(A3): 239-242.

Karandikar B. M., Morsi B. I., Shah Y. T., Carr N. L. (1987). "Effect of water on the solubilities and mass transfer coefficients of gases in a heavy fraction of fischer-tropsch products." *The Canadian Journal of Chemical Engineering*, 65(6): 973–981.

Karatza D., Prisciandaro M., Lancia A., Musmarra D. (2010). "Sulfite oxidation catalyzed by cobalt ions in flue gas desulfurization processes." *Journal of the Air & Waste Management Association*, 60(6): 675–680.

Kawase Y., Moo-Young M. (1992). "Correlations for liquid-phase mass transfer coefficient in bubble column reactors with newtonian and non-newtonian fluids." *The Canadian Journal of Chemical Engineering*, 70: 48–54.

Khopkar A. R., Aubin J., Xuereb C., Sauze N. L., Bertrand J., Ranande V. V. (2003). "Gas-liquid flow generated by a pitched-blade turbine: particle image velocimetry measurements and computational fluid dynamics simulations." *Industrial and Engineering Chemistry Research*, 42(21): 5318–5332.

Kiepe J., Horstmann S., Fischer K., Gmehling J. (2002). "Experimental determination and prediction of gas solubilitz data for CO_2 +H_2O mixtures containing NaCl or KCl at temperatures between 313 and 393 K and pressure up to 10 MPa." *Industrial and Engineering Chemistry Research*, 41: 4393–4398.

Kierzkowska-Pawlak H., Zarzycki R. (2000). "Calorimetric studies of CO_2 absorption into toluene/water emulsions." *Chemical Papers*, 54(6b): 437-441.

Kluytmans J. H. J., Wachem B. G. M., Kuster B. F. M., Schouten J. C. (2003). "Mass transfer in sparged and stirred reactors: influence of carbon particles and electrolyte." *Chemical Engineering Science*, 58(20): 4719–4728.

Kordac M., Linek V. (2008). "Dynamic measurement of carbon dioxide volumetric mass transfer coeficient in a well-mixed reactor using a ph probe: analysis of the salt and saturation effects." *Industrial and Engineering Chemistry Research*, 47: 1310–1317.

Kundu A., Dumont E., Duquenne A., Delmas H. (2003). "Mass transfer characteristics in gas-liquid-liquid system." *The Canadian Journal of Chemical Engineering*, 81(3–4): 640–646.

Laity D. S., Treybal R. E. (1957). "Dynamics of liquid agitation in the absence of an air-liquid interface." *AIChE Journal*, 3(2): 176–180.

de Lamotte A., Delafosse A., Calvo S., Delvigen F., Toye D. (2017). "Investigating the effets of hydrodynamics and mixing on mass transfer through the free-saurface in stirred tank bioreactors." *Chemical Engineering Science*, 172: 125-142.

Ledakowicz S., Nettelhoff H., Deckwer W. D. (1984). "Gas-liquid mass transfer data in a stirred autoclave reactor." *Industrial and Engineering Chemistry Fundamentals*, 23(4): 510–512.

Lee D. J., Lou X., Fan L. S. (1999). "Gas disengagement technique in a slurry bubble column operated in the coalesced bubble regime." *Chemical Engineering Science*, 54: 2227-2236.

Lekhal A., Chaudhari R. V., Wilhelm A. M., Delmas H. (1997). "Gas-liquid mass transfer in gas-liquid-liquid dispersions." *Chemical Engineering Science*, 52(21-22): 4069–4077.

Lewis W. K., Whitman W. G. (1924). "Principles of gas absorption." *Industrial and Engineering Chemnisty*, 16(12): 1215–1220.

Lide D. R. (2003). "CRC Handbook of Chemistry and Physics." *CRC Press, 84th edition*.

Linek V., Beneš. P. (1976). "A study of the mechanism of gas absorption into oil-water emulsions." *Chemical Engineering Science*, 31(11): 1037–1046.

Linek V., Kordač M., Fujasová M., Moucha T. (2004). "Gas-liquid mass transfer coefficient in stirred tanks interpreted through models of idealized eddy structure of turbulence in the bubble vicinity." *Chemical Engineering and Processing: Process Intensification*, 43(12): 1511–1517.

Linek V., Tvrdik J. (1971). "A generalization of kinetic data on sulphite oxidation systems." *Biotechnology and Bioengineering*, 13(3): 353–369.

Linek V., Vacek V. (1981). "Chemical engineering use of catalyzed sulfite oxidation kinetiks for the determination of mass transfer characteristics of gas-liquid contactors." *Chemical Engineering Science*, 36(11): 1747–1768.

Luewisutthichat W., Tsutsumi A., Yoshida K. (1997). "Chaotic hydrodynamics of continuous single-bubble flow systems." *Chemical Engineering Science*, 52: 3685–3691.

Maalej S., Benadda B., Otterbein M. (2001). "Influence of pressure on the hydrodynamics and mass transfer parameters of an agitated bubble reactor." *Chemical Engineering and Technology*, 24(1): 77–84.

Martín M., Montes F. J., Galán M. A. (2008a). "Bubbling process in stirred tank reactors II: Agitator effect on the mass transfer rates." *Chemical Engineering Science*, 63: 3223-3232.

McFarlane C. M., Zhao X., Nienow A. W. (1995). "Studies of high solidity ratio hydrofoil impellers for aerated bioreactors. 2. air—water studies." *Biotechnology Progress*, 11(6): 608–618.

Mehta V. D., Sharma M. M. (1971). "Mass transfer in mechanically agitated gas-liquid contactors." *Chemical Engineering Science*, 26(3): 461–479.

Miller S. A., Ekstrom A., Foster N. R. (1990). "Solubility and mass-transfer coefficients for hydrogen and carbon monoxide in n-octacosane." *Journal of Chemical and Engineering Data*, 35(2): 125–127.

Mishra V. P., Dyster K. N., Jaworski Z., Nienow A. W., McKemmie J. (1998). "A study of an up- and a down-pumping wide blade hydrofoil impeller; Part I. LDA measurements." *The Cansdian Journal of Chemical Engineering*, 76: 577–588.

Mishra M., Muthuprasanna P., .Surya prabha K., Sobhita rani P., Satish babu A., Sarath Chandiran I., Arunachalam G., Shalini S. (2009). "Basics and potential applications of surfactants - A review." *International Journal of PharmTech Research*, 1(4): 1354–1365.

Martín M., García J. M., Montes F. J., Galán M. A. (2008b). "On the effect of the orifice configuration on the coalescence of growing bubbles." Chemical Engineering and Processing: Process Intensification, 47(9-10): 1799-1809.

Morelli J. J., Szajer G. (2000). "Analysis of surfactants – Part I" *Journal of Surfactants and Detergents*, 3(4): 539–551.

Ngo T. H., Schumpe A. (2012a). "Absorption of CO_2 into alkane/water emulsions in a stirred tank." *Journal of Chemical Engineering of Japan*, 45(9): 737-741.

Ngo T. H., Schumpe A. (2012b). "Oxygen absorption into stirred emulsions of n-alkanes." *International Journal of Chemical Engineering*, 2012: 1-7.

Nielsen D. R., Daugulis A. J., P. McLellan P. J. (2003). "A novel method of simulating oxygen mass transfer in two-phase partitioning bioreactors." *Biotechnology and Bioengineering*, 83(6): 735–742.

Nienow A. W. (1990). "Gas dispersion performance in fermenter operation." *Chemical Engineering progress*, 61–71.

Nocentini M., Fajner D., Pasquali G., Magelli F. (1992). "Gas-liquid mass transfer and holdup in vessels stirred with multiple rushton turbines: Water and water-glycerol solutions." *American Chemical Society*, 32(1): 19-26.

Oliveira R. C. G., Gonzalez G., Oliveira J. F. (1999). "Interfacial studies on dissolved gas flotation of oil droplets for water purification." *Colloids and Surfaces A: Physicochemical Engineering Aspects*, 154: 127-135.

Onda K., Takeuchi H., Maeda Y. (1972). "The absorption of oxygen into sodium sulphite solutions in a packed column." *Chemical Engineering Science*, 27(2): 449–451.

Oyevaar M. H., Westerterp K. R. (1989). "The use of the chemical method for the determination of interfacial areas in gas-liquid contactors." *Chemical Engineering Science*, 44(11): 2691–2701.

Özcan-Taşkin G., Wei H. (2003). "The effect of impeller-to-tank diameter ratio on draw down of solids." *Chemical Engineering Science*, 58(10): 2011–2022.

Painmanakul P., Loubière K., Hèbrard G., Mietton-Peuchot M., Roustan M. (2005). "Effect of surfactants on liquid-side mass transfer coefficients." *Chemical Engineering Science*, 60(22): 6480–6491.

Pal R. (1993). "Pipeline flow of unstable and surfactant stabilizes emulsions." *AIChE Journal*, 39(11): 1754–1764.

Perazzo A., Preziosi V., Guido S. (2015). "Phase inversion emulsification: Current understanding and applications." *Advances in Colloid and Interface Science*, 222: 581-599.

Pinho H. J. O., Alves S. S. (2010). "Effect of spreading coefficient on gas-liquid mass transfer in gas-liquid-liquid dispersions in a stirred tank." *Chemical Engineering Communications*, 197(12): 1515–1526.

Pizzino A., Cattè M., Van Hecke E., Salager J. L., Aubry J. M. (2009). "On-line light backscattering tracking of the transitional phase inversion of emlsions." *Colloids and Surfaces A: Physicochemical Engineering Aspects*, 338: 148-154.

Posocco P., Perazzo A., Preziosi V., Laurini E., Pricl S., Guido S. (2016). "Interfacial tension of oil/water emulsions with mixed non-ionic surfactants: comparison between experiments and molecular simulations." *RSC Advances*, 6(6): 4723–4729.

Preziosi V., Perazzo A., Caserta S., Tomaiuolo G., Guido S. (2013). "Phase inversion emulsification." *Chemical Engineering Transactions*, 32: 1585-1590.

Reid R. C., Praunsnitz J. M., Sherwood T. K. (1977). "The properties og gases and liquids." *McGraw-Hill. New York, 3rd edition.*

Rols J. L., Condoret J. S., Fonade C., Goma G. (1990). "Mechanism of enhanced oxygen transfer in fermentation using emulsified oxygen-vectors." *Biotechnology and bioengineering*, 35(4): 427–435.

Rols, J. L., Goma G. (1991). "Enhanced oxygen transfer rates in fermentation using soyabean oil-in-water dispersions." *Biotechnology Letters*, 13(1): 7–12.

Rosu M., Schumpe A. (2006). "Influence of surfactants on gas absorption into aqueous suspensions of activated carbon." *Chemical Engineering Science*, 62(18–20): 5458–5463.

Sardeing R., Aubin J., Poux M., Xuereb C. (2004a). "Gas–liquid mass transfer: influence of sparger location." *Chemical Engineering Research and Design*, 82(9): 1161–1168.

Sardeing R., Aubin J., Xuereb C. (2004b). "Gas–liquid mass transfer a comparison of down- and up-pumping axial flow impellers with radial impellers." *Chemical Engineering Research and Design*, 82(12): 1589–96.

Sauid M., Suhaila, Krishnan J., Ling T. H., Veluri M. (2013). "Enhancement of oxygen mass transfer and gas holdup using palm oil in stirred tank bioreactors with xanthan solutions as simulated viscous fermentation broths." *BioMed Research International*, 2013: 1-9.

Schramm L. L., Marangoni G. (2000). "Surfactants: fundamentals and applications in the petroleum industry." *Cambridge University Press, 1st edition*.

Schweitzer J-M., Bayle J., Gauthier T. (2001). "Local gas hold-up measurements in fluidized bed and slurry bubble column." *Chemical engineering Science*, 56: 1103-1110.

Schumpe A. (1993). "The estimation of gas solubilities in salt solutions." *Chemical engineering Science*, 48: 153-158.

Schumpe A., Deckwer W. D. (1980). "Analysis of chemical methods for determination of interfacial areas in gas-in-liquid dispersions with non-uniform bubble sizes." *Chemical engineering Science*, 35: 2221-2233.

Schumpe A., Quicker, G., Deckwer W. D. (1982). "Gas solubilities in microbial culture media." *Advances in Biochemical Engineering*, 24: 1-38.

Schumpe A., Saxena A. K., Fang L. K. (1986). "Gas/liquid mass transfer in slurry bubble column." *Chemical engineering Science*, 42(7): 1787-1796.

Sivaji K., Murty G. S. R. N. (1982). "Kinetics of sulfite oxidation reaction." *Industrial and Engineering Chemistry Fundamentals* 21(4): 344–352.

Srivastava R. D., Mcmillan A. F., Harris I. J. (1968). " The kinetiks of oxidation of sodium sulphite." *The Canadian Journal of Chemical Engineering*, 46: 181-184.

Springer T. G., Pigford R. L. (1970). "Influence of surface turbulence and surfactants on gas transport through liquid interfaces." *Industrial and Engineering Chemistry Fundamentals*, 9(3): 458-465

Stegeman D, Ket P. J., Kolk H. A. v.d., Bolk J. W., Knop P. A., Westerterp K. R. (1995). "Interfacial area and gas holdup in a bubble column reactor at elevated pressures." *Industrial & Engineering Chemistry Research*, 34: 59-71.

Taylor G. I. (1932). "The viscosity of a fluid containing small drops of another fluid." *Proceedings of the Royal Society of London Series A*, 138: 41–48.

Tyrode E., Allouche J., Choplin L., salager J. L. (2005). "Emulsion catastrophic inversion from abnormal to normal morphology. 4.Following the emulsion viscosity during three inversion protocols and extending the critical dispersed-phase concept." *Industrial & Engineering Chemistry Research*, 44: 67-74.

Tekie Z, Li J., Morsi B. I. (1997). "Mass transfer parameters of O_2 and N_2 in cyclohexane under elevated pressures and temperatures: A statistical approach." *Industrial & Engineering Chemistry Research*, 36: 3879–3888.

Treybal R. E. (1981). "Mass-transfer operations." *McGraw-Hill, New York*, 3rd edition.

Vaessen G. E. J. (1996). "Predicting catastrophic phase inversion in emulsions." *Eindhoven Univeristy of Technology, Eindhoven*.

Van Ede C. J., Houten R. V., Beenackers A. A. C. M. (1995). "Enhancement of gas to water mass transfer rates by a dispersed organic phase." *Chemical Engineering Science*, 50(18): 2911–2922.

Vázquez G., Cancela M. A., Varela R., Alvarez E., Navaza J. M. (1997). "Influence of surfactants on absorption of co2 in a stirred tank with and without bubbling." *Chemical Engineering Journal*, 67(2): 131–137.

Vázquez G., Cancela M. A., Riverol C., Alvarez E., Navaza J. M. (2000). "Determination of interfacial areas in a bubble column by different chemical methods." *Industrial & Engineering Chemistry Research*, 39(7): 2541–2547.

Vermeulen T., Williams G. M., Langlois G. E. (1955). "Interfacial area in liquid–liquid and gas–liquid agitation." *Chemical Engineering Progress*, 51 (2): 85–94.

de Waal K. J. A., Okeson J. C. (1966). "The oxidation of aqueous sodium sulphite solutions." *Chemical Engineering Science*, 21(6-7): 559–572.

Wang X., Conway W., Burns R., McCann N., Maeder M. (2010). "Comprehensive study of the hydration and dehydration reactions of carbon dioxide in aqueous solution." *The Journal of physical Chemistry*, 114(4): 1734–1740.

Weisenberger s., Schumpe A. (1996). "Estimation of gas solubilities in salt solutions at temperature from 273 K to 363 K." *AIChE Journal*, 42(1): 298-300.

Weiss R. F. (1974). "Carbon dioxide in water and seawater: The solubility of a non-ideal gas." *Marine Chemistry*, 2: 203-215.

Wilhelm E., Battino R., Wilcock R. J. (1977). "Low-pressure solubility of gases in liquid water." *Chemical Reviews*, 77(2): 219-262.

Wilke C. R., Chang P. (1955) "Correlation of diffusion coefficients in dilute solutions." *AIChE Journal*, 1(2): 264-270.

Worden R. M., Bredwell M. D. (1998). "Mass transfer properties of microbubbles: II. Analysis using a dynamic model." *Biotechnology Progress*, 14(1): 39-46.

Yagi S., Inoue H. (1962). "The absorption of oxygen into sodium sulphite solution." *Chemical Engineering Science*, 17(6): 411–421.

Yagi S., Yoshida F. (1975). "Gas absorption by newtonian and non-newtonian fluids in sparged agitated vessels." *Industrial & Engineering Chemistry Process Design and Development*, 14(4): 488–493.

Yoshida F., Tsuneo Y., Yoshio M. (1970). "Oxygen absorption into oil-in-water emulsions. a study on hydrocarbon fermentors." *Industrial & Engineering Chemistry Process Design and Development*, 9(4): 570–577.

Yoshimoto M., Suenaga S., Furumoto K., Fukunaga K., Nakao K. (2007). "Gas-liquid interfacial area, bubble size and liquid-phase mass transfer coefficient in a three-phase external loop airlift bubble column." *Chemical and biochemical engineering quarterly*, 21(4): 365–372.

Zeppieri S., Rodríguez, J., López de Ramos A. L. (2001). "Interfacial tension of alkane+water systems." *Journal of Chemical and Engineering Data*, 46(5): 1086-1088.

Zhang Z., Chen W., Yu S., Li W. (2010). "Enhancement of gas-to-water mass-transfer rates by the second liquid phase." *Industrial and Engineering Chemistry Research*, 49(7): 3223–3227.

Zhao B., Li Y., Huiling T., Zhuo Y., Zhang L., Shi J., Chen C. (2005). "study on the reaction rate of sulfite oxidation with cobalt ion catalyst." *Chemical Engineering Science*, 60: 863–868.

Zokaei-Kadijani S., Safdari J., Mousavian M. A., Rashidi A. (2013). "Study of oxygen mass transfer coefficient and oxygen uptake rate in a stirred tank reactor for uranium ore bioleaching." *Annals of Nuclear Energy*, 53: 280–287.